

THE UNIVERSITY OF CALGARY

PHASE BEHAVIOUR AND VISCOSITY OF BITUMEN
FRACTIONS SATURATED WITH CO₂

by

ROBERT ROY EASTICK

A THESIS

SUBMITTED TO THE FACULTY OF GRADUATE STUDIES
IN PARTIAL FULFILLMENT OF THE REQUIREMENTS FOR THE DEGREE OF
MASTER OF SCIENCE

DEPARTMENT OF CHEMICAL AND PETROLEUM ENGINEERING

CALGARY, ALBERTA, CANADA

OCTOBER, 1989

© ROBERT ROY EASTICK 1989



National Library
of Canada

Bibliothèque nationale
du Canada

Canadian Theses Service Service des thèses canadiennes

Ottawa, Canada
K1A 0N4

The author has granted an irrevocable non-exclusive licence allowing the National Library of Canada to reproduce, loan, distribute or sell copies of his/her thesis by any means and in any form or format, making this thesis available to interested persons.

The author retains ownership of the copyright in his/her thesis. Neither the thesis nor substantial extracts from it may be printed or otherwise reproduced without his/her permission.

L'auteur a accordé une licence irrévocable et non exclusive permettant à la Bibliothèque nationale du Canada de reproduire, prêter, distribuer ou vendre des copies de sa thèse de quelque manière et sous quelque forme que ce soit pour mettre des exemplaires de cette thèse à la disposition des personnes intéressées.

L'auteur conserve la propriété du droit d'auteur qui protège sa thèse. Ni la thèse ni des extraits substantiels de celle-ci ne doivent être imprimés ou autrement reproduits sans son autorisation.

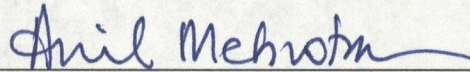
ISBN 0-315-54212-0

THE UNIVERSITY OF CALGARY
FACULTY OF GRADUATE STUDIES

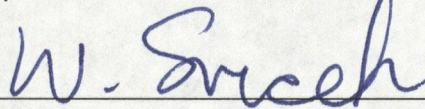
The undersigned certify that they have read, and recommend to the
Faculty of Graduate Studies for acceptance, a thesis entitled,

"PHASE BEHAVIOUR AND VISCOSITY OF BITUMEN FRACTIONS
SATURATED WITH CO₂"

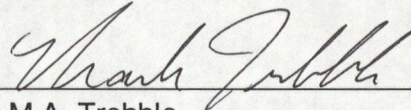
submitted by Robert Roy Eastick in partial fulfillment of the requirements for the
degree of Master of Science.



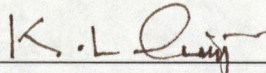
Dr. A.K. Mehrotra, Committee Chairman
Department of Chemical & Petroleum Engineering



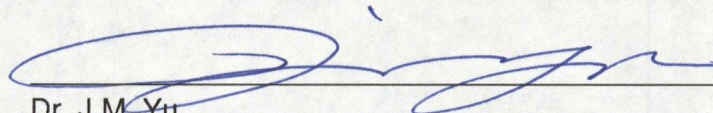
Dr. W.Y. Svrcek,
Department of Chemical & Petroleum Engineering



Dr. M.A. Trebble,
Department of Chemical & Petroleum Engineering



Dr. K.L. Chowdhury,
Department of Survey Engineering



Dr. J.M. Yu,
Esso Resources Canada Ltd., External Examiner

October 5, 1989

Date

ABSTRACT

New data for the viscosity, density, and gas-solubility of CO₂-saturated bitumen fractions are presented. These fractions were obtained by dividing a sample of Cold Lake bitumen into five fractions based on boiling point. The lightest two fractions (bp < 510°C) were clear liquids, whereas the third and fourth fractions (bp > 510°C) were dark and viscous. The fifth fraction was a glass-like solid at room temperature, with a softening temperature of approximately 100°C. The gas-solubility, density, and viscosity of each of these fractions saturated with CO₂ were measured. The properties of the CO₂-saturated whole bitumen were measured as well.

The viscosity behaviour of the bitumen fractions were found to be well correlated with a two parameter double-log correlation that has been shown to be valid generally for Alberta bitumens. A mixing rule for bitumen fractions is also presented.

The phase behaviour of the bitumen fractions were correlated using three equations-of-state (EOS): the Soave-Redlich-Kwong EOS (1972), the Peng-Robinson EOS (1976), and the Patel-Teja EOS (1982). The fractions were characterized as individual pseudocomponents, with critical properties estimated from correlations proposed by Kesler and Lee (1976), Cavett (1962), Sim and Daubert(1980), Whitson (1980), Twu (1984), and Watanasiri *et al* (1985). Correlation was performed by optimizing the EOS binary interaction parameter in the equations-of-state to match the

solubility data, and by optimizing the pseudocomponent critical pressure to match the density data.

The bitumen fraction characterizations were then blended to predict the CO₂-solubility of the whole bitumen. Interactions between the bitumen fractions are suggested by the results. Finally, the predictions are compared with the experimental data.

ACKNOWLEDGEMENTS

The author wishes to express his gratitude to Dr. Anil Mehrotra for his support and encouragement in supervising this project. His contagious enthusiasm is responsible for much of this work.

Thanks also go to Mr. Rod Rundle for his assistance in the collection of data and for the forthcoming preparation of the final project report.

Special thanks go to fellow graduate students John Nighswander and Bruce Milne, whose helpful discussions, be they in the bowels of the Engineering Building or on the summit of some lofty peak, are greatly appreciated.

The help of Ian Mikalson in the construction of the Low Viscosity Apparatus is also appreciated.

A special appreciation goes to Bernie Sheehan, who provided support and encouragement when they were needed most.

Financial support by the Alberta Oil Sands Technology and Research Authority (AOSTRA) and the Department of Chemical and Petroleum Engineering at the University of Calgary is gratefully acknowledged.

TABLE OF CONTENTS

	Page
Abstract	iii
Acknowledgements	v
Table of Contents	vi
List of Tables	ix
List of Figures	xi
List of Symbols	xiii
CHAPTER 1 - INTRODUCTION	1
CHAPTER 2 - LITERATURE REVIEW	6
2.1 CO ₂ -Saturated Bitumen Data	6
2.2 Characterization of Bitumen for Data Correlation and Prediction	8
2.2.1 The Kesler and Lee Correlations	9
2.2.2 The Cavett Correlations	10
2.2.3 The Sim and Daubert Correlations	11
2.2.4 The Whitson Correlations	11
2.2.5 The Twu Correlations	12
2.2.6 The Watanasiri <i>et al.</i> Correlations	14
2.2.7 Acentric Factor Correlations	15
2.3 Equation of State Considerations	16
2.3.1 The Soave-Redlich-Kwong Equation of State	16
2.3.2 The Peng-Robinson Equation of State	18
2.3.3 The Patel-Teja Equation of State	19
CHAPTER 3 - DESCRIPTION OF BITUMEN FRACTIONS	21
3.1 Physical and Chemical Analyses of Bitumen Fractions	21
3.1.1 Molar Mass Measurements	22
3.1.2 Asphaltenes Content Measurements	22
3.1.3 SIMDIST Distillations	24
3.1.4 Elemental Composition Analyses	24
3.1.5 Room Temperature Density Measurements	26

3.2	Viscosity Measurements and Correlation	26
3.2.1	A Correlation for Bitumen Fraction Viscosity	27
3.2.2	Prediction of Whole Bitumen Viscosity	33
CHAPTER 4 - EXPERIMENTAL		38
4.1	High Viscosity Apparatus	38
4.2	Low Viscosity Apparatus	41
4.3	Depressurization Apparatus	43
CHAPTER 5 - DATA FOR THE PROPERTIES OF CO₂-SATURATED BITUMEN FRACTIONS		46
5.1	Results for CO ₂ -Saturated Whole Cold Lake Bitumen	46
5.2	Results for CO ₂ -Saturated Cut 1	49
5.3	Results for CO ₂ -Saturated Cut 2	52
5.4	Results for CO ₂ -Saturated Cut 3	52
5.5	Results for CO ₂ -Saturated Cut 4	52
5.6	Results for CO ₂ -Saturated Cut 5	59
CHAPTER 6 - CORRELATION OF CO₂-SOLUBILITY AND DENSITY DATA		62
6.1	Definition of Optimization Criterion	62
6.2	Characterization of Bitumen Fractions	64
6.2.1	Estimation of Critical Temperature	65
6.2.2	Estimation of Critical Pressure	65
6.2.3	Estimation of Acentric Factor	69
6.3	Calculation Method	72
6.4	Correlation of Whole Bitumen Solubility Data	72
6.4.1	Comparison of Critical Property Correlations	72
6.4.2	Comparison of Equations of State	74
6.5	Correlation of Bitumen Fraction Solubility Data	78
6.5.1	Correlation of Cut 1 Solubility Data	78
6.5.2	Correlation of Cut 2 Solubility Data	82
6.5.3	Correlation of Cut 3 Solubility Data	84
6.5.4	Correlation of Cut 4 Solubility Data	84
6.5.5	Correlation of Cut 5 Solubility Data	84
6.6	Temperature-Dependence of the Interaction Parameter	91

6.7	Correlation of Density Data	93
6.7.1	Estimation of Critical Pressure from Density Data	94
6.8	Use of Regressed Critical Pressure with the P-R EOS	97
6.9	Summary	105
CHAPTER 7 - WHOLE BITUMEN GAS-SOLUBILITY PREDICTIONS		110
CONCLUSIONS AND RECOMMENDATIONS		115
	Conclusions	115
	Recommendations	116
REFERENCES		118
APPENDIX A - Constants in the Cavett Correlations		123
APPENDIX B - SIMDIST Distillation Data		124
APPENDIX C - Supplement to Chapter 6		127

LIST OF TABLES

Table	Page
3.1 Measured Data and Properties of Cold Lake Bitumen and Its Fractions	23
3.2 Effect of Temperature on the Density of Cut 1	28
3.3 Viscosity-Temperature Data for Cold Lake Bitumen and Its Fractions	30
3.4 Correlation of Gas-Free Viscosities of Samples with Equation 3.1	32
5.1 CO ₂ -Saturated Whole Bitumen Data	47
5.2 CO ₂ -Saturated Cut 1 Data	50
5.3 CO ₂ -Saturated Cut 2 Data	53
5.4 CO ₂ -Saturated Cut 3 Data	55
5.5 CO ₂ -Saturated Cut 4 Data	57
5.6 CO ₂ -Saturated Cut 5 Data	60
6.1 Critical Property Estimations for Bitumen Fractions	66
6.2 Acentric Factor Estimations for Bitumen Fractions	70
6.3 Comparison of Characterizations for the Correlation of Whole Bitumen Solubility Data Using the P-R EOS	73
6.4 Comparison of Equations of State for the Correlation of Whole Bitumen Solubility Data with the Twu Characterization	76
6.5 Comparison of Characterizations for the Correlation of Cut 1 Solubility Data with the P-R EOS	79
6.6 Comparison of Characterizations for the Correlation of Cut 2 Solubility Data with the P-R EOS	82
6.7 Comparison of Characterizations for the Correlation of Cut 3 Solubility Data with the P-R EOS	85
6.8 Comparison of Characterizations for the Correlation of Cut 4 Solubility Data with the P-R EOS	87
6.9 Comparison of Characterizations for the Correlation of Cut 5 Solubility Data with the P-R EOS	89
6.10 Comparison of Characterizations for the Correlation of Whole Bitumen Solubility Data with Temperature Dependent Interaction Parameters	92

6.11	Correlation of Sample Solubility and Density Data with the P-T EOS	98
7.1	Prediction of Whole Bitumen Solubility Data using Five-Pseudocomponent Characterizations	113

LIST OF FIGURES

Figure	Page
3.1 Sample SIMDIST Distillations	25
3.2 Comparison of Viscosities of Cold Lake Bitumen Samples	29
3.3 Viscosities of Bitumen Fractions Correlated with Equation 3.1	31
3.4 Relationship Between b_1 and b_2 for Bitumen Fractions and Alberta Bitumens	34
3.5 Cold Lake Bitumen Viscosity Predicted with Equation 3.2	35
3.6 Relationship Between b_1 and b_2 and Bitumen Fraction Molar Mass	37
4.1 The High Viscosity Apparatus	39
4.2 The Low Viscosity Apparatus	42
4.3 The Depressurization Apparatus	45
5.1 CO ₂ -Saturated Whole Bitumen Data	48
5.2 CO ₂ -Saturated Cut 1 Data	51
5.3 CO ₂ -Saturated Cut 2 Data	54
5.4 CO ₂ -Saturated Cut 3 Data	56
5.5 CO ₂ -Saturated Cut 4 Data	58
5.6 CO ₂ -Saturated Cut 5 Data	61
6.1 Estimates of Bitumen Fraction Critical Temperatures	67
6.2 Estimates of Bitumen Fraction Critical Pressures	68
6.3 Estimates of Bitumen Fraction Acentric Factors	71
6.4 Whole Bitumen CO ₂ -Solubility Data Correlated with the P-R EOS	75
6.5 Whole Bitumen CO ₂ -Solubility Data Correlated with the Twu Characterization	77
6.6 Cut 1 CO ₂ -Solubility Data Correlated with the P-R EOS	80
6.7 Cut 2 CO ₂ -Solubility Data Correlated with the P-R EOS	83
6.8 Cut 3 CO ₂ -Solubility Data Correlated with the P-R EOS	86
6.9 Cut 4 CO ₂ -Solubility Data Correlated with the P-R EOS	88
6.10 Cut 5 CO ₂ -Solubility Data Correlated with the P-R EOS	90
6.11 Cut 3 Density Data Correlated with the P-T EOS and the Kesler-Lee Characterization	96
6.12 Whole Bitumen CO ₂ -Solubility and Density Data Correlated with the P-T EOS	99

6.13	Cut 1 CO ₂ -Solubility and Density Data Correlated with the P-T EOS	100
6.14	Cut 2 CO ₂ -Solubility and Density Data Correlated with the P-T EOS	101
6.15	Cut 3 CO ₂ -Solubility and Density Data Correlated with the P-T EOS	102
6.16	Cut 4 CO ₂ -Solubility and Density Data Correlated with the P-T EOS	103
6.17	Cut 5 CO ₂ -Solubility and Density Data Correlated with the P-T EOS	104
6.18	Cut 2 CO ₂ -Solubility Data Correlated with the P-R EOS and P _c estimated from Equation 6.6	106
6.19	Cut 4 CO ₂ -Solubility Data Correlated with the P-R EOS and P _c estimated from Equation 6.6	107
7.1	Whole Bitumen CO ₂ -Solubility Predictions	114

LIST OF SYMBOLS

a	equation of state parameter
API	API gravity
b	equation of state parameter
b_1, b_2	parameters in Equation 3.1
bp	boiling point
c	equation of state parameter
K	Watson characterization factor
k_{ij}	binary interaction parameter between components i and j
k_α, k_β	constants in Equation 6.5
MW	molar mass, g/mol
N	number of data points
P	pressure
P	number of adjustable parameters in a model
P_c	critical pressure
SG	specific gravity
T	temperature
T_b	normal boiling point
T_c	critical temperature
v	critical volume
x_i	mole fraction of component i
y_i	data point i
Z_c	critical compressibility

Greek Symbols

μ	dynamic viscosity, Pa·s
ρ	density, kg/m ³
σ_i	standard deviation of data point i
ω	acentric factor

Superscripts

\circ	reference fluid (n -alkanes)
\wedge	correlated value

Subscripts

m mixture, whole bitumen
r reduced value

Abbreviations

AAD average absolute deviation
SIMDIST simulated distillation analysis

Other symbols with more localized use are defined in the text.

CHAPTER 1

INTRODUCTION

As the availability of conventional crude oil continues to dwindle, the viability of bitumen as an energy resource increases. Yet, our knowledge of the behaviour of this substance is still limited. Due to the heavy, viscous nature of bitumen, enhanced techniques must be used to recover and transport the bitumen. An increase in temperature greatly reduces the viscosity of bitumen, as does the dissolution of gases or liquid diluents in the bitumen. Accurate prediction of the diluent requirement is important if recovery is to be efficient and economical, and prediction of the phase behaviour of the mixture as conditions change is important in the design of transportation and downstream facilities.

Many aspects of bitumen behaviour have been correlated, but the prediction of the responses of bitumens to different conditions, given only a few bulk properties of the bitumen, is still in its infancy. A number of predictive methods, developed for use with conventional crudes, have been extended to bitumens; but the unique aspects of bitumens — such as the high molar mass and the high asphaltenes content — indicate that these methods might be improved upon.

The measurement of the viscosity, density, and gas solubility of bitumens saturated with gases at various temperatures and pressures has been underway since the beginning of this decade, when Jacobs *et al.* (1980) reported the viscosity of Athabasca bitumen saturated with CO₂, CH₄, and N₂. Svrcek and Mehrotra (1982) provided gas solubility and

density in addition to viscosity data. The behaviour of Athabasca bitumen saturated with a synthetic combustion gas mixture was documented as well (Mehrotra and Svrcek, 1982; Mehrotra and Svrcek, 1985a). Similar data for Athabasca bitumen have also been provided by Fu *et al.* (1985). Measurements have also been made with Marguerite Lake Phase-A bitumen (Mehrotra and Svrcek, 1984), Peace River bitumen (Mehrotra and Svrcek, 1985b; Svrcek and Mehrotra, 1989), Wabasca bitumen (Mehrotra and Svrcek, 1985c), and Cold Lake bitumen (Fu *et al.*, 1988; Mehrotra and Svrcek, 1988a; Yu *et al.*, 1989). Various gases were used in these investigations, including N_2 , CO, CH_4 , CO_2 , C_2H_6 , and mixtures of gases resembling field gas mixtures. A good compendium of experimental data may be found in the AOSTRA Data Book (AOSTRA, 1984).

Empirical correlations of measured properties of these bitumens were provided by Mehrotra and Svrcek (1982, 1984). Generally, these correlations are polynomial in nature. Characterization techniques, in which the bitumen is represented by a number of pseudocomponents for use in equations of state, have also been considered. In this method, used commonly with conventional crudes, critical properties of the pseudocomponents are estimated from readily measured properties of the sample, such as density, molar mass, or normal boiling point. With the bitumen so represented, gas solubility may be predicted with an equation of state.

Predictions of gas-saturated bitumen phase equilibria using an equation of state were examined by Bishnoi *et al.* (1977). A typical Athabasca bitumen sample was arbitrarily broken into five pseudocompo-

nents, with critical properties of these pseudocomponents obtained from their estimated physical properties. Predictions, however, were not compared with any experimental data. Mehrotra *et al.* (1985) used the Peng-Robinson equation of state to predict the gas solubility and density of Athabasca and Peace River bitumens, comparing a number of characterization methods. Characterizations have also been developed for Athabasca (GCOS) bitumen, Athabasca (ARC) bitumen, Marguerite Lake Phase-A bitumen, Peace River (PRISP) bitumen, and Wabasca bitumen (Mehrotra and Svrcek, 1987, 1988; Mehrotra *et al.*, 1989), and for Cold Lake bitumen (Mehrotra and Svrcek, 1988).

Prediction of the viscosity of bitumen was also undertaken using characterization schemes. Johnson *et al.* (1987) and Mehrotra and Svrcek (1987) used the extended principle of corresponding states to model the viscosity of Athabasca, Peace River, Marguerite Lake, and Wabasca bitumens.

In all the previous studies, it should be noted that the fractionation of the bitumen to generate pseudocomponents was performed theoretically; *i. e.*, the bitumen samples were not physically subdivided into individual fractions. The theoretical fractionation was typically based on the solubility of the bitumen in a solvent to obtain an asphaltenes fraction, and on a distillation (such as a SIMDIST distillation) of the asphaltenes-free bitumen to elucidate distillable and undistillable maltenes fractions. Definitions of such fractions, however, are purely arbitrary, and vary from characterization scheme to characterization

scheme.

What all of the previous correlation schemes lack is a precise knowledge of the equation of state (EOS) binary interaction parameters for gas-bitumen pairs. These are typically set to match the experimental data, making these predictive methods an exercise in correlation. Not considered in these schemes are pseudocomponent-pseudocomponent interaction parameters, which have been neglected due to a lack of any experimental data that would allow these parameters to be determined.

For this work, a sample of Cold Lake bitumen was fractionated into five samples by distillation by Esso Resources Canada Ltd., Calgary. These fractions, or "cuts", range from a light clear liquid (Cut 1), to a fraction resembling the whole bitumen (Cut 3), to a brittle glass-like solid with a softening temperature of approximately 100°C (Cut 5). The viscosity, density, and gas solubility of each of these cuts saturated with CO₂ were measured at temperatures ranging from 25°C to 150°C and at pressures up to 10 MPa. In addition, properties of the gas-saturated whole bitumen were measured as well.

The collected phase behaviour data have been correlated using three equations of state, with each cut being represented by a single pseudocomponent. For estimating critical properties for each pseudocomponent, six different correlations for critical temperature and critical pressure, and three correlations for acentric factor were screened. Interaction parameters for each CO₂-pseudocomponent pair were regressed from the

CO₂-solubility data. All five pseudocomponents were then used to model the whole bitumen. The results suggest the presence of pseudocomponent-pseudocomponent interactions.

CHAPTER 2

LITERATURE REVIEW

The scope of this work considers the behaviour of undefined hydrocarbon mixtures, and the correlation of their properties. As such, the literature review was limited to these areas. Primary emphasis was placed on heavy oils and bitumens. In terms of data pertaining to this work, screening was limited to literature on bitumens saturated with CO₂, and did not consider the properties of bitumens saturated with other gases.

The review of correlational and predictive methods was limited to equations-of-state based methods, which have found a great deal of acceptance in the petroleum industry. With these methods, the undefined hydrocarbon mixture is represented by a number of pseudocomponents, whose properties are estimated through the use of correlations. The correlations used in this study all use some readily measured properties of the mixture to estimate critical properties of the pseudocomponents. Correlations that require some sort of definition of the molecular structure of the mixture were not considered.

2.1 CO₂-Saturated Bitumen Data

Data for the solubility of CO₂ in a number of Alberta bitumens have been presented. Svrcek and Mehrotra (1982) gave 29 data points for the viscosity, density, and gas solubility of CO₂-saturated Athabasca bitumen. Temperatures and pressures varied from 23.0°C to 97.4°C, and from 1.72 MPa to 6.38 MPa. Viscosity was found to decrease significantly with increases in temperature and pressure, ranging from a high of 22.9 Pa·s at 25.7°C and 1.72 MPa to a low of 0.073 Pa·s at 96.8°C and 6.38 MPa. The density

of the gas-saturated bitumen was found to be unaffected by pressure but decreased with temperature from approximately 1040 kg/m^3 at 23°C to about 985 kg/m^3 at 100°C . Solubility of CO_2 in the bitumen was found to increase with pressure and decrease with temperature. A maximum value of 8.77 wt% CO_2 was obtained at 23.8°C and 5.75 MPa.

The properties of CO_2 -saturated Marguerite Lake bitumen have also been studied (Mehrotra and Svrcek, 1984). The range of pressures and temperatures considered was essentially the same as for the Athabasca bitumen experiments, except an isotherm was added at 12°C . At pressures above 4.5 MPa for this isotherm, the CO_2 liquefies and the viscosity and gas solubility of the bitumen become less sensitive to changes in pressure.

Peace River and Wabasca bitumens also exhibit similar behaviour when saturated with CO_2 (Mehrotra and Svrcek, 1985a, 1985b). The Wabasca bitumen is much less viscous than the bitumens mentioned above and exhibited a higher CO_2 -solubility at a given temperature and pressure than the other bitumens.

Properties of Cold Lake bitumen saturated with CO_2 were presented by Mehrotra and Svrcek (1988). It was reported that the data agreed qualitatively with trends exhibited by other Alberta bitumens. Experiments were performed at temperatures spanning a range from 15°C to 98°C , but the pressure range went up to 10 MPa with this bitumen. This gave a number of points in the liquid CO_2 region. The 15°C isotherms leveled out at a viscosity of approximately $0.7 \text{ Pa}\cdot\text{s}$ and a solubility of 12.3 wt% CO_2 as

the liquid CO₂ region was encountered at a pressure of about 5 MPa. Similarly, the 25°C isotherm leveled out at a viscosity of 0.36 Pa·s and a solubility of approximately 12.8 wt% CO₂ at about 6 MPa as well. The density of the gas saturated bitumen samples was once again found to be insensitive to pressure, but decreased with temperature. Densities ranged from approximately 1020 kg/m³ at 12°C to 970 kg/m³ at 98°C.

Yu *et al.* (1989) have extended the range of data available for Cold Lake bitumen to temperatures of 250°C and pressures of 16 MPa. Their data at 50°C and 100°C were found to be in agreement with the data of Mehrotra and Svrcek (1988).

2.2 Characterization of Bitumen for Data Correlation and Prediction

Correlation of the properties of bitumens has been successfully performed with EOS based characterization methods. With these methods, a hydrocarbon mixture is arbitrarily broken into a number of pseudocomponents whose properties are estimated through the use of these correlations. These pseudocomponents are then used to represent the mixture in the calculation of the mixture properties. The number of pseudocomponents used to represent a given mixture can vary depending on the accuracy required, the degree to which the mixture will be separated (such as in refinery simulation where a hydrocarbon mixture will be split into many different streams), or whether there are physical characteristics which can be used to represent different portions of the mixture (such as asphaltenes, distillable and undistillable maltenes, *etc.*).

A wealth of correlations are available to estimate the critical

properties of undefined hydrocarbon mixtures. Most of these were developed by correlating the critical properties of compounds that are similar in nature to the hydrocarbon mixture under consideration. These correlations are usually extrapolated beyond their limits, but many have been found that work well with conventional oils.

Fu *et al.* (1986) recommended the use of a modified Black and Twu (1983) correlation for the estimation of bitumen critical properties. Unfortunately, this approach requires the breakdown of the bitumen into specific structural groups (such as *n*-alkanes, *n*-alkyl aromatics, *etc.*). Since no data were available to break the cuts into these groups, the correlation was not considered.

Based on evidence of their success, six different correlations for the prediction of critical pressure and critical temperature were considered. These were: the Kesler and Lee (1976) correlations, Cavett's (1962) correlations, Sim and Daubert's (1980) correlation of Winn's (1957) nomograph, Whitson's (1980) correlations, Twu's (1984) correlations, and the correlations of Watanasiri *et al.* (1985). Three correlations were considered for the estimation of pseudocomponent acentric factor: Kesler and Lee's (1976), Edmister's (1958), and the correlation of Watanasiri *et al.* (1985).

2.2.1 The Kesler and Lee Correlations

Kesler and Lee (1976) presented a number of correlations to improve enthalpy predictions of petroleum fractions. The equations for critical

temperature, critical pressure and molar mass are as follows:

$$T_c = 341.7 + 811 SG + (0.4244 + 0.1174 SG) T_b + (0.4669 - 3.2623 SG) 10^5 / T_b \quad (2.1)$$

$$\begin{aligned} \ln P_c = & 8.3634 - 0.0566 / SG \\ & - (0.24244 + 2.2898 / SG + 0.11857 / SG^2) 10^{-3} T_b \\ & + (1.4685 + 3.648 / SG + 0.47227 / SG^2) 10^{-7} T_b^2 \\ & - (0.42019 + 1.6977 / SG^2) 10^{-10} T_b^3 \end{aligned} \quad (2.2)$$

$$\begin{aligned} MW = & -12272.6 + 9486.4 SG + (4.6523 - 3.3287 SG) T_b \\ & + (1 - 0.77084 SG - 0.02058 SG^2)(1.3437 - 720.79 / T_b) 10^7 / T_b \\ & + (1 - 0.80882 SG + 0.02226 SG^2)(1.8828 - 181.98 / T_b) 10^{12} / T_b^3 \end{aligned} \quad (2.3)$$

The temperatures T_c and T_b are in Rankine, the pressure P_c is in psia, MW is the molar mass, and SG is the specific gravity. Kesler and Lee stated that Equations (2.1) and (2.2) can be extrapolated beyond the 1 200°F limit of the data used. Equation (2.3) was regressed using molar masses up to 650 g/mol.

2.2.2 The Cavett Correlations

Cavett (1962) proposed correlations relating critical temperature and critical pressure to the API gravity of the fraction and its boiling point. The equations are as follows:

$$\begin{aligned} T_c = & a_0 + a_1 T_{bm} + a_2 T_{bm}^2 + a_3 (API) T_{bm} + a_4 T_{bm}^3 + \\ & a_5 (API) T_{bm}^2 + a_6 (API)^2 T_{bm}^2 \end{aligned} \quad (2.4)$$

$$\log P_c = b_0 + b_1 T_b + b_2 T_b^2 + b_3 (API) T_b + b_4 T_b^3 + b_5 (API) T_b^2 + b_6 (API)^2 T_b + b_7 (API)^2 T_b^2 \quad (2.5)$$

With these correlations, T_c is in Rankine, and P_c is in psia. T_b represents the molal average boiling point, and T_{bm} represents the mean average boiling point (the average of the molal average boiling point and the cubic average boiling point). Values for the constants a_0 through a_6 and b_0 through b_7 are provided in Appendix A.

2.2.3 The Sim and Daubert Correlations

Sim and Daubert's (1980) correlation was included as part of a rigorous analysis of available vapour-liquid equilibrium (VLE) calculation methods (Sim and Daubert, 1980). The correlations were used in a comparison of the Chao-Seader (1961), Grayson-Streed (1963), and Soave (1972) methods of VLE calculation.

$$T_c = \exp \left[4.2009 T_b^{0.08615} SG^{0.04614} \right] / 1.8 \quad (2.6)$$

$$P_c = 6.1483 (10^{12}) T_b^{-2.3177} SG^{2.4853} \quad (2.7)$$

$$MW = 5.805 (10^{12}) \left[T_b^{2.3776} / SG^{0.9371} \right] \quad (2.8)$$

In this set of equations, T_b and T_c are in Kelvin, and P_c is in Pa. No indication is given as to the range of applicability of these equations.

2.2.4 The Whitson Correlations

Whitson (1980) extended the correlations of Riazi and Daubert (1980)

to temperatures of 1 200°F. The following correlations were proposed:

$$T_b = 52.60 MW^{0.45533} SG^{0.4628} \quad (2.9)$$

$$T_c = 19.0623 T_b^{0.58848} SG^{0.3596} \quad (2.10)$$

$$P_c = 5.53028 (10^9) T_b^{-2.3125} SG^{2.3201} \quad (T_b < 850^\circ \text{F}) \quad (2.11)$$

$$P_c = 1.71589 (10^{14}) T_b^{-3.86618} SG^{4.2448} \quad (T_b > 850^\circ \text{F}) \quad (2.12)$$

Here, T_b and T_c are in Kelvin, and P_c is in kPa.

2.2.5 The Twu Correlations

Twu (1984) presented correlations for critical temperature, critical pressure, molecular weight, and critical volume given only normal boiling point and specific gravity as input data. The systems investigated had normal boiling points that ranged up to 1 778°R (998 K) and specific gravities up to 1.436. The correlations are given as perturbations from a reference system (the normal alkanes). Correlations for the reference system considered alkanes of carbon numbers up to 100 (the superscript "°" refers to the normal alkanes):

$$T_c^\circ = T_b \left[0.533272 + 0.191017(10^{-3})T_b + 0.779681(10^{-7})T_b^2 - 0.284376(10^{-10})T_b^3 + 0.959468(10^{28})/T_b^{13} \right]^{-1} \quad (2.13)$$

$$SG^\circ = 0.843593 - 0.128624\alpha - 3.36158\alpha^3 - 13749\alpha^{12} \quad (2.14)$$

$$T_b = \exp(5.71419 + 2.71579\theta - 0.286590\theta^2 - 39.8554/\theta - 0.122488/\theta^2) - 24.7522\theta + 35.3155\theta^2 \quad (2.15)$$

$$v_c^\circ = \left[1 - (0.419869 - 0.505839\alpha - 1.56436\alpha^3 - 9481\alpha^{14}) \right]^{-8} \quad (2.16)$$

$$P_c^\circ = \left(3.83354 + 1.19629\alpha^{0.5} + 34.8888\alpha + 36.1952\alpha^2 + 104.193\alpha^4 \right)^2 \quad (2.17)$$

where

$$\alpha = 1 - T_b / T_c^\circ \quad (2.18)$$

and

$$\theta = \ln MW^\circ \quad (2.19)$$

T_c and T_b are in Rankine, P_c is in psia, and SG is taken at 60°F . The perturbation equations are all based on a Taylor expansion about the n -alkane properties:

$$T_c = T_c^\circ \left[(1 + 2f_T) / (1 - 2f_T) \right]^2 \quad (2.20)$$

$$f_T = \Delta SG_T \left[-0.362456 / T_b^{0.5} + (0.0398285 - 0.948125 / T_b^{0.5}) \Delta SG_T \right] \quad (2.21)$$

$$\Delta SG_T = \exp \left[4(SG^\circ - SG) \right] - 1 \quad (2.22)$$

$$v_c = v_c^\circ \left[(1 + 2f_v) / (1 - 2f_v) \right]^2 \quad (2.23)$$

$$f_v = \Delta SG_v \left[0.466590 / T_b^{0.5} + (-0.182421 + 3.01721 / T_b^{0.5}) \Delta SG_v \right] \quad (2.24)$$

$$\Delta SG_v = \exp \left[4(SG^{\circ 2} - SG^2) \right] - 1 \quad (2.25)$$

$$P_c = P_c^\circ (T_c / T_c^\circ) (v_c^\circ / v_c) \left[(1 + 2f_p) / (1 - 2f_p) \right]^2 \quad (2.26)$$

$$f_p = \Delta SG_p \left[(2.53262 - 46.1955 / T_b^{0.5} - 0.00127885 T_b) \right. \\ \left. + (-11.4277 + 252.140 / T_b^{0.5} + 0.00230535 T_b) \Delta SG_p \right] \quad (2.27)$$

$$\Delta SG_p = \exp \left[0.5(SG^\circ - SG) \right] - 1 \quad (2.28)$$

$$\ln MW = \ln MW^\circ \left[(1 + 2f_M) / (1 - 2f_M) \right]^2 \quad (2.29)$$

$$f_M = \Delta SG_M \left[|x| + (-0.0175691 + 0.193168 / T_b^{0.5}) \Delta SG_M \right] \quad (2.30)$$

$$|x| = |0.0175691 + 0.193168 / T_b^{0.5}| \quad (2.31)$$

$$\Delta SG_M = \exp \left[5(SG^\circ - SG) \right] - 1 \quad (2.32)$$

2.2.6 The Watanasiri et al. Correlations

Watanasiri *et al.* (1985) proposed correlations for T_c , P_c , v_c , ω , and dipole moment based on 115 compounds, most of which were "model coal compounds." These included benzenic, naphthalenic, and polycyclic compounds. The highest molar mass used in the correlation was 283 g/mol, and the authors made no claim about the validity of extrapolated values.

$$\begin{aligned} \ln T_c = & -0.00093906 T_b + 0.030950 \ln(MW) + 1.11067 \ln(T_b) \\ & + MW (0.078154 SG^{0.5} - 0.061061 SG^{1/3} - 0.016943 SG) \end{aligned} \quad (2.33)$$

$$\begin{aligned} \ln v_c = & 80.4479 - 129.8083 SG + 63.1750 SG^2 - 13.1750 SG^3 \\ & + 1.10108 \ln(MW) + 42.1958 \ln(SG) \end{aligned} \quad (2.34)$$

$$\begin{aligned} \ln P_c = & 3.95431 + 0.70682(T_c / v_c)^{0.8} - 4.8400 MW / T_c \\ & - 0.15919 T_b / MW \end{aligned} \quad (2.35)$$

Critical temperature and the normal boiling point are in Kelvin. Critical pressure is in atm and critical volume is in cm^3/mol . The values for T_c and v_c in Equation (2.35) are obtained from Equations (2.33) and (2.34) respectively.

2.2.7 Acentric Factor Correlations

Correlations of acentric factors are not as prevalent in the literature as correlations of critical properties. Three correlations were considered in this work for modeling the bitumen fractions.

Kesler and Lee (1976) presented two correlations based on data for paraffinic, aromatic, and naphthenic compounds. The first correlation is to be used for reduced normal boiling points (T_{br}) above 0.8:

$$\begin{aligned} \omega = & -7.904 + 0.1352 K - 0.007465 K^2 + 8.359 T_{br} \\ & + (1.408 - 0.01063 K) / T_{br} \end{aligned} \quad (2.36)$$

$(T_{br} > 0.8)$

The second equation is to be used for T_{br} below 0.8:

$$\begin{aligned} \omega = & \left[\ln P_{br}^S - 5.92714 + 6.09648 / T_{br} + 1.28862 \ln T_{br} \right. \\ & \left. - 0.169347 T_{br}^6 \right] \cdot \left[15.2518 - 15.6875 / T_{br} \right. \\ & \left. - 13.4721 \ln T_{br} + 0.43577 T_{br}^6 \right] \end{aligned} \quad (2.37)$$

$(T_{br} < 0.8)$

In these equations, T_{br} represents the reduced normal boiling point, K is the Watson characterization factor (defined as $T_b^{1/3}/SG$), and P_{br}^S is the reduced vapour pressure at T_b .

A correlation that is commonly referred to (Pedersen *et al.*, 1983; Sim and Daubert, 1980; Whitson, 1980) is Edmister's (1958) acentric factor correlation:

$$\omega = (3 / 7) \left[\frac{\log(P_c) \cdot T_r}{T_r - 1} \right] - 1 \quad (2.38)$$

Here, P_c is in atm.

Watanasiri *et al.* (1985) also presented a correlation for the acentric factor of the compounds they studied.

$$\begin{aligned} \omega = & \left[0.922170(10^{-3}) T_b + 0.507288 T_b / MW + 382.904 / MW \right. \\ & + 0.2420(10^{-5}) (T_b / SG)^2 - 0.2165(10^{-4}) T_b \cdot MW \\ & + 0.1261(10^{-2}) SG \cdot MW + 0.1265(10^{-4}) MW^2 \\ & + 0.2016(10^{-4}) SG \cdot MW^2 - 80.6495 T_b^{1/3} / MW \\ & \left. - 0.3780(10^{-2}) T_b^{2/3} / SG^2 \right] \cdot \left[T_b / MW \right] \end{aligned} \quad (2.39)$$

As with their other correlations, T_b is in Kelvin.

2.3 Equation of State Considerations

The use of equation of state (EOS) based models in the calculation of hydrocarbon properties has become accepted throughout the petroleum industry. The ease of calculation and reliability of results has made the use of more complex models almost obsolete. Of the three equations-of-state considered here, the Soave-Redlich-Kwong EOS and the Peng-Robinson EOS are two parameter equations, while the Patel-Teja EOS is a three parameter equation.

2.3.1 The Soave-Redlich-Kwong Equation of State

The Soave-Redlich-Kwong (S-R-K) equation (1972) was the first cubic EOS to gain acceptance in industry. Soave's modification to the Redlich-Kwong equation was in the temperature dependence of the attractive term. The equation is able to match hydrocarbon vapour-liquid equilibria

very well. The S-R-K equation is as follows:

$$P = \frac{RT}{v - b} - \frac{a(T)}{v(v + b)} \quad (2.40)$$

Application of the van der Waals conditions at the critical point yields the following equations:

$$a_c = 0.42747 \frac{R^2 T_c^2}{P_c} \quad (2.41)$$

$$b_c = 0.08664 \frac{R T_c}{P_c} \quad (2.42)$$

$$Z_c = 0.3333 \quad (2.43)$$

where

$$Z_c = \frac{P_c v_c}{R T_c} \quad (2.44)$$

At temperatures different from the critical, a_c is multiplied by a temperature dependency term:

$$a = a_c \cdot \alpha(T) \quad (2.45)$$

The value for b is simply b_c , as there is no temperature dependence in this term.

The form of $\alpha(T)$ considers the reduced temperature of a compound and its acentric factor:

$$\alpha^{0.5} = 1 + \kappa(1 - T_r^{0.5}) \quad (2.46)$$

$$\kappa = 0.480 + 1.574\omega - 0.176\omega^2 \quad (2.47)$$

For mixtures of compounds, a is summed geometrically and b is summed

arithmetically:

$$a = \sum_i \sum_j x_i x_j a_{ij} \quad (2.48)$$

$$a_{ij} = (a_i a_j)^{0.5} (1 - k_{ij}) \quad (2.49)$$

$$b = \sum_i \sum_j x_i x_j \frac{b_i + b_j}{2} \quad (2.50)$$

The constant k_{ij} in Equation (2.48) is an interaction parameter for the species i and j which is determined empirically. By definition, $k_{ij} = k_{ji}$ and $k_{ii} = k_{jj} = 0$.

2.3.2 The Peng-Robinson Equation of State

Peng and Robinson (1976) made certain modifications to the S-R-K equation, and the resulting equation has come to be quite popular. The modifications made by Peng and Robinson came about in an effort to improve liquid density predictions without sacrificing the accurate vapour pressures and equilibrium ratios generated by the S-R-K equation. A change to the attractive term in Equation (2.40) was the major modification introduced in the Peng-Robinson (P-R) equation:

$$P = \frac{RT}{v - b} - \frac{a(T)}{v(v + b) + b(v - b)} \quad (2.51)$$

The constants in Equations (2.41), (2.42), (2.43), and (2.47) were changed as well:

$$a_c = 0.45724 \frac{R^2 T_c^2}{P_c} \quad (2.52)$$

$$b_c = 0.07780 \frac{R T_c}{P_c} \quad (2.53)$$

$$Z_c = 0.3074 \quad (2.54)$$

$$\kappa = 0.37464 + 1.54226\omega - 0.26992\omega^2 \quad (2.55)$$

All other term are defined the same as those in the S-R-K EOS.

2.3.3 The Patel-Teja Equation of State

Although the aim of the Peng-Robinson equation was to improve liquid density predictions, the fact that the critical compressibility is still a set value for all compounds hinders its ability to do this. Patel and Teja (1982) addressed this issue by making the critical compressibility factor (Z_c) variable. In fact, the optimum value for Z_c in the equation is not necessarily the compound's actual critical compressibility, so the value is referred to as ζ_c . The resulting equation was the Patel-Teja (P-T) equation of state.

The variable critical compressibility factor arises from the introduction of a third parameter in the equation of state.

$$P = \frac{RT}{v - b} - \frac{a(T)}{v(v + b) + c(v - b)} \quad (2.56)$$

Applying the van der Waals constraints at the critical point yields:

$$a = \Omega_a \frac{R^2 T_c^2}{P_c} \quad (2.57)$$

$$b = \Omega_b \frac{R T_c}{P_c} \quad (2.58)$$

$$c = \Omega_c \frac{R T_c}{P_c} \quad (2.59)$$

where

$$\Omega_c = 1 - 3\zeta_c \quad (2.60)$$

$$\Omega_a = 3\zeta_c^2 + 3(1 - 2\zeta_c)\Omega_b + \Omega_b^2 + 1 - 3\zeta_c \quad (2.61)$$

and Ω_b is the smallest positive root of:

$$\Omega_b^3 + (2 - 3\zeta_c)\Omega_b^2 + 3\zeta_c^2\Omega_b - \zeta_c^3 = 0 \quad (2.62)$$

Temperature dependence of the a -term is the same as for the S-R-K and P-R equations (Equation (2.46)) with κ given by:

$$\kappa = 0.452413 + 1.30982\omega - 0.295937\omega^2 \quad (2.63)$$

Patel and Teja also correlated values of ζ_c :

$$\zeta_c = 0.329032 - 0.076799\omega + 0.0211947\omega^2 \quad (2.64)$$

The mixing rules for a and b are as for the S-R-K and P-R equations, with c being mixed arithmetically.

CHAPTER 3

DESCRIPTION OF BITUMEN FRACTIONS

The bitumen samples used in this project were supplied by Esso Resources Canada Ltd., Calgary. A total of six samples were provided: five samples fractionated from the bitumen, and a sample of the whole bitumen itself. The fractions (or "cuts") were obtained by vacuum distillation, providing a good variation in properties between the samples. The boiling point (bp) ranges of Cuts 1 and 2 (as supplied by Esso) were as follows: $bp < 343^{\circ}\text{C}$ for Cut 1 and $343^{\circ}\text{C} < bp < 510^{\circ}\text{C}$ for Cut 2. These cuts represented 10.3 mass % and 28.3 mass % of the whole bitumen respectively. The three heavier cuts (Cuts 3 through 5) had initial boiling points greater than 510°C . Cut 3 represented 16.8 mass % of the whole bitumen, Cut 4 represented 6.5 mass %, and Cut 5 represented 38.1 mass %.

The lighter cuts (Cuts 1 and 2) were clear liquids with relatively low viscosities. Cuts 3 and 4 resembled the whole bitumen in terms of colour and consistency. Cut 5 was a brittle glass-like solid at room temperature that softened at a temperature of approximately 100°C .

3.1 Physical and Chemical Analyses of Bitumen Fractions

A number of initial tests were run on the samples to gain information on compositional differences in the bitumen. These tests included molar mass analysis, asphaltenes content measurement, SIMDIST analysis, elemental composition analyses, and density measurement. The results of these analyses are given in Table 3.1.

3.1.1 Molar Mass Measurements

The molar masses of all six samples were obtained by the freezing point method by CORE Laboratories. Values ranged from 209 g/mol for Cut 1 to 2500 g/mol for Cut 5. The molar mass of the whole bitumen (577 g/mol) is somewhat higher than the value of 533 g/mol reported by Fu *et al.* (1986). Since Cut 5 was a solid at room-temperature, its molar mass could not be measured directly by this technique. Rather, a sample was dissolved in benzene and the analysis was performed on the solution. The resulting molar mass was then used to obtain the molar mass of Cut 5.

It should be noted that if the molar mass of the whole bitumen is determined from a mole balance of the cuts, a value of only 529 g/mol results. This inconsistency appears to be indicative of the limitations of the freezing point method when applied to bitumen.

3.1.2 Asphaltenes Content Measurements

The asphaltenes content of a bitumen is defined as the portion of the bitumen which is insoluble in *n*-pentane. Table 3.1 gives the asphaltenes content of the six samples on a mass basis. Note that Cuts 1 through 4 have virtually no asphaltenes content, while nearly one half of Cut 5 is asphaltenes.

TABLE 3.1

Measured Data and Properties of Cold Lake Bitumen and Its Fractions

Sample	Mass fraction of whole bitumen	Molar mass (g/mol)	Density (g/cm ³)	Asphaltenes (mass %)	Maltenes (mass %)		Elemental analyses (mass %)				
					Distillable bp < 550°C	Undistillable bp > 550°C	C	H	N	S	O*
whole bitumen	1.000	577	0.995	16.7	47.8	35.5	82.09	10.87	0.47	4.35	2.22
Cut 1	0.103	209	0.879	0.0	100.0	0.0	83.17	13.06	0.17	1.75	1.85
Cut 2	0.283	310	0.941	0.0	100.0	0.0	83.86	11.87	0.15	3.09	1.03
Cut 3	0.168	667	0.990	2.2	67.1	30.7	83.05	11.18	0.40	4.22	1.15
Cut 4	0.065	800	0.999	1.7	20.3	78.0	83.58	11.18	0.52	4.38	0.34
Cut 5	0.381	2500	1.072	49.5	0.0	50.5	80.39	9.48	0.94	n.a.	--

* oxygen content obtained by difference.

3.1.3 SIMDIST Analyses

A SIMDIST analysis is a chromatographic simulation of an atmospheric pressure batch distillation that generates an analog to a true boiling point curve. The effective range of the distillation extends to a maximum temperature of approximately 550°C. Generally, this temperature is used as a marker to differentiate between the "distillable" and "undistillable" maltenes fractions in a bitumen.

SIMDIST curves for the lightest four cuts and the whole bitumen are given in Figure 3.1. A curve for Cut 5 is not shown, since its initial boiling point was above 550°C. Data for this figure are provided in Appendix B. Table 3.1 shows the distillable and undistillable maltene contents based on these data and the asphaltenes content data. The boiling point ranges for Cut 1 and Cut 2 are in general agreement with the data provided by Esso.

3.1.4 Elemental Composition Analyses

Two elemental composition analyses were performed on each sample: a C/H/N analysis and a sulphur analysis, with the oxygen content obtained by difference. Results are given in Table 3.1. Because Cut 5 is a solid at room temperature, its sulphur content could not be measured. It is expected that it would be quite high. Note that the hydrogen content of the cuts decreases with molar mass, indicating a greater degree of aromaticity in the heavier fractions.

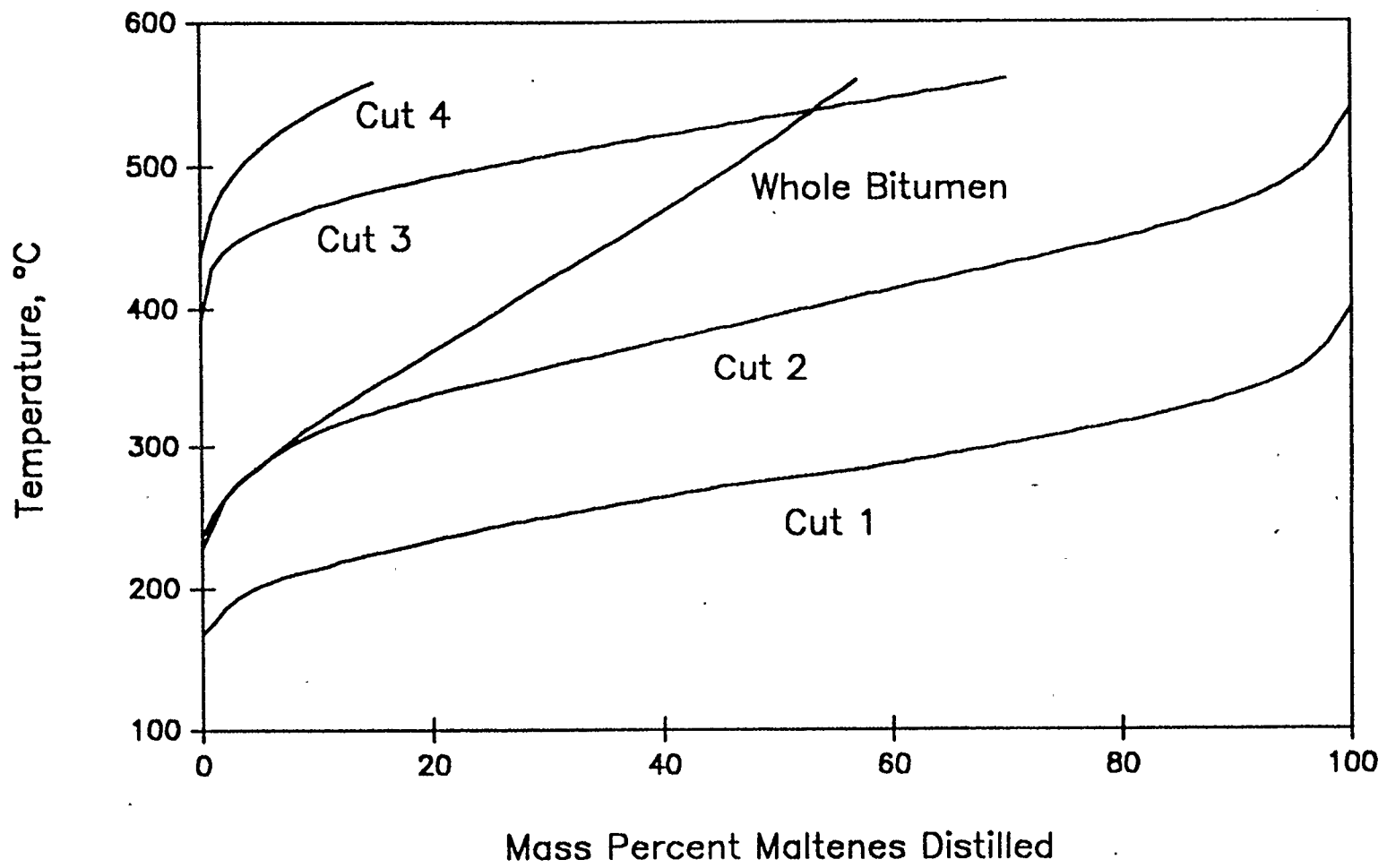


Figure 3.1: Sample SIMDIST Distillations

3.1.5 Room Temperature Density Measurements

The densities of all six samples at room temperature were measured with pycnometers. Results are given in Table 3.1. Values ranged from a low of 879 kg/m³ for Cut 1 to 1 072 kg/m³ for Cut 5. The density of the whole bitumen was measured as 995 kg/m³.

If the specific volumes of the fraction may be considered additive, the following equation may be used to estimate the density of the whole bitumen from the densities of the cuts:

$$\bar{\rho} = \left(\sum x_i \rho_i \right)^{-1} \quad (3.1)$$

where x_i is the mass fraction of cut i . The estimated bitumen density obtained from this equation from the density data of the cuts is 992 kg/m³, which is in good agreement with the measured value of 995 kg/m³.

3.2 Viscosity Measurements and Correlation

The effect of temperature on the apparent viscosities of each of the samples was also examined. The dynamic viscosities of Cuts 2 through 5 were obtained on an RV8 viscometer from Viscometers (UK) Ltd. Data were taken over a temperature range of at least 60°C, and at least two different shear rates were used at most temperatures. Because of the low viscosity of Cut 1, its kinematic viscosity was obtained with a Cannon-Fenske viscometer. To obtain the dynamic viscosity of Cut 1, the variation of its density with temperature was measured. The data given in

Table 3.2 and are correlated well with the following equation:

$$\rho(T) = 0.8908 - 0.513(10^{-3}) \cdot T \quad (3.2)$$

where T is the temperature in Celsius and ρ is in kg/m^3 .

The viscosity data for the whole bitumen are plotted in Figure 3.2, along with the data reported by Mehrotra and Svrcek (1988a). This sample of Cold Lake bitumen is more viscous than that of Mehrotra and Svrcek, which was taken from the Alberta Research Council Sample Bank. This is consistent with the lower molar mass of 533 g/mol which they assumed was representative of their sample.

3.2.1 A Correlation for Bitumen Fraction Viscosity

Data for each of the cuts and the whole bitumen summarized in Table 3.3 and are plotted in Figure 3.3. The viscosities of Cuts 1 and 2 are very low, less than 70 $\text{mPa}\cdot\text{s}$ at 30°C. Cut 5 has a very high viscosity, about 800 000 $\text{mPa}\cdot\text{s}$ at 120°C. The viscosities of Cut 3 and the whole bitumen are remarkably close, although plots of viscosity versus temperature show slightly different curvatures.

The viscosity-temperature data were correlated with the following equation (Mehrotra *et al.*, 1989):

$$\log \log (\mu + 0.7) = b_1 + b_2 \log (T) \quad (3.1)$$

The temperature is in Kelvin, and the viscosity is in $\text{mPa}\cdot\text{s}$. This correlation was found to work well with several bitumens (Khan *et al.*, 1984, Mehrotra and Svrcek, 1984, 1987, Svrcek and Mehrotra, 1988). Values of b_1 and b_2 for each sample, regressed from the data, are given in Table 3.4. Predictions from this correlation are plotted as the solid lines in Figure 3.3.

TABLE 3.2

Effect of Temperature on the Density of Cut 1

Temperature (°C)	Density (g/mL)
25.0	0.879
45.0	0.867
60.0	0.861

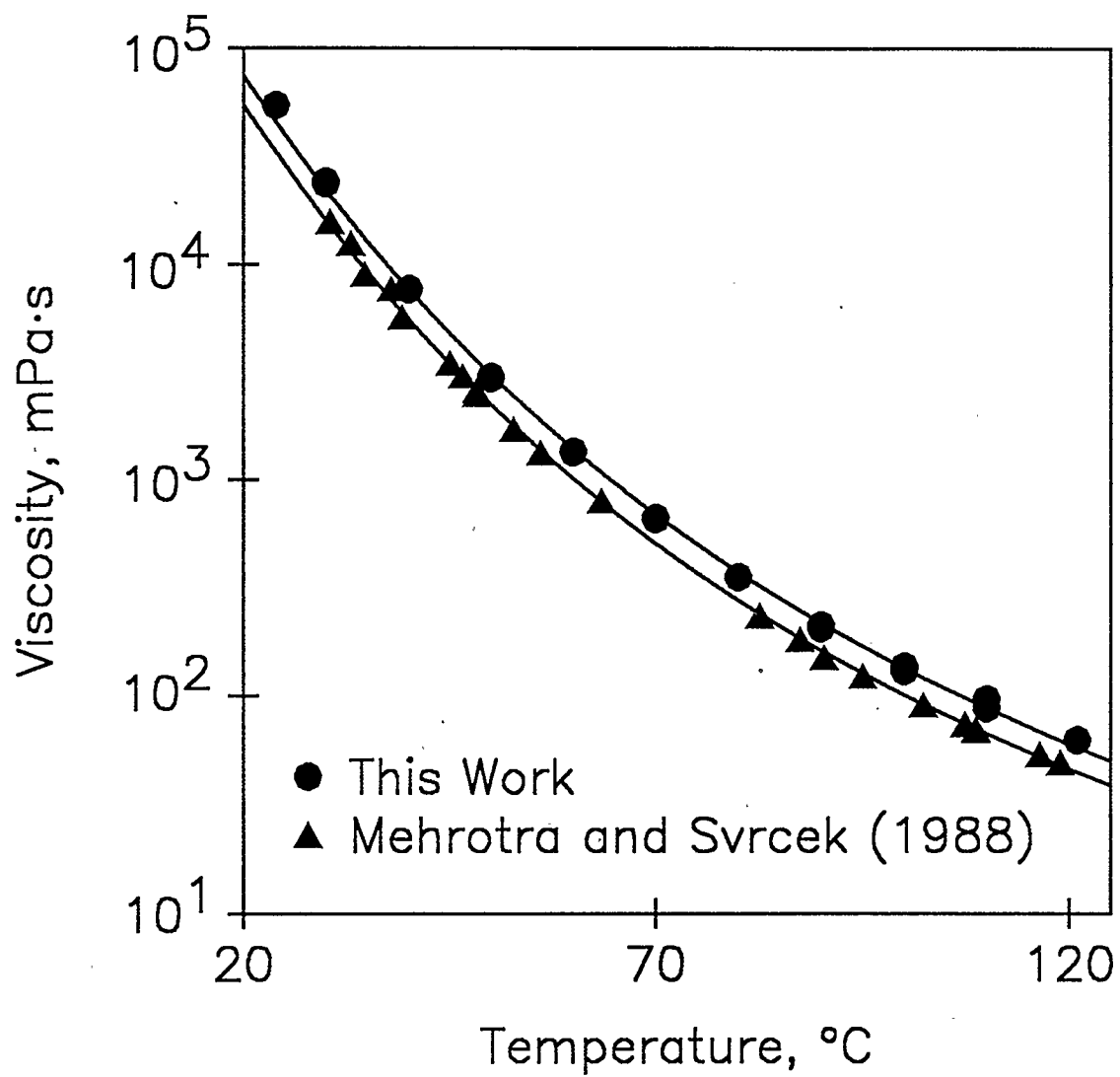


Figure 3.2: Comparison of Viscosities of Cold Lake Bitumen Samples

TABLE 3.3
Viscosity-Temperature Data for Cold Lake Bitumen and Its Fractions

Whole bitumen		Cut 1		Cut 2		Cut 3		Cut 4		Cut 5	
T (°C)	μ (mPa·s)	T (°C)	μ (mPa·s)	T (°C)	μ (mPa·s)	T (°C)	μ (mPa·s)	T (°C)	μ (mPa·s)	T (°C)	μ (mPa·s)
23.9	54500	22.4	5.04	30.1	74.2	26.1	43300	30.2	430000	120.0	835000
29.9	24100	22.4	5.03	30.1	74.4	30.0	26200	39.9	95600	120.0	822000
29.9	23600	22.4	5.02	30.1	76.3	30.0	25700	39.9	94100	130.1	265000
40.0	7640	27.0	4.29	40.2	41.3	40.3	7530	39.9	93400	130.1	274000
40.0	7690	27.0	4.28	40.2	42.2	40.4	7100	50.2	23900	140.1	94500
50.0	2970	30.0	4.01	40.2	43.2	40.3	7150	50.2	23700	140.1	97700
50.0	3020	30.0	3.99	45.0	32.3	50.4	2480	50.2	23500	150.1	39400
60.0	1340	30.0	3.98	45.0	33.1	50.4	2520	60.4	7970	150.1	39700
60.0	1350	40.1	3.07	45.0	34.2	60.6	1090	60.4	7740	160.1	19000
70.0	655	40.1	3.07	50.0	25.4	60.6	1050	60.4	7640	160.1	19300
70.0	664	40.1	3.06	50.0	25.9	60.6	1020	70.0	3120	170.0	9500
80.0	354	50.0	2.46	54.9	20.5	70.4	516	70.0	3000	170.0	9600
80.0	355	50.0	2.46	54.9	20.6	70.4	490	70.0	2940	180.0	5300
90.0	205	50.0	2.44	59.9	16.8	70.4	474	80.3	1390	180.0	5450
90.0	211	60.0	2.01	59.9	17.0	70.3	470	80.3	1320	190.0	3050
100.1	130	60.0	2.00	65.0	13.9	79.9	271	80.3	1300	190.0	3150
100.1	136	60.0	1.99	65.0	14.1	79.9	256	90.5	650	199.9	1900
110.0	87.5	69.9	1.72	70.0	11.7	79.8	253	90.5	631	210.0	1300
110.0	96.2	69.9	1.69	74.9	10.1	89.9	144	100.4	344		
121.0	62.5	69.9	1.68	80.0	8.48	89.9	141	105.7	262		
		80.0	1.44	84.9	7.36	100.0	87.5				
		80.0	1.43	89.9	6.40						
		80.0	1.42								
		89.9	1.23								
		89.9	1.22								
		89.9	1.21								
		93.6	1.16								
		93.6	1.15								
		93.6	1.15								

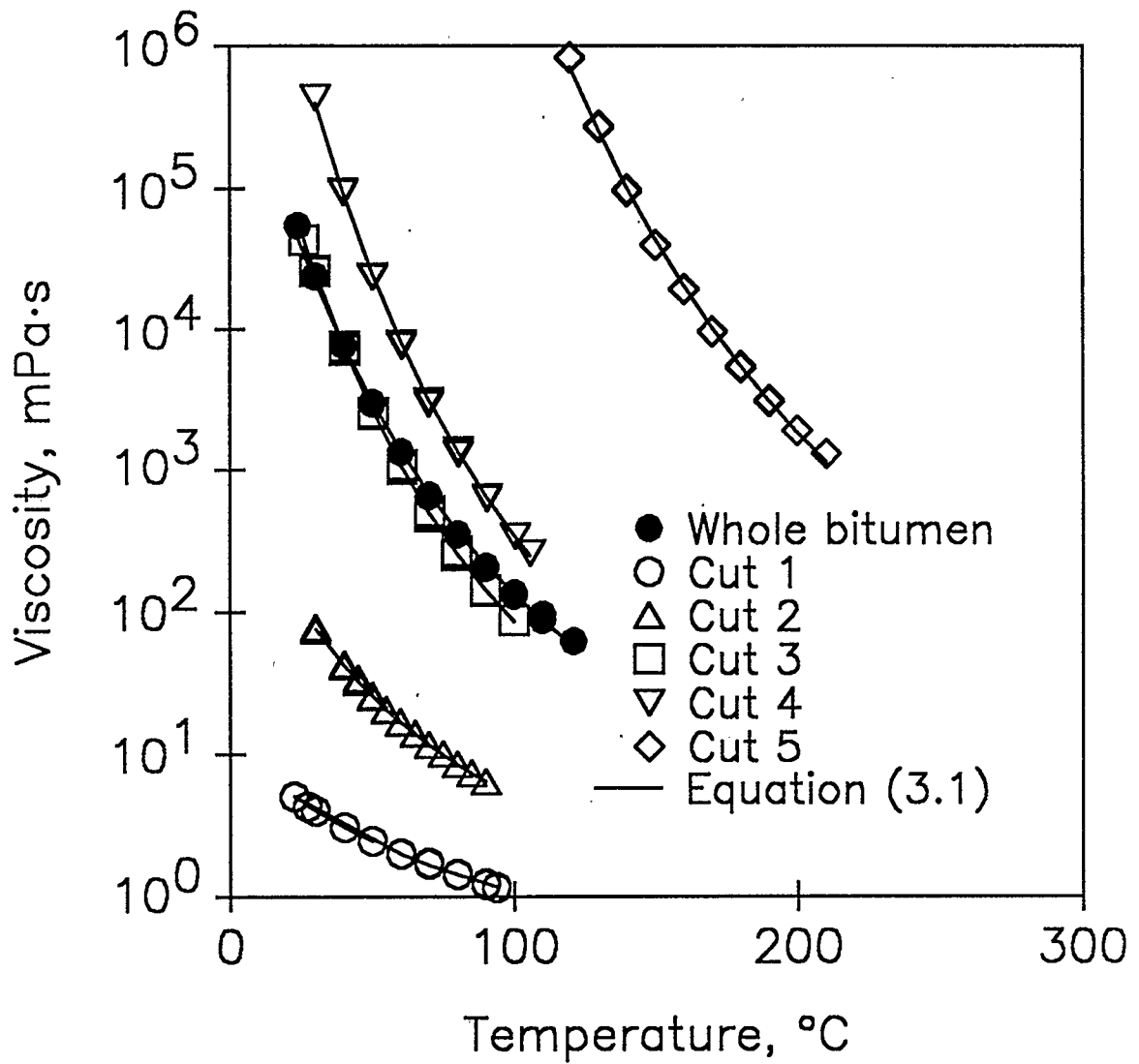


Figure 3.3: Viscosities of Bitumen Fractions Correlated with Equation 3.1

TABLE 3.4

Correlation of Gas-Free Viscosities of Samples with Equation 3.1

Sample	b_1	b_2	AAD*
whole bitumen	9.1451	-3.4281	4.3%
Cut 1	11.6244	-4.7535	0.9%
Cut 2	11.2120	-4.4068	1.2%
Cut 3	10.2535	-3.9527	2.3%
Cut 4	10.1941	-3.8061	3.1%
Cut 5	8.9592	-3.1573	6.6%

$$*AAD = (1/N) \sum_{i=1}^N |\mu_{\text{exp}} - \mu_{\text{corr}}| / \mu_{\text{exp}}$$

A relationship between values of b_1 and b_2 for each cut can be seen in Figure 3.4, which plots values of b_2 against values of b_1 for the five cuts. All points lie close to a straight line, suggesting some sort of correlation between the parameters. Also shown in the figure are values for other Alberta bitumens (Svrcek and Mehrotra, 1988) and for the whole Cold Lake bitumen used in this work. These points lie below and to the left of the line connecting the cut points. This behaviour has been discussed in more detail elsewhere (Eastick and Mehrotra, 1989).

3.2.2 Prediction of the Whole Bitumen Viscosity

In an effort to predict the viscosity of the whole bitumen from the viscosity behaviour of the cuts, mixing rules of the following form were investigated:

$$f(\mu_m) = \sum_{i=1}^N x_i f(\mu_i) \quad (3.2)$$

where $f(\mu)$ is some function of the viscosity, and x_i is either mole fraction, mass fraction, or volume fraction.

When $f(\mu)$ is defined as $\log(\mu + 0.7)$, Equation 3.2 may be rewritten as:

$$\log(\mu_m + 0.7) = \sum_{i=1}^N x_i \log(\mu_i + 0.7) \quad (3.3)$$

Predictions of the whole bitumen viscosity with this equation are given in Figure 3.5 for cases when x_i is defined as mole fraction, mass fraction, and volume fraction. Both the mass fraction and volume fraction definition tend to over-predict the whole bitumen viscosity data by one to two orders of magnitude, while the mole fraction definition under-predicts the data by one order of magnitude.

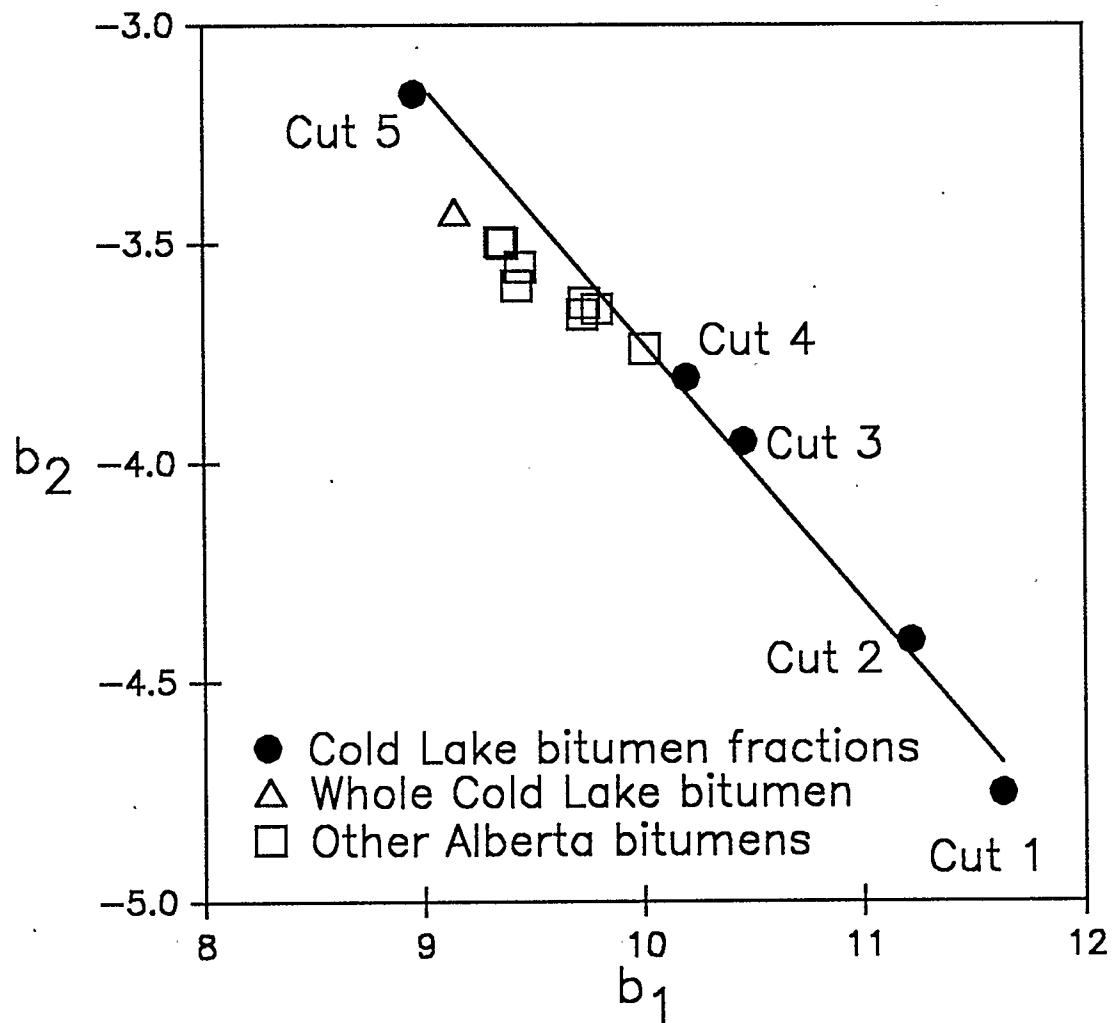


Figure 3.4: Relationship Between b_1 and b_2 for Bitumen Fractions and Alberta Bitumens

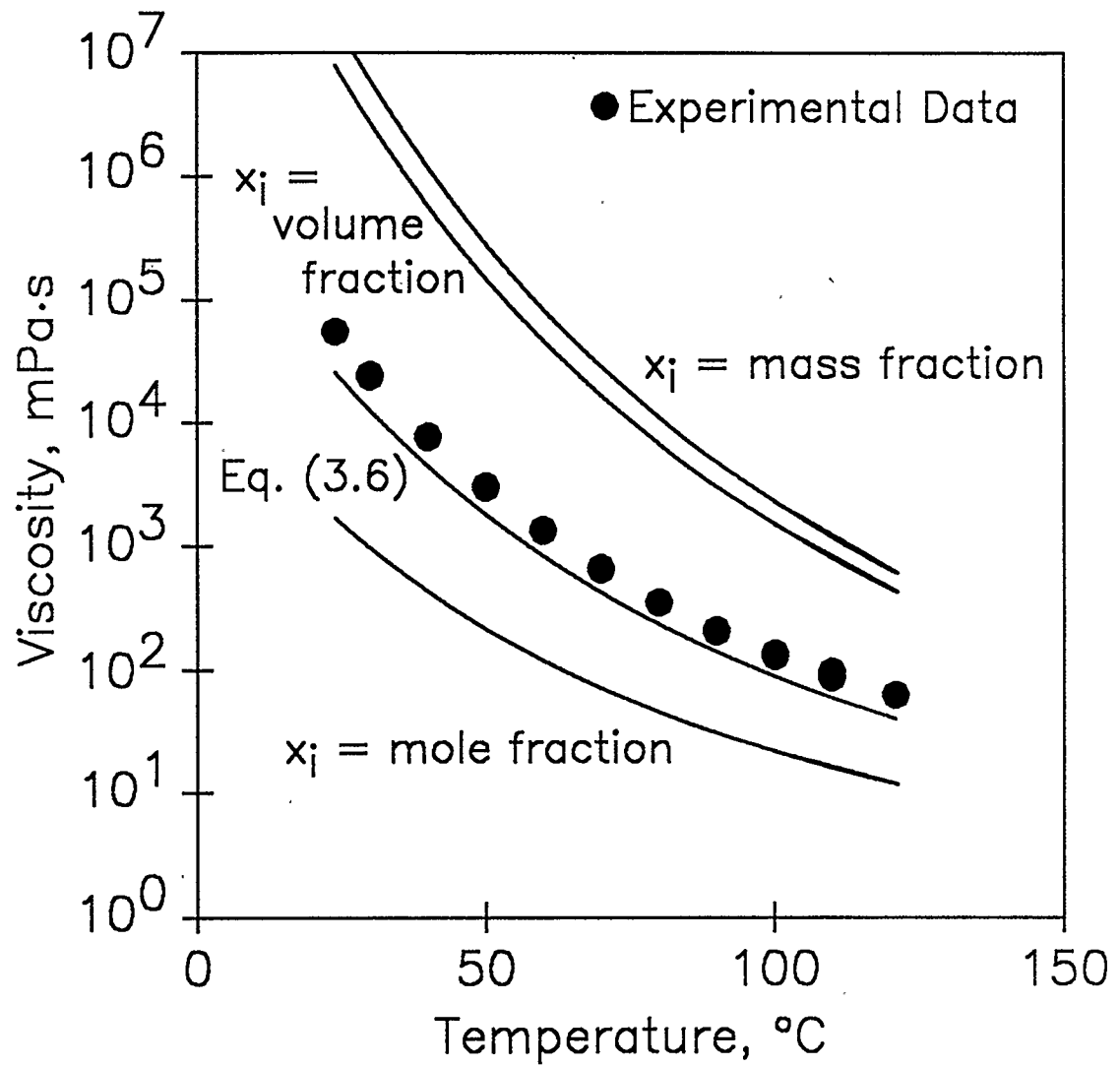


Figure 3.5: Cold Lake Bitumen Viscosity Predicted with Equation 3.2

A number of modifications to the definition of $f(\mu)$ were investigated in an effort to improve the whole bitumen viscosity predictions. A form that gave considerable improvement is:

$$f(\mu) = (MW)^{0.5} \log (\mu + 0.7) \quad (3.4)$$

where MW represents the molar mass. Equation 3.3 may be rewritten as:

$$(\overline{MW})^{0.5} \log (\mu_m + 0.7) = \sum_{i=1}^N x_i (MW_i)^{0.5} \log (\mu_i + 0.7) \quad (3.5)$$

Here, \overline{MW} represents the molar mass of the mixture. When x_i is taken to be the mole fraction of the cut in the whole bitumen, predictions of the whole bitumen viscosity are now well within an order of magnitude of the data, and the average absolute deviation obtained is 38%. Predictions are shown in Figure 3.5.

It is interesting to note that if Equation 3.5 is rewritten as follows:

$$\log (\mu_m + 0.7) = \sum_{i=1}^N \left[x_i (MW_i / \overline{MW})^{0.5} \right] \log (\mu_i + 0.7) \quad (3.6)$$

the term $\left[x_i (MW_i / \overline{MW})^{0.5} \right]$ is actually the geometric mean of the mass and mole fractions of Cut i .

A relationship between the molar mass of the cuts and their parameters in Equation 3.1 is shown in Figure 3.6. Generalization of b_1 and b_2 in terms of molar mass has been investigated by Eastick and Mehrotra (1989).

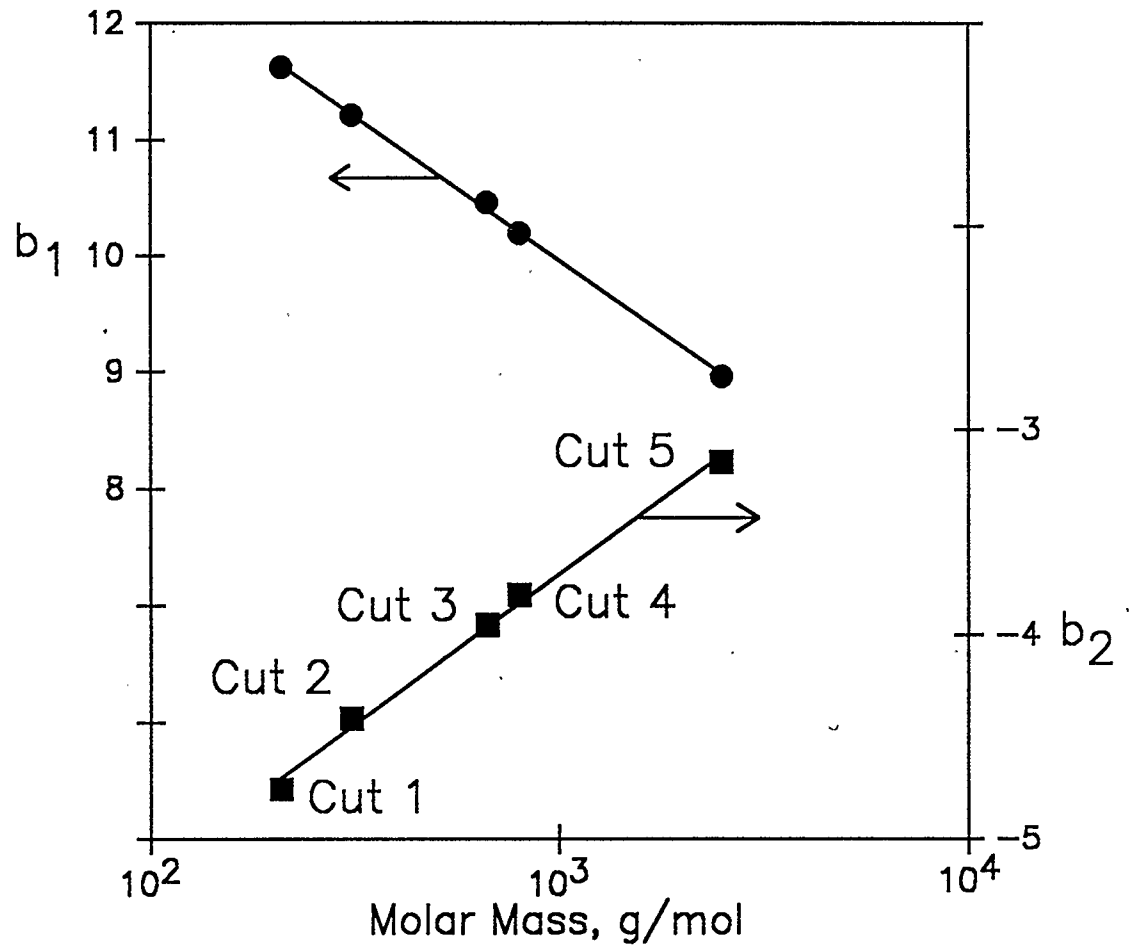


Figure 3.6: Relationship Between b_1 and b_2 and Bitumen Fraction Molar Mass

CHAPTER 4

EXPERIMENTAL

As was shown in Chapter 3, the viscosities of the samples used in this project varied by many orders of magnitude at a given temperature. Two of the five cuts — Cuts 3, and 4 — could be considered to have viscosities on the same scale as the whole bitumen. The viscosity of Cut 5 is four orders of magnitude greater than that of the whole bitumen at 120°C, and the viscosities of the two lighter cuts — Cuts 1 and 2 — are four to five orders of magnitude less than that of the whole bitumen.

Because of these extreme variations in viscosity, two different apparatuses were required to perform experiments on all fractions. An apparatus, called the High Viscosity Apparatus, used previously to measure the properties of other gas-saturated bitumens, was adequate for measuring the properties of the whole bitumen as well as Cuts 3, 4, and 5. It could not, however, be used to test Cuts 1 or 2, since their very low viscosities would have been out of the range of the viscometer in the apparatus. Another apparatus, called the Low Viscosity Apparatus, was designed and constructed for measuring the properties of the two lighter cuts.

4.1 High Viscosity Apparatus

Experiments on Cuts 3, 4, and 5, as well as on the whole bitumen, were performed on the High Viscosity Apparatus (HVA). The apparatus has been described previously (Jacobs *et al.*, 1980, Svrcek and Mehrotra, 1982, Mehrotra and Svrcek, 1988a). The apparatus is shown schematically in Figure 4.1.

- 1 MIXING CELL
- 2 SAMPLE CELL
- 3 CONTRAVES DC44 VISCOMETER
- 4 LUWA GEAR PUMP
- 5 MOTOR
- 6 1-INCH VALVE
- 7 GAS SUPPLY
- 8 HEATED AIR BATH

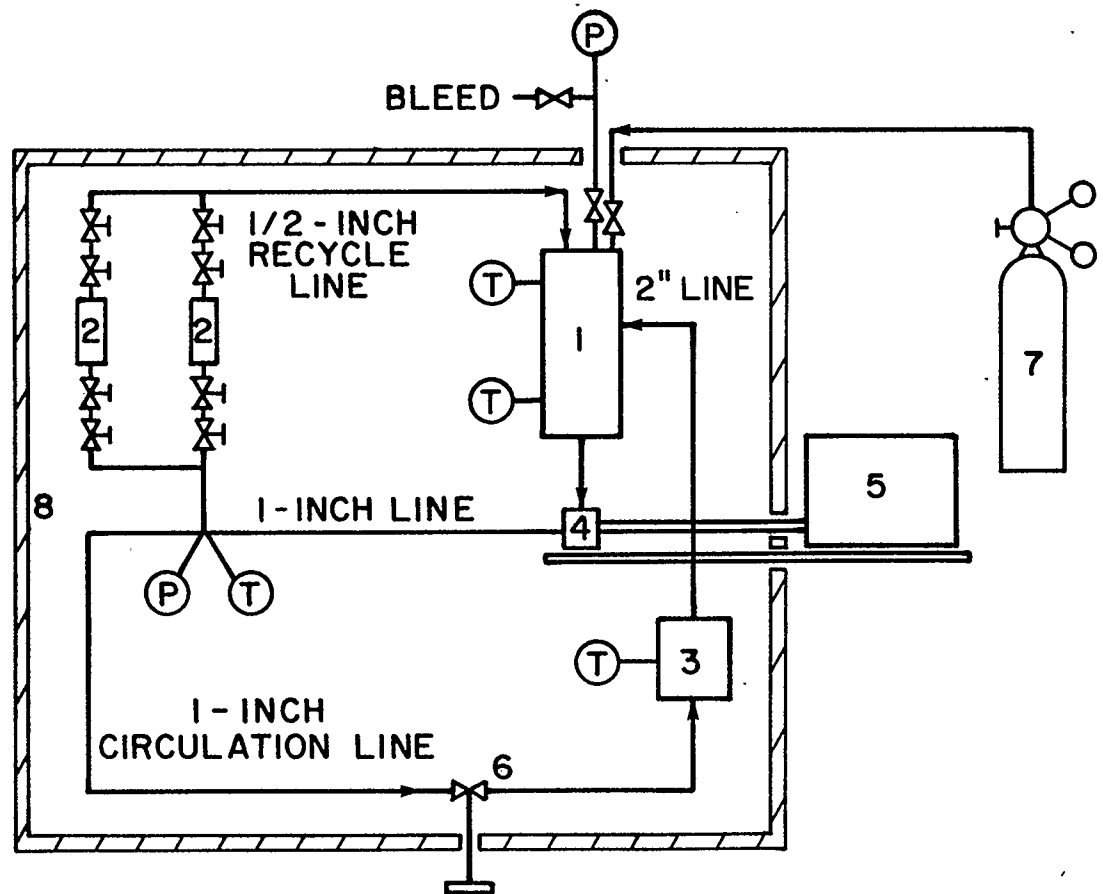


Figure 4.1: The High Viscosity Apparatus

The apparatus consisted of a mixing cell, a gas supply, a gear pump, a Contraves DC44 viscometer, and a pair of removable sample cells. The complete apparatus, except the gas supply and the instrumentation on the viscometer, was contained within a heated air-bath. The volume of the mixing cell is approximately 2 litres. The sample cells were calibrated for volume and mass, and hold about 6 mL of sample each.

A typical experiment in the HVA began with the introduction of the gas to the sample in the apparatus. As CO_2 is only available at a pressure of 6 MPa, external heating was required to raise the pressure to over 10 MPa before it was introduced to the HVA. After the introduction of the gas, the supply was isolated from the mixing cell and bitumen circulation was begun. The gate valve in the 1-inch circulation line was opened such that there was flow through both the circulation line and the recycle line. The sample was reintroduced to the mixing cell through a distributor at the top — ensuring ample gas-liquid contact area. The sample was allowed to equilibrate for a minimum of twenty-four hours, and the approach to equilibrium was monitored through the viscosity readings of the viscometer.

When equilibrium was reached, as indicated by a steady viscosity reading, the temperature and pressure of the mixing cell were recorded, as was the viscosity of the sample. The air-bath was then opened and one of the sample cells was isolated and removed. If more experiments were required at the same temperature, gas was released from the apparatus until the pressure had reached the desired level. If experiments were to be performed at a new temperature, the temperature of the air-bath was

adjusted and more gas was introduced to the system. The system was then allowed to equilibrate at the new conditions.

After removal from the apparatus, the sample cell was cleaned and weighed. The density of the sample was determined from the calibrated volume and mass of the cell. The sample was then degassed in the depressurization apparatus (described in Section 4.3) to determine the amount of gas in the bitumen. When this was complete, the cell was cleaned and weighed to get an empty mass of the cell.

4.2 Low Viscosity Apparatus

Since the HVA was originally designed to measure properties of gas-saturated bitumen, it was never intended to be used for fluids with the low viscosities of Cuts 1 and 2. Because of this, another apparatus was designed to handle the low viscosities of these two cuts.

The new Low Viscosity Apparatus (LVA) consisted of a 1.5 litre mixing cell, a Gilson High Pressure Liquid Chromatography (HPLC) pump, a capillary viscometer, and a 6 mL sample cell. The complete apparatus was contained within a Blue M oven. Circulation was provided by the HPLC pump, which also acted as a flow regulator for the capillary viscometer. A bypass line was available to allow circulation to continue when the sample cell was out for degassing. The circulating fluid was passed through a distributor at the top of the sample cell to provide gas-liquid contact. A schematic diagram of the apparatus is shown in Figure 4.2.

Blue M Oven

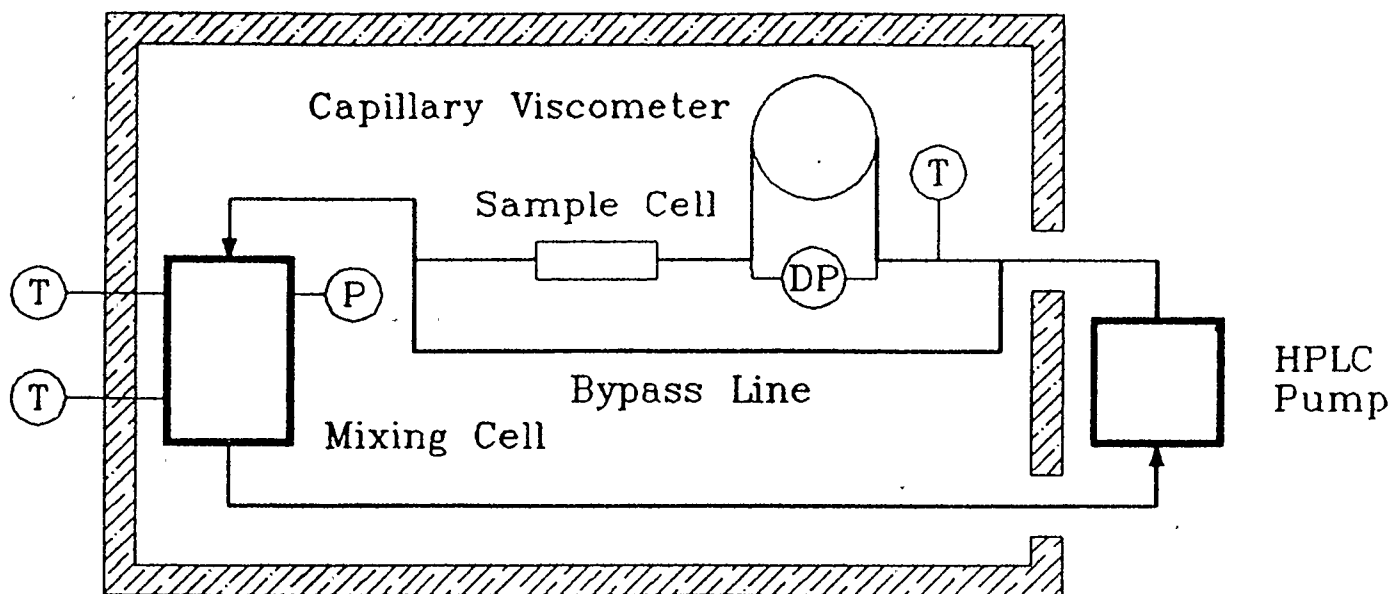


Figure 4.2: The Low Viscosity Apparatus

The capillary viscometer consisted of a 5 m length of 1/8-inch stainless-steel tubing and two Rosemount differential pressure transmitters. The transmitters were calibrated for ranges of 0-150 inches of water and 0-30 inches of water. Pressure taps were placed approximately 50 cm from the tubing connection points, and the tubing was coiled with a 30 cm diameter. Flow through the coil was regulated by the HPLC pump, which could deliver up to 25 mL/min in increments of 0.025 mL/min. Knowing the flow of fluid through the tubing (metered by the HPLC pump) and the pressure drop induced by this flow (measured by the DP cells) the viscosity of the sample could be determined. Calibration of the viscometer was performed at several temperatures with a Cannon viscosity standard, which had viscosities of approximately 75 mPa·s at 25°C and 5 mPa·s at 100°C.

A typical experiment in the LVA was much the same as one in the HVA. Equilibrium was achieved in the same manner, although the approach to equilibrium was much quicker (typically less than six hours for Cut 2, approximately four hours for Cut 1). Experiments in the liquid-CO₂ region with these light fractions were avoided, as there was no way to ensure that there was no entrainment of the liquid-CO₂ phase in the hydrocarbon phase.

4.3 Depressurization Apparatus

To determine the CO₂ content of the saturated bitumen sample, the contents of the sample cell were depressurized and the quantity of gas released was recorded. The apparatus consisted of a mercury-filled depressurization cell, a Heise pressure gauge, and a Ruska pump attached

to the mercury reservoir of the depressurization cell. The depressurization cell was contained within an oven. Figure 4.3 shows a schematic of the depressurization apparatus.

After the sample cell was cleaned, dried, and weighed, it was attached to the depressurization apparatus. The "dead volume" of the apparatus (the volume remaining with a full mercury reservoir) was measured by monitoring the pressure response to changes in the volume of mercury in the reservoir. The "dead air" in the cell was computed with the ideal gas law. When the dead volume had been determined, the sample cell was opened and the gas in solution in the bitumen released. The apparatus was heated to a temperature of at least 110°C (higher in the case of Cut 5) to ensure that all the gas in the bitumen was liberated. After cooling, the pressure of the apparatus was recorded at a number of volumes, and the number of moles of gas released was calculated from the ideal gas law. The gas solubility in the bitumen was then computed from the molar mass of the gas and the mass of gas-saturated bitumen in the sample cell.

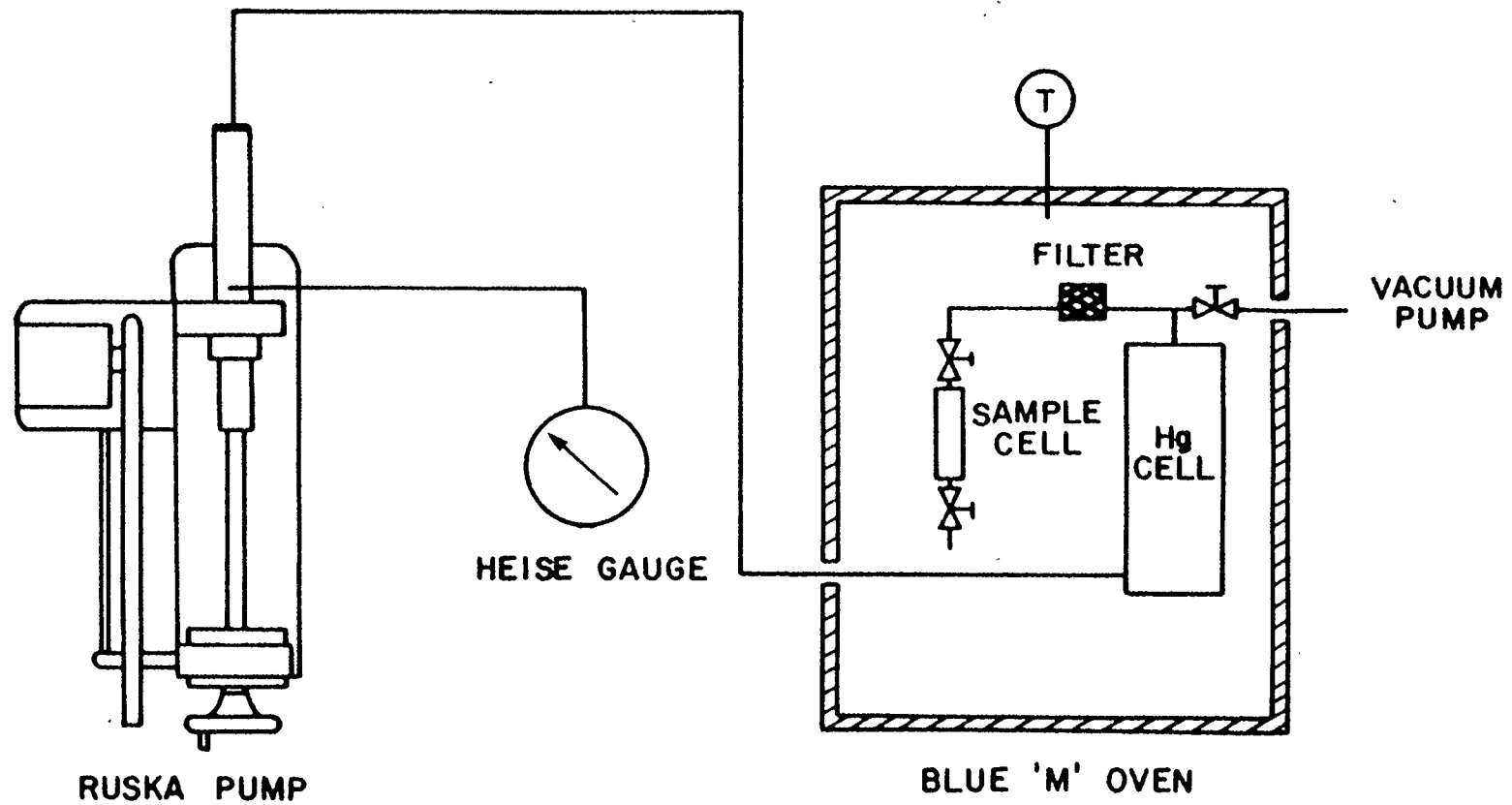


Figure 4.3: The Depressurization Apparatus

CHAPTER 5

DATA FOR THE PROPERTIES OF CO₂-SATURATED BITUMEN FRACTIONS

Experiments on the gas-saturated bitumen fractions were designed such that the effects of both temperature and pressure on the properties of the fractions could be investigated. A total of ninety data points were collected for the solubility, density, and viscosity of the cuts. Where possible, data points were also collected in the liquid-CO₂ region. Data points on four isotherms (spanning a 75°C temperature range) were taken for all but one cut. Isotherms were chosen such that the temperatures investigated for adjacent cuts (e.g., Cut 3 and Cut 4) overlapped to some extent.

5.1 Results for CO₂-Saturated Whole Cold Lake Bitumen

To provide a base-line for examining potential predictive methods, and to check the reproducibility of the experiments, CO₂-solubility experiments were first performed on the whole Cold Lake bitumen sample. Sixteen data points were collected on four isotherms, with pressures ranging up to 10 MPa. Two data points were collected in the liquid-CO₂ region.

The data collected from these experiments are given in Table 5.1. The solubility and viscosity data are plotted in Figure 5.1. In this figure, the lines connecting the data points simply highlight the isotherms; they do not imply any kind of model or correlation.

TABLE 5.1

CO₂-Saturated Whole Bitumen Data

Point	Pressure (MPa)	Temperature (°C)	Viscosity (Pa·s)	Density (kg/m ³)	CO ₂ -Solubility (mass %)
1	10.54	25.4	0.236	1036	12.35
2	7.72	24.4	0.240	1028	12.44
3	5.47	25.4	0.485	1031	9.65
4	2.55	23.5	3.040	1025	4.16
5	10.15	50.6	0.065	1001	11.55
6	7.55	50.7	0.110	993	7.55
7	5.43	50.5	0.193	979	5.87
8	2.85	52.1	0.570	963	2.85
9	10.47	75.7	0.037	971	9.49
10	7.43	74.7	0.065	973	6.90
11	5.16	74.5	0.108	957	4.98
12	2.51	73.1	0.206	972	2.13
13	10.33	99.4	0.028	932	7.86
14	7.56	96.6	0.041	944	5.94
15	5.25	96.4	0.058	937	4.25
16	2.57	95.3	0.094	940	2.15

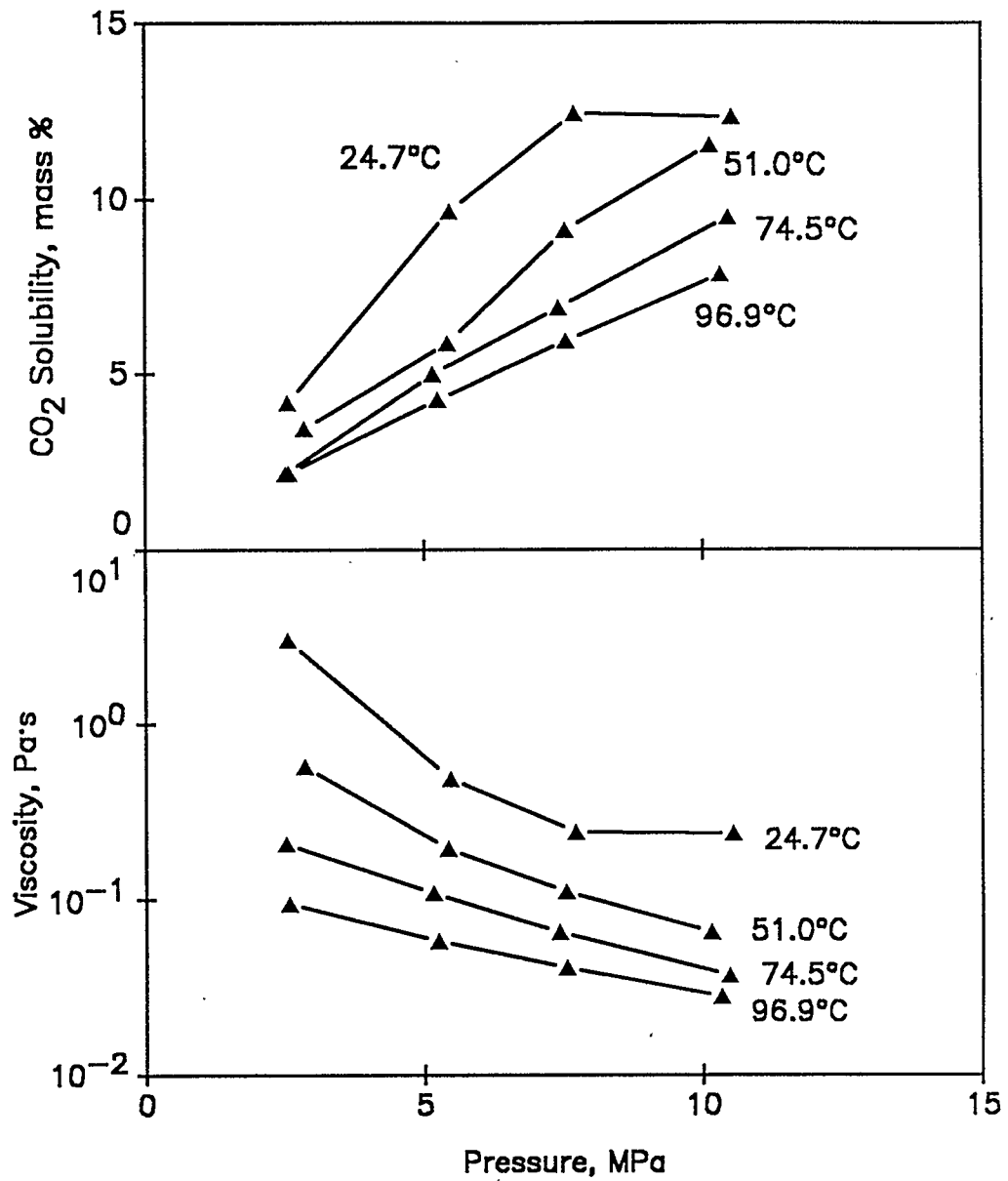


Figure 5.1: CO₂-Saturated Whole Bitumen Data

The CO₂-solubility data follow the trends shown by other bitumens: increased solubility with increased pressure, with the characteristic flattening of the room-temperature isotherm at pressures above the vapour pressure of CO₂. The density of the gas-saturated bitumen does not show any definite trend with pressure, although it is clearly a function of temperature. The viscosity data also show the effects of the liquid-CO₂ on the room-temperature isotherm.

5.2 Results for CO₂-Saturated Cut 1

Experiments on Cut 1 were performed in the LVA. Seventeen data points were collected on four isotherms at pressures up to 6 MPa. Pressures above 6 MPa caused erratic behaviour in the HPLC pump and were avoided. Thus, no data points were collected in the liquid-CO₂ region.

The Cut 1 data are provided in Table 5.2. The solubility and viscosity data are also plotted in Figure 5.2. The solubility and viscosity data show no flattening of the room temperature isotherm is observed, as no data points were collected in the liquid-CO₂ region. The density data again show no apparent trend with pressure, but do show a decrease in density with an increase in temperature.

TABLE 5.2

CO₂-Saturated Cut 1 Data

Point	Pressure (MPa)	Temperature (°C)	Viscosity (mPa·s)	Density (kg/m ³)	CO ₂ -Solubility (mass %)
1	4.49	25.1	1.47	856	16.25
2	3.91	25.1	1.84	888	12.03
3	2.30	24.4	3.05	901	5.89
4	0.99	25.6	4.18	895	2.21
5	6.20	51.9	1.11	865	13.44
6	4.73	51.9	1.40	830	9.80
7	3.14	51.8	1.65	857	5.79
8	2.09	51.8	1.88	847	3.52
9	6.19	73.5	1.07	867	10.57
10	4.57	72.9	1.23	884	7.53
11	3.52	73.9	1.31	821	5.53
12	2.65	73.5	1.50	822	3.71
13	6.34	97.5	1.00	831	8.91
14	4.48	98.0	1.09	799	6.04
15	3.14	97.9	1.22	823	3.97
16	2.14	98.0	1.34	820	2.37

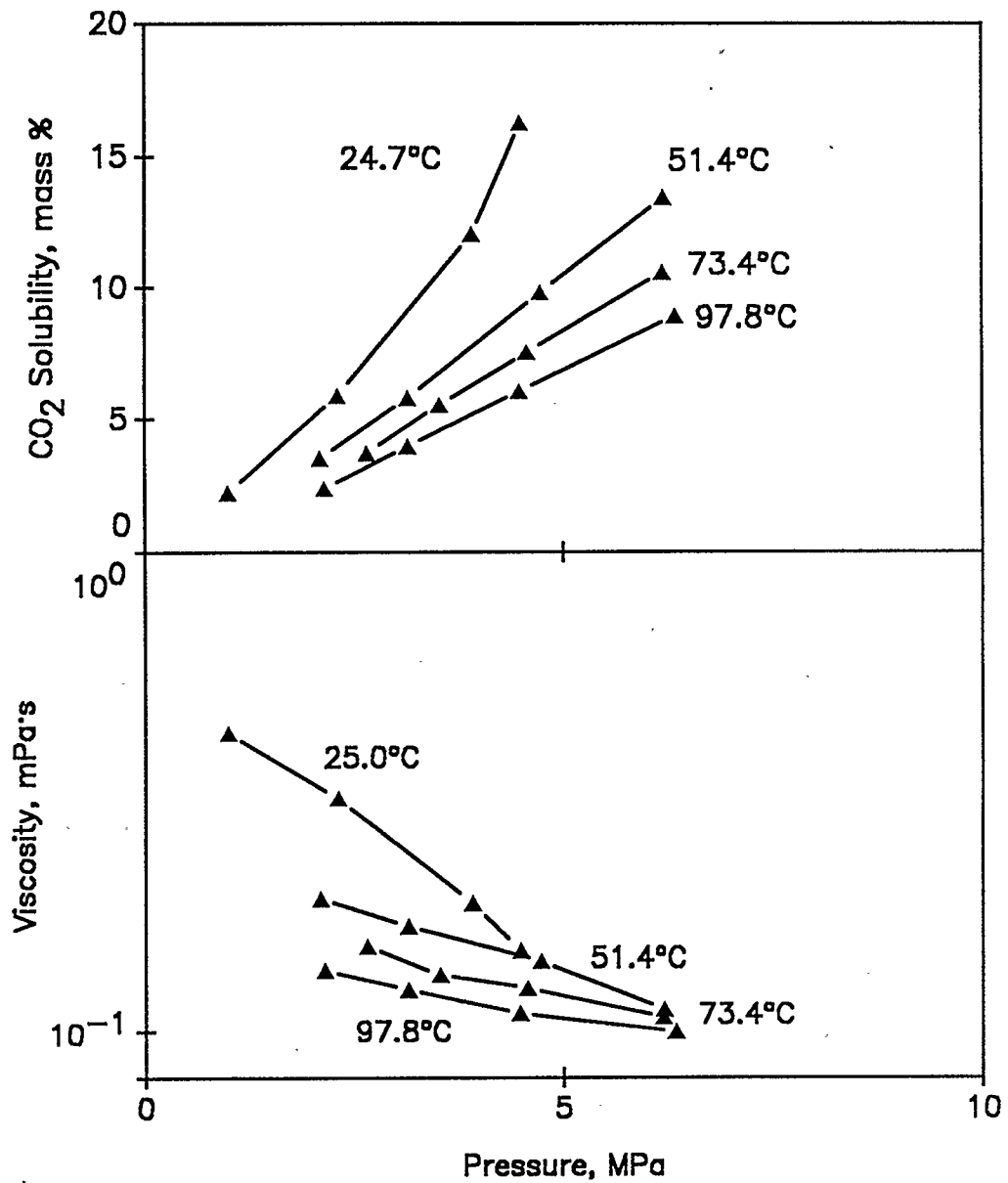


Figure 5.2: CO₂-Saturated Cut 1 Data

5.3 Results for CO₂-Saturated Cut 2

Data for Cut 2, like the data for Cut 1, were collected in the LVA. A total of 14 data points were collected on four isotherms — at 25°C, 50°C, 75°C, and 100°C — at pressures up to a maximum of 10 MPa. Again, no data were collected in the liquid-CO₂ region. The data are given in Table 5.3, and are presented in Figure 5.3. The same observations made for Cut 1 (no flattening of the room temperature isotherm, no apparent effect of pressure on density) can be made for Cut 2. The CO₂-solubility of Cut 2 is slightly less than that of Cut 1.

5.4 Results for CO₂-Saturated Cut 3

Cut 3 was the first of the cuts to be tested in the HVA. As with the gas-free properties of this fraction (discussed in Chapter 3), the gas-saturated properties are remarkably similar to those of the whole bitumen. Seventeen data points were collected, including two points in the liquid-CO₂ region. The data are presented in Table 5.4 and in Figure 5.4.

5.5 Results for CO₂-Saturated Cut 4

Fifteen data points were collected for gas-saturated Cut 4 at four temperatures in the HVA. Because the viscosity of the sample at room temperature was out of the range of the Contraves DC44 viscometer, data were collected at 50°C, 75°C, 100°C, and 125°C, at pressures up to 10 MPa. The data are presented in Table 5.5 and Figure 5.5.

TABLE 5.3

CO₂-Saturated Cut 2 Data

Point	Pressure (MPa)	Temperature (°C)	Viscosity (mPa·s)	Density (kg/m ³)	CO ₂ -Solubility (mass %)
1	6.09	24.1	5.00	964	16.04
2	4.81	24.3	—	946	11.80
3	4.78	24.0	10.10	—	—
4	3.89	25.4	23.50	963	8.88
5	2.79	24.1	25.80	902	5.57
6	10.08	49.9	1.98	934	17.04
7	8.85	49.8	3.31	943	14.65
8	4.91	49.9	7.01	931	7.61
9	2.65	49.4	11.03	938	4.26
10	7.17	74.8	3.43	914	8.58
11	5.08	73.8	4.62	914	5.93
12	3.12	75.0	5.50	909	3.73
13	2.18	74.5	5.89	905	2.37
14	3.77	99.6	3.86	868	3.45
15	2.59	103.5	3.88	891	2.16

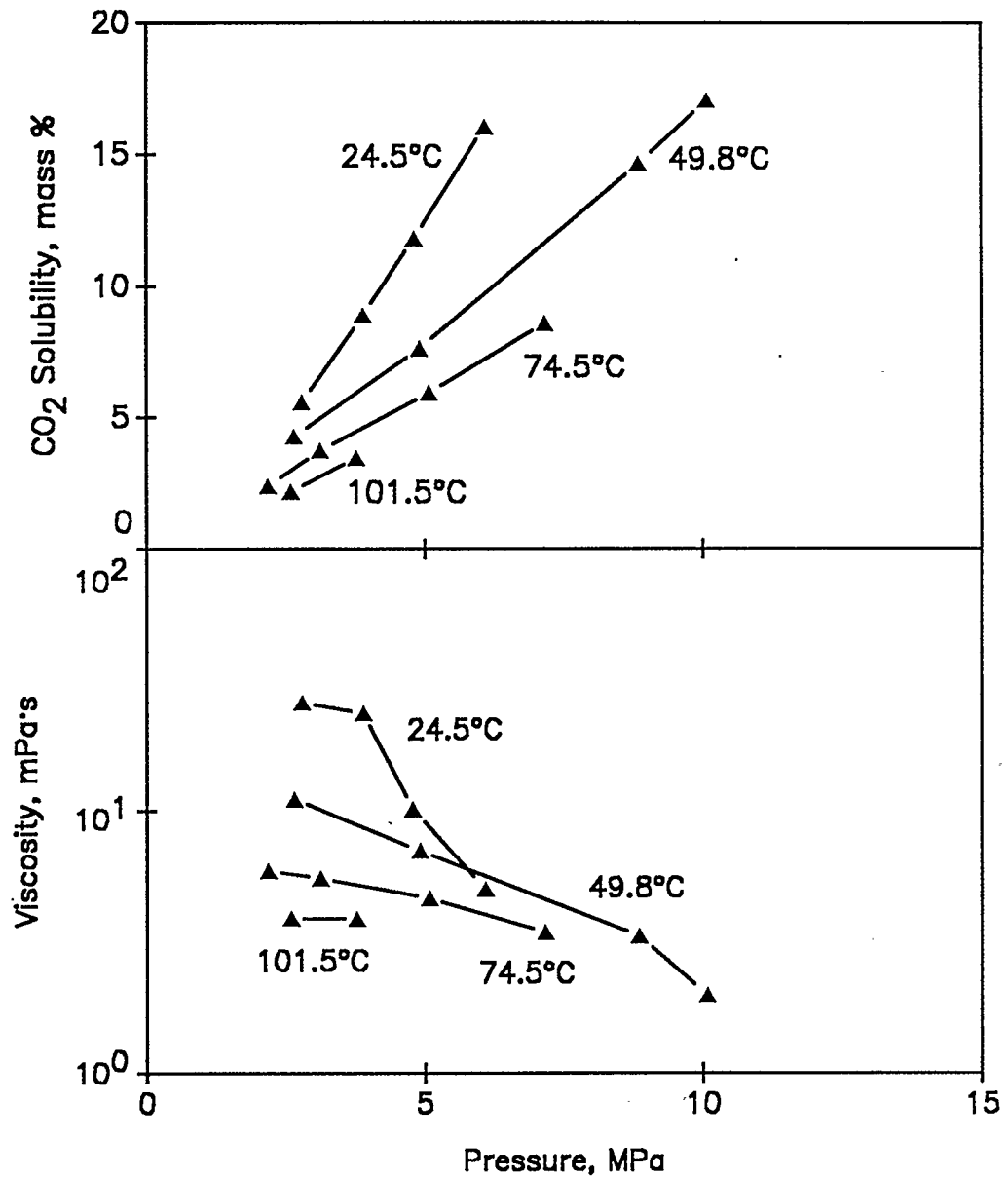


Figure 5.3: CO₂-Saturated Cut 2 Data

TABLE 5.4

CO₂-Saturated Cut 3 Data

Point	Pressure (MPa)	Temperature (°C)	Viscosity (Pa·s)	Density (kg/m ³)	CO ₂ -Solubility (mass %)
1	10.24	23.2	0.156	1037	11.66
2	7.59	23.1	0.164	1039	11.32
3	4.71	23.2	0.550	1025	7.77
4	2.11	23.7	3.930	1036	3.47
5	10.26	50.8	0.047	1013	10.12
6	10.09	54.2	—	1032	10.61
7	7.66	54.0	—	991	8.40
8	5.23	51.6	0.145	1006	5.87
9	2.69	50.9	0.525	1010	2.97
10	10.06	74.4	0.030	999	8.39
11	7.67	75.6	0.042	990	6.56
12	5.45	74.5	0.071	990	4.92
13	2.71	73.9	0.153	1002	2.40
14	10.79	111.1	0.012	958	6.94
15	7.50	104.0	0.019	975	4.91
16	5.65	102.5	0.025	959	4.08
17	2.63	108.1	0.032	954	1.78

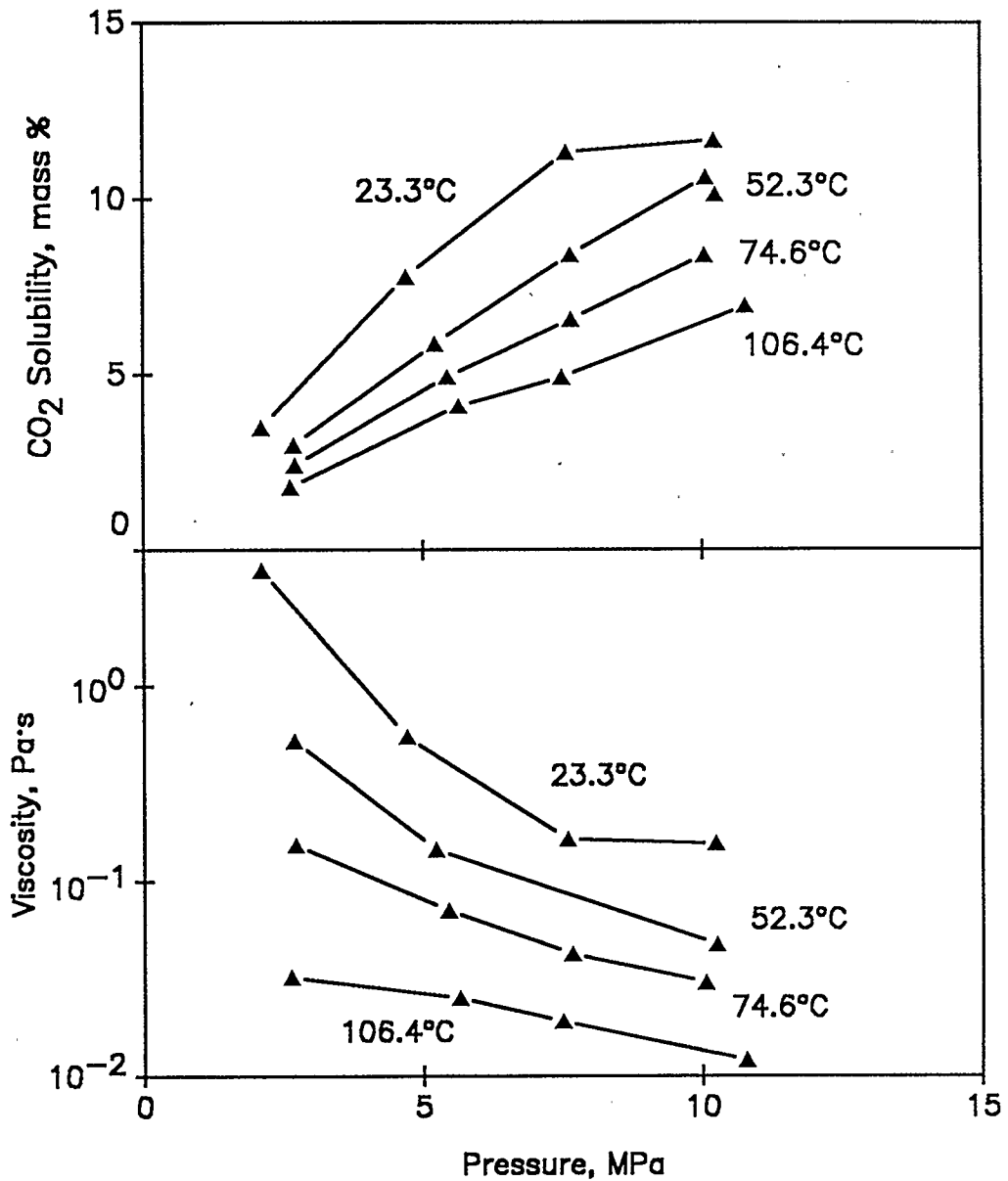


Figure 5.4: CO₂-Saturated Cut 3 Data

TABLE 5.5

CO₂-Saturated Cut 4 Data

Point	Pressure (MPa)	Temperature (°C)	Viscosity (Pa·s)	Density (kg/m ³)	CO ₂ -Solubility (mass %)
1	8.72	54.0	0.230	1020	8.20
2	5.45	52.6	0.736	1009	5.20
3	2.85	50.5	2.746	1012	2.94
4	9.94	73.3	0.091	998	7.48
5	7.69	73.7	0.132	1001	5.96
6	5.84	77.0	0.182	1004	4.71
7	2.59	75.8	0.748	989	1.89
8	11.95	100.7	0.034	985	7.79
9	7.95	101.2	0.055	974	5.07
10	5.89	101.0	0.076	980	3.99
11	3.08	102.0	0.130	977	2.08
12	9.49	128.2	0.026	976	5.14
13	7.80	126.1	0.030	961	4.28
14	5.74	129.8	0.034	966	2.97
15	2.96	123.6	0.060	961	1.53

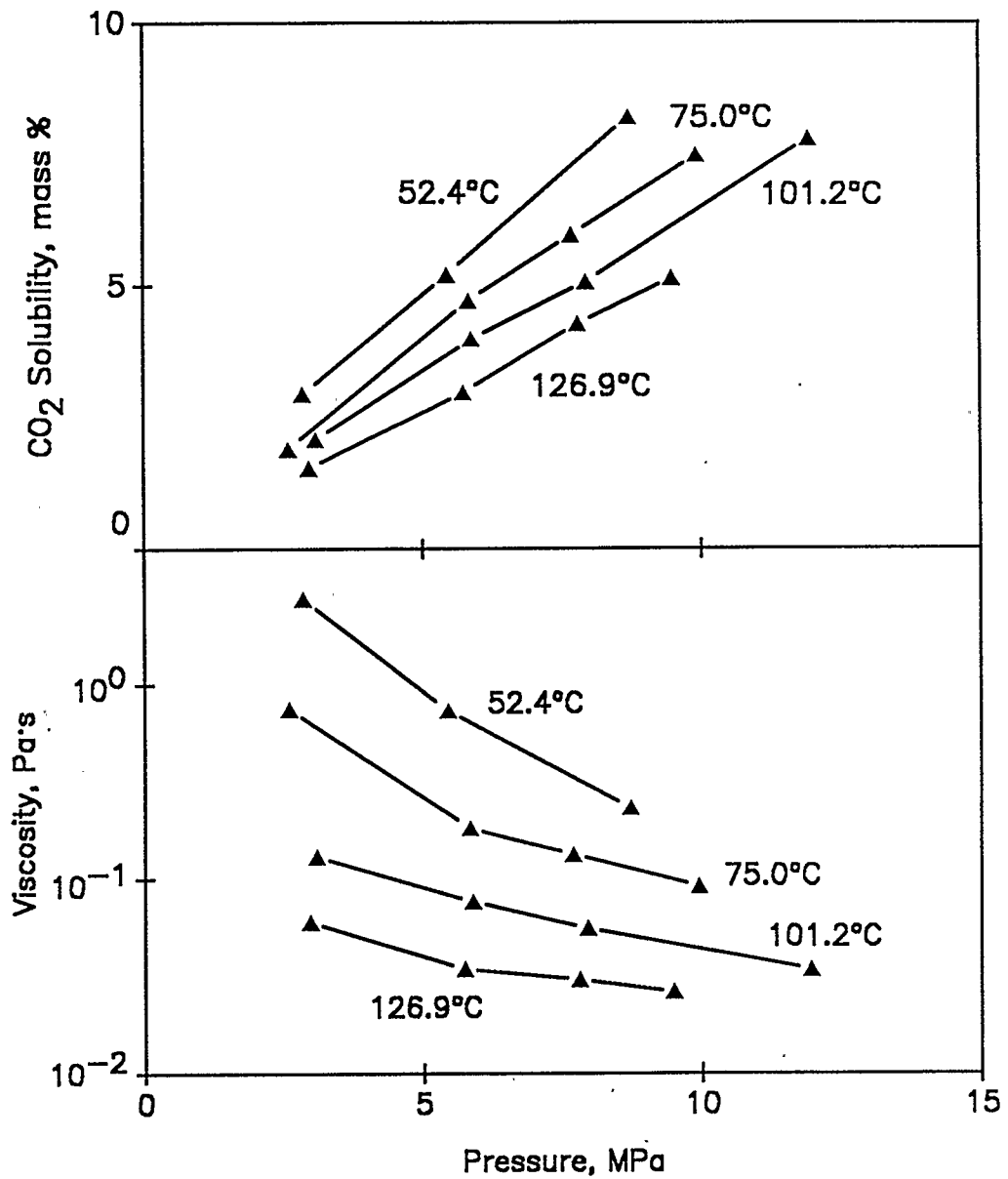


Figure 5.5: CO₂-Saturated Cut 4 Data

5.6 Results for CO₂-Saturated Cut 5

Experiments on Cut 5 were performed in the HVA as well. Once again, the sample was too viscous to perform any experiments at room temperature, or at any temperatures below 100°C for that matter. Three isotherms were collected (at temperatures near 155°C, 125°C, and 110°C) at pressures up to 10 MPa.

The data are presented in Table 5.6 and Figure 5.6. The values obtained for the CO₂-solubility are low, relative to values obtained in experiments with the other cuts, and as such appear more scattered than values from the other cuts.

TABLE 5.6
CO₂-Saturated Cut 5 Data

Point	Pressure (MPa)	Temperature (°C)	Viscosity (Pa·s)	Density (kg/m ³)	CO ₂ -Solubility (mass %)
1	6.45	109.7	193.4	1047	3.68
2	4.88	111.8	252.6	1014	2.75
3	2.01	114.3	844.0	970	1.43
4	9.14	125.3	23.5	1000	3.96
5	6.73	120.1	56.4	1022	3.08
6	5.03	117.6	144.6	974	2.71
7	2.80	124.9	277.4	953	1.28
8	9.52	153.7	7.52	978	3.07
9	7.19	154.3	6.01	979	2.58
10	5.19	154.3	11.6	1009	1.43
11	3.14	158.6	14.7	997	1.15

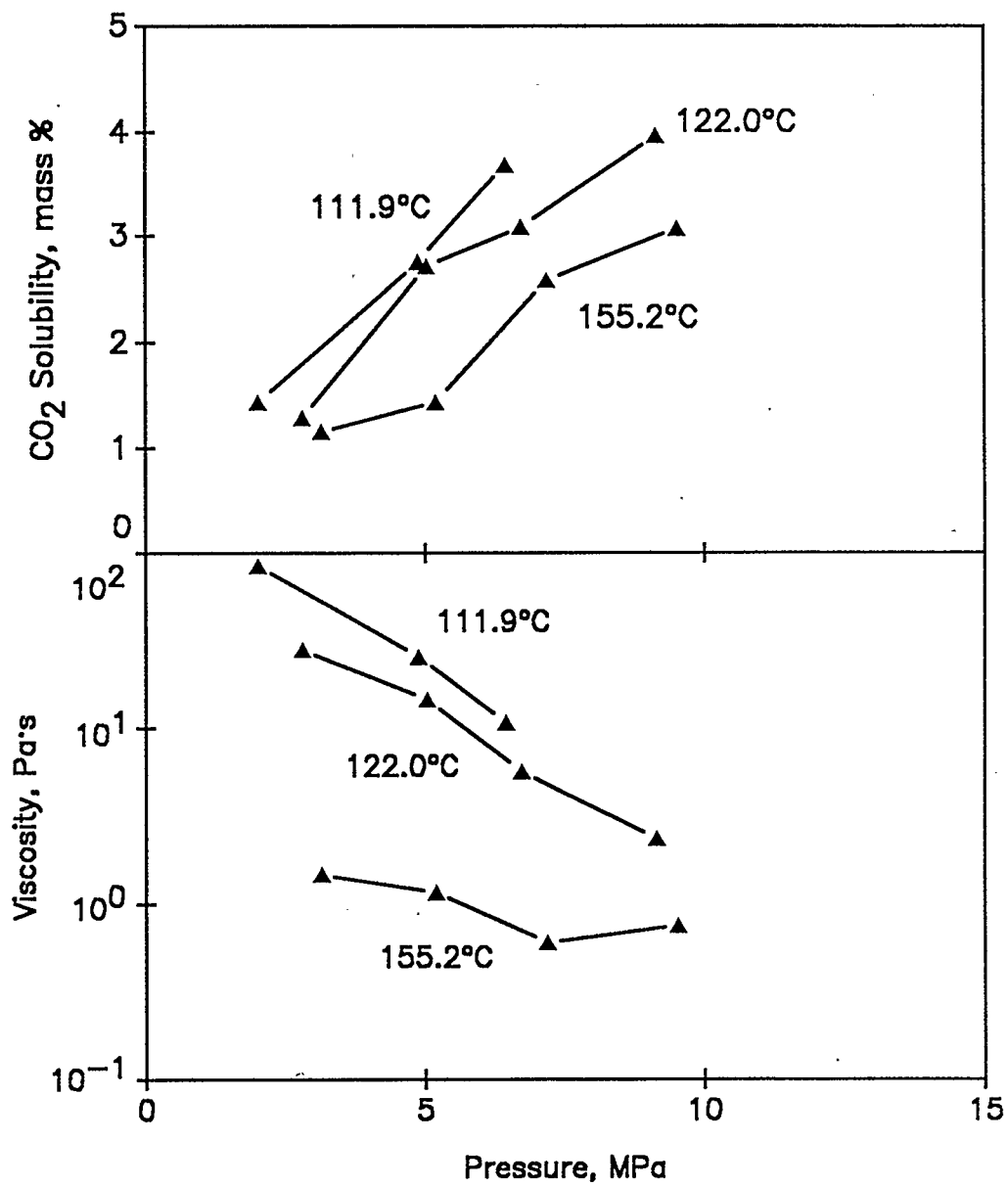


Figure 5.6: CO₂-Saturated Cut 5 Data

CHAPTER 6

CORRELATION OF CO₂-SOLUBILITY AND DENSITY DATA

A number of different approaches were looked at in correlating the experimental data with an equation of state. Primarily, the chief method of correlation was optimization of the interaction parameter in Equation 2.49 to match the experimental data. Temperature dependence in this parameter was also investigated. The optimization of another parameter in the characterization of a given cut (such as critical pressure) to match the density data was also explored. The relative merits of the equations of state considered in this project — aside from the obvious advantage of the P-T equation in density predictions — are also examined.

6.1 Definition of Optimization Criterion

To correlate the CO₂-solubility and density data, some sort of objective function was required that would give an indication of the goodness-of-fit of the model. Typically, average absolute deviation (AAD) is used, but this tends to place greater emphasis on data points that are small in value:

$$\text{AAD} = \sum_{i=1}^N \left(\frac{|y_i - \hat{y}_i|}{y_i} \right) \quad (6.1)$$

In this equation, N is the number of data points, y_i is data point i , and \hat{y}_i is the correlated value of data point i .

A better method would be to take the confidence in individual data points into account, so that data points which one has more confidence in

are more heavily weighted. With this type of objective function, data of different types (such as CO₂-solubility and density data) can be included simultaneously in the objective function.

This latter type of objective function was used in this work. The function used is as follows:

$$R = \sum_{i=1}^N \left(\frac{y_i - \hat{y}_i}{\sigma_i} \right)^2 \quad (6.2)$$

Here, the residual, R , is the value to be minimized. The standard deviation for data point i (σ_i) arises from normally distributed errors in the sampling procedure, and is an indication of the confidence in the data point. For CO₂-solubility data points, a standard deviation of 0.5 wt% is assumed, and for density data points, a value of 8 kg/m³ is assumed. If one assumes goodness-of-fit of the model, a residual value approximately equal to the degrees of freedom in the model is expected (Press *et al.*, 1988).

Knowing that a residual value approximately equal to the degrees of freedom in the model can be expected, one can produce an estimate of the average standard deviation of the data with the following function:

$$\bar{\sigma} = \sqrt{\sum_{i=1}^N \frac{(y_i - \hat{y}_i)^2}{N - P}} \quad (6.3)$$

where P is the number of parameters in the model.

If one assumes that the model describes the behaviour of the system, the following equation may be used to generate 95% confidence limits for

the optimized parameter :

$$\text{confidence in parameter } j = \sqrt{\sum_{i=1}^N \left(\frac{\partial \hat{y}_i}{\partial a_j} \right)^2} \cdot t \quad (6.4)$$

where a_j is parameter j , and t is the value of the t -statistic at a confidence level of 95%.

6.2 Characterization of Bitumen Fractions

As has been mentioned in Chapter 2, six critical property correlations were considered in estimating the critical properties of the samples and three correlations were considered in estimating acentric factors. Properties of the samples that were used to generate the predictions were limited to density and molar mass. For some correlations, a value of the boiling point was required, and this value was taken from the SIMDIST distillations of the samples. For Cut 5, the value was chosen such that the mass average boiling point of the samples was that of the whole bitumen. All types of boiling points (mean, molal average, cubic average) were assumed to be equal to the boiling point determined from the SIMDIST distillations.

At first, it may seem improper to use these correlations to estimate the critical properties of Cut 5, which is a solid at room temperature; however, if one considers this sample to be a very viscous fluid — so viscous that flow is practically impossible — the validity of this approach is not so questionable. The ultimate test of this assumption, in fact, would be from the actual correlation of the phase behaviour data.

6.2.1 Estimation of Critical Temperature

Estimations of the critical temperatures of the samples are fairly consistent from correlation to correlation. For Cut 1, five of the six correlations give values in the 700 K range; the exception is the Cavett correlation which gives a value of 957 K. This trend is also apparent with Cuts 2 through 4 and the whole bitumen.

For Cut 5, however, the estimated critical temperatures are scattered over a much wider range. The Cavett correlation, which gives the highest T_c estimations for the other samples, gives the lowest estimation for Cut 5 (1355 K). The highest estimation comes from the correlation of Watanasiri *et al.*, which gives a value of 2043 K. The T_c estimations are compared in Figure 6.1.

6.2.2 Estimation of Critical Pressure

Critical pressure estimates — shown in Table 6.1 and in Figure 6.2 — are much more varied from correlation to correlation than the critical temperature estimates. For example, Cut 1 values range from 1891 kPa (Twu) to 2627 kPa (Cavett). Cut 2 values are the most consistent (1348 kPa from Whitson to 1674 kPa from Kesler-Lee). The values obtained for Cut 5 seem to be the best indication of the way a correlation may behave when extrapolated: The Cavett correlation was found to go through a minimum between Cut 4 and Cut 5 so that the P_c value for Cut 5 is actually greater than that for Cut 4. A number of correlations (Kesler-Lee, Winn, Whitson, and Watanasiri *et al.*) predicted critical pressures below atmospheric pressure.

TABLE 6.1

Critical Property Estimations for Bitumen Fractions

Correlation	whole bitumen		Cut 1		Cut 2		Cut 3		Cut 4		Cut 5	
	T _c (K)	P _c (kPa)										
Kesler-Lee	1019	813	733	2219	840	1675	1052	641	1113	466	1797	101
Cavett	1215	1014	958	2628	1110	1392	1225	961	1257	910	1355	1111
Sim-Daubert	1036	914	732	2039	846	1545	1072	793	1133	674	1634	248
Whitson	1077	511	757	2285	878	1348	1114	397	1176	294	1669	47
Twu	1037	757	765	1891	883	1362	1055	658	1093	556	1406	359
Watanasiri	1042	477	716	2059	884	1461	1059	328	1116	210	2044	17

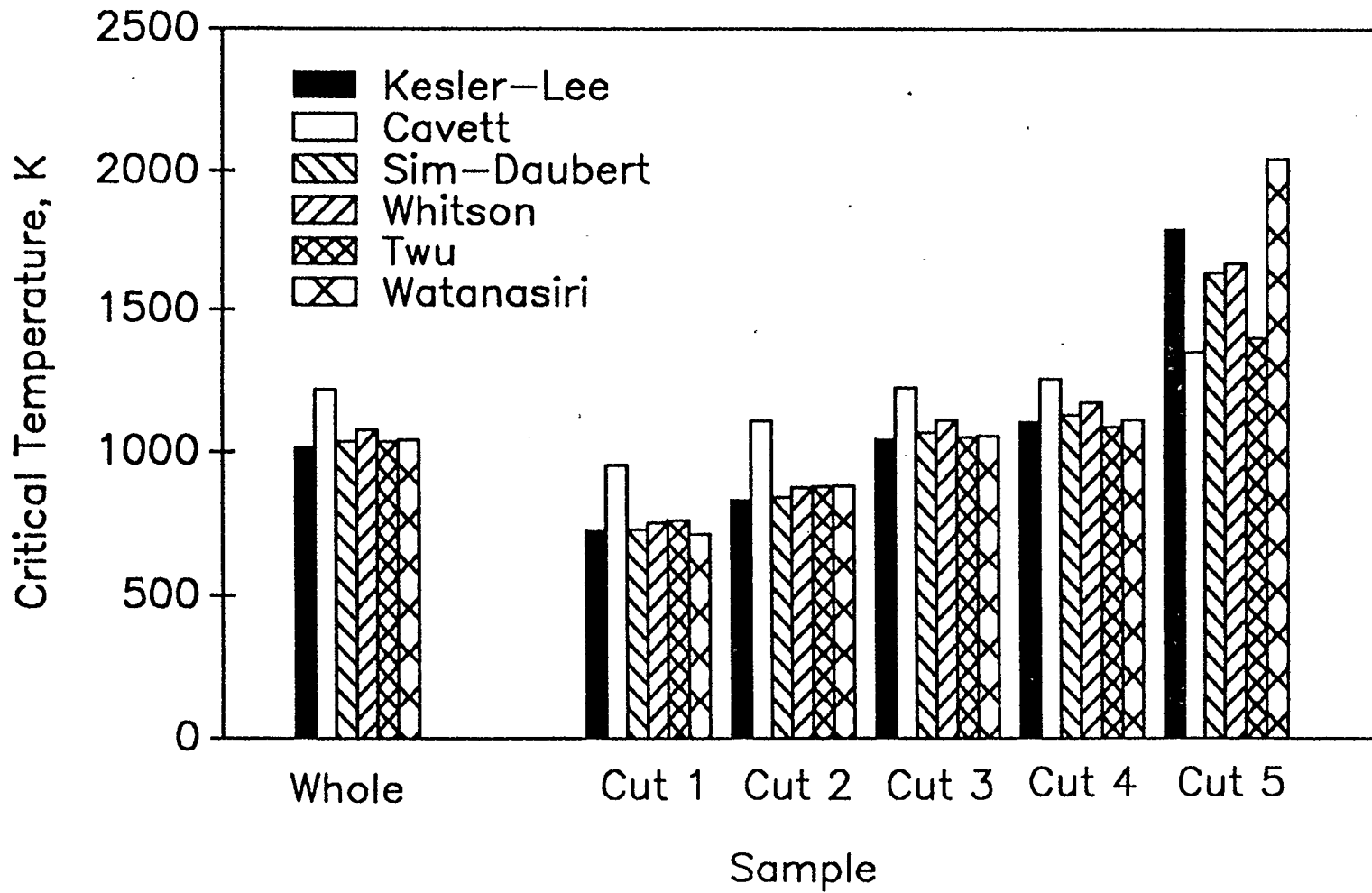


Figure 6.1: Estimates of Bitumen Fraction Critical Temperatures

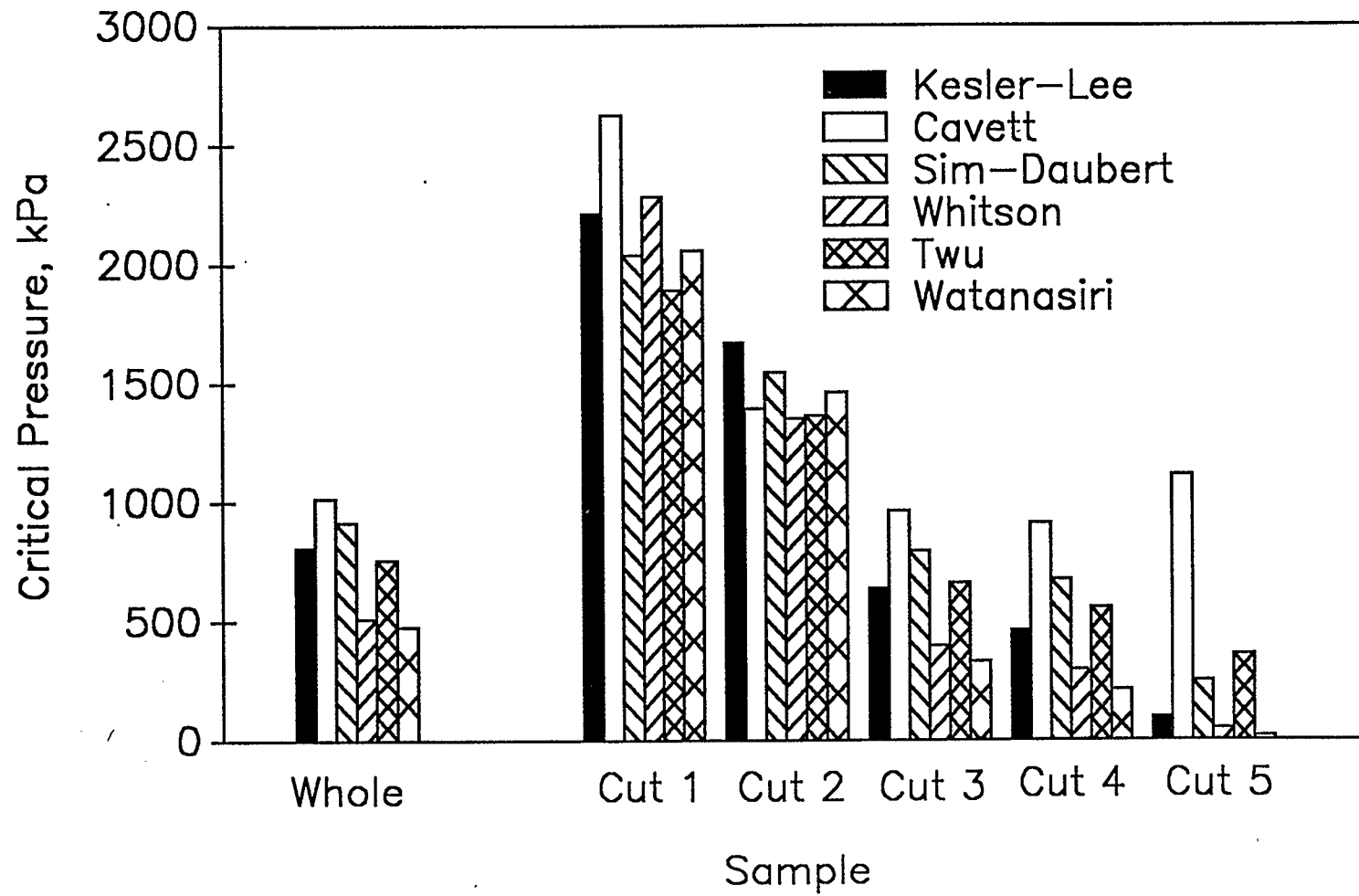


Figure 6.2: Estimates of Bitumen Fraction Critical Pressures

It should also be noted that the value of α in the Twu correlation (Equation 2.18) was negative with Cut 5. This caused numerical problems in Equation 2.17, so α was set equal to zero. While this resulted in a reasonable value for the critical pressure of Cut 5, further extrapolation of the correlation would result in an increase in the value of P_c . This is because the value of P_c° is held constant by holding α at zero, while the perturbation function increases.

6.2.3 Estimation of Acentric Factor

Only one of the three correlations for the acentric factor that were evaluated in this study gave reasonable results for all six samples: the Kesler-Lee correlation. The Edmister correlation often went through a maximum as the molar mass of the sample increased, and frequently gave negative values. The correlation of Watanasiri *et al.* gave exorbitantly large values for the samples with molar masses above 500. The estimations are given in Table 6.2 and are compared in Figure 6.3. The values given for the Edmister correlation are arrived at using the Kesler-Lee critical pressure and critical temperature estimations. Since the Kesler-Lee correlation was the only one to give consistent results, it was the only one used in all subsequent calculations for correlating the data.

TABLE 6.2
Acentric Factor Estimations for Bitumen Fractions

Correlation	whole bitumen	Cut 1	Cut 2	Cut 3	Cut 4	Cut 5
Kesler-Lee	1.378	0.662	0.873	1.529	1.734	3.417
Edmister	0.139	0.605	0.826	1.816	2.437	-1.001
Watanasiri	5.220	0.514	1.048	6.975	10.124	64.195

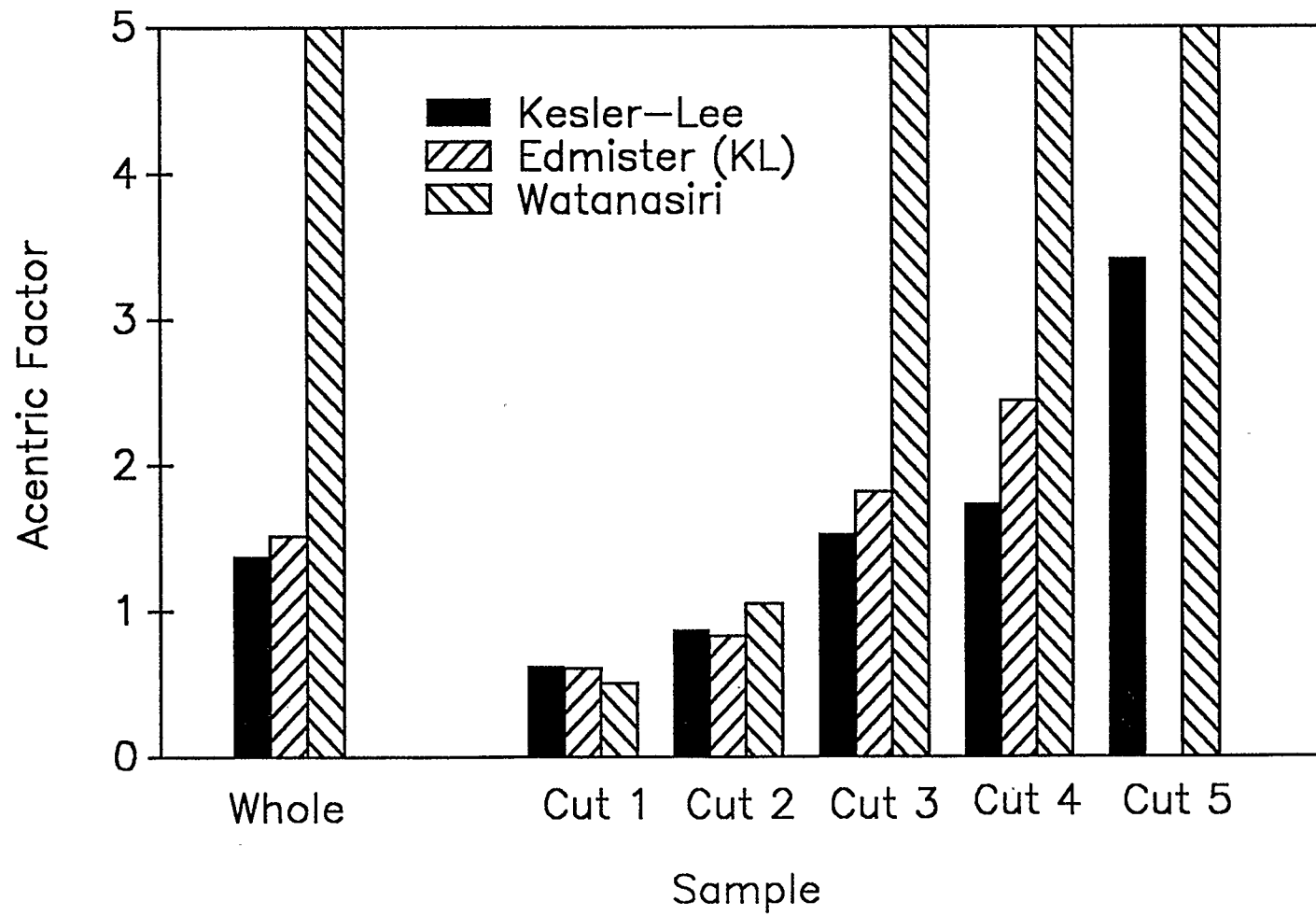


Figure 6.3: Estimates of Bitumen Fraction Acentric Factors

6.3 Calculation Method

Calculation of the CO₂-solubility and density of the saturated fractions was performed with the method presented by Nghiem *et al.* (1983). Essentially, the requirement of equal fugacities in both the hydrocarbon and the CO₂-rich phases was met for each component. Because of the negligible solubility of the fractions in CO₂, three phases were not expected. Thus only two-phase flash calculations were required. The selection of the correct root from the cubic EOS for each phase was performed such that the Gibb's free energy of the phase was minimized. This allowed calculations to be performed correctly in the liquid-CO₂ region. The critical properties of CO₂ were taken from Reid *et al.*

6.4 Correlation of Whole Bitumen Solubility Data

The sixteen gas-solubility data points collected for the whole bitumen were correlated with the one-pseudocomponent bitumen characterizations presented in Table 6.1 and with the Kesler-Lee acentric factor estimation in Table 6.2. All three equations of state were used as well. Computation of the CO₂-pseudocomponent phase equilibria was

6.4.1 Comparison of Critical Property Correlations

The results of the correlation of the gas solubility data are given in Table 6.3. The optimized interaction parameter, the 95% confidence interval, the residual (minimum of the objective function), and the average absolute deviations (AAD) are shown for correlation with the P-R EOS.

TABLE 6.3
 Comparison of Characterizations for the Correlation of
 Whole Bitumen Solubility Data Using the P-R EOS

Characterization	Optimized k_{ij}	95% Confidence Interval	Residual	AAD
Kesler-Lee	0.0884	0.0007	19.2	9.7%
Cavett	0.064	0.001	77.6	17.0%
Sim-Daubert	0.0806	0.0005	36.5	12.5%
Whitson	0.1097	0.0009	16.2	5.9%
Twu	0.09090	0.00005	13.9	8.4%
Watanasiri	0.1163	0.0003	27.6	6.7%

Figure 6.4 compares the experimental data for the 24.7°C and 96.9°C isotherms with with predictions generated by use of the different correlations. Note that for some correlations (such as Whitson's), an interaction parameter that increases with temperature would appear to improve the correlation, while for others (such as the Kesler-Lee correlations), an interaction parameter that decreases with temperature appears more justified. The use of a temperature-dependent interaction parameter is explored in more detail in Section 6.8.

6.4.2 Comparison of the Equations of State

Four isotherms generated by the three equations of state (using the correlations of Twu) are compared with the experimental data in Table 6.4 and Figure 6.5. The P-R EOS and the S-R-K EOS gave almost identical predictions, although the values of the interaction parameter are different. The P-T EOS shows very different results for the best fit of the data. The isotherms are much more spread out than with the other two equations, and the use of a temperature dependent interaction parameter appears necessary.

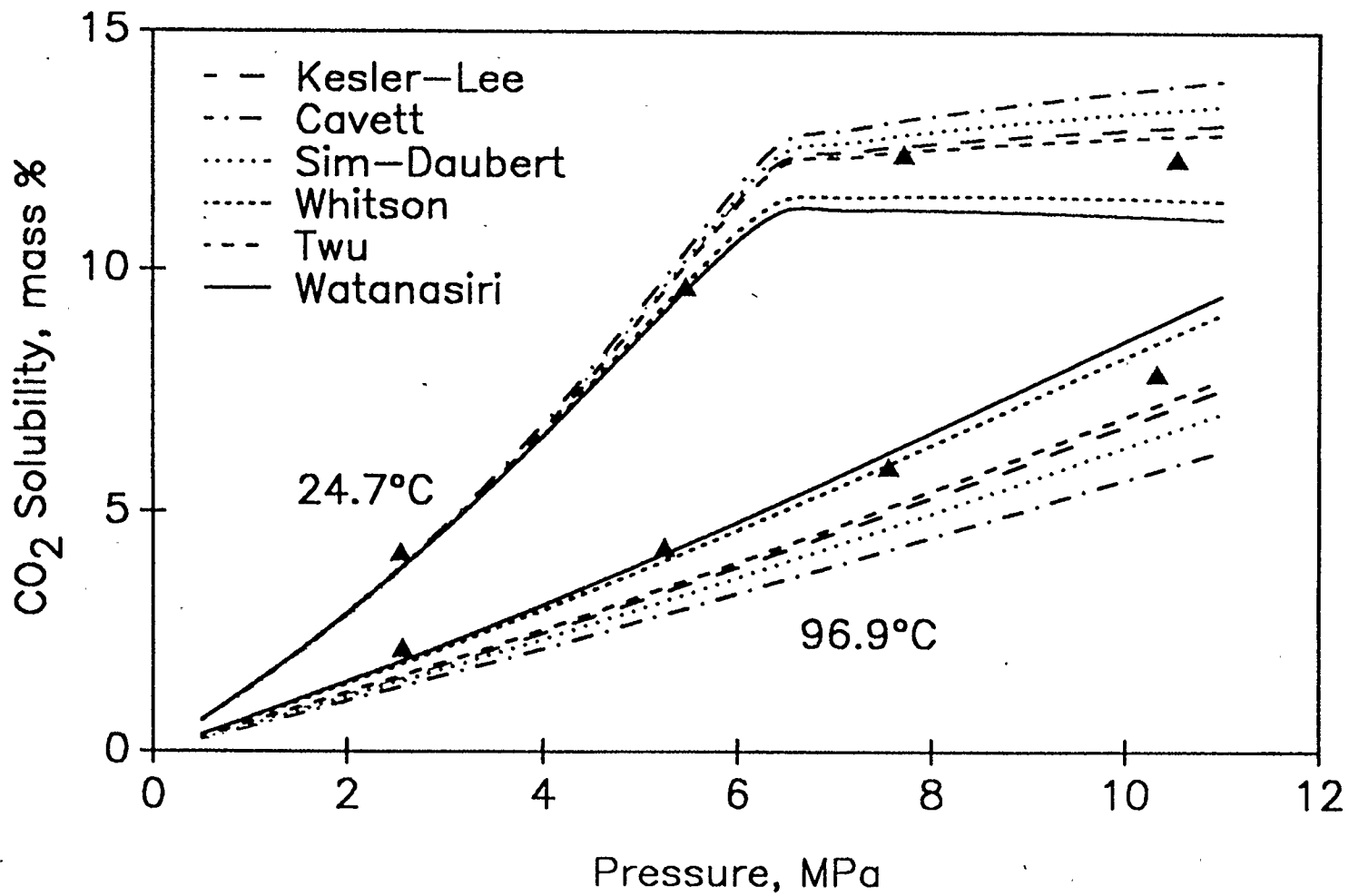


Figure 6.4: Whole Bitumen CO₂-Solubility Data Correlated with the P-R EOS

TABLE 6.4
Comparison of Equations of State for the Correlation of
Whole Bitumen Solubility Data with the Twu Characterization

Equation of State	Optimized k_{ij}	95% Confidence Interval	Residual	AAD
S-R-K	0.1020	0.0006	15.6	8.9%
P-R	0.09089	0.00005	13.9	8.4%
P-T	0.005	0.007	60.1	15.5%

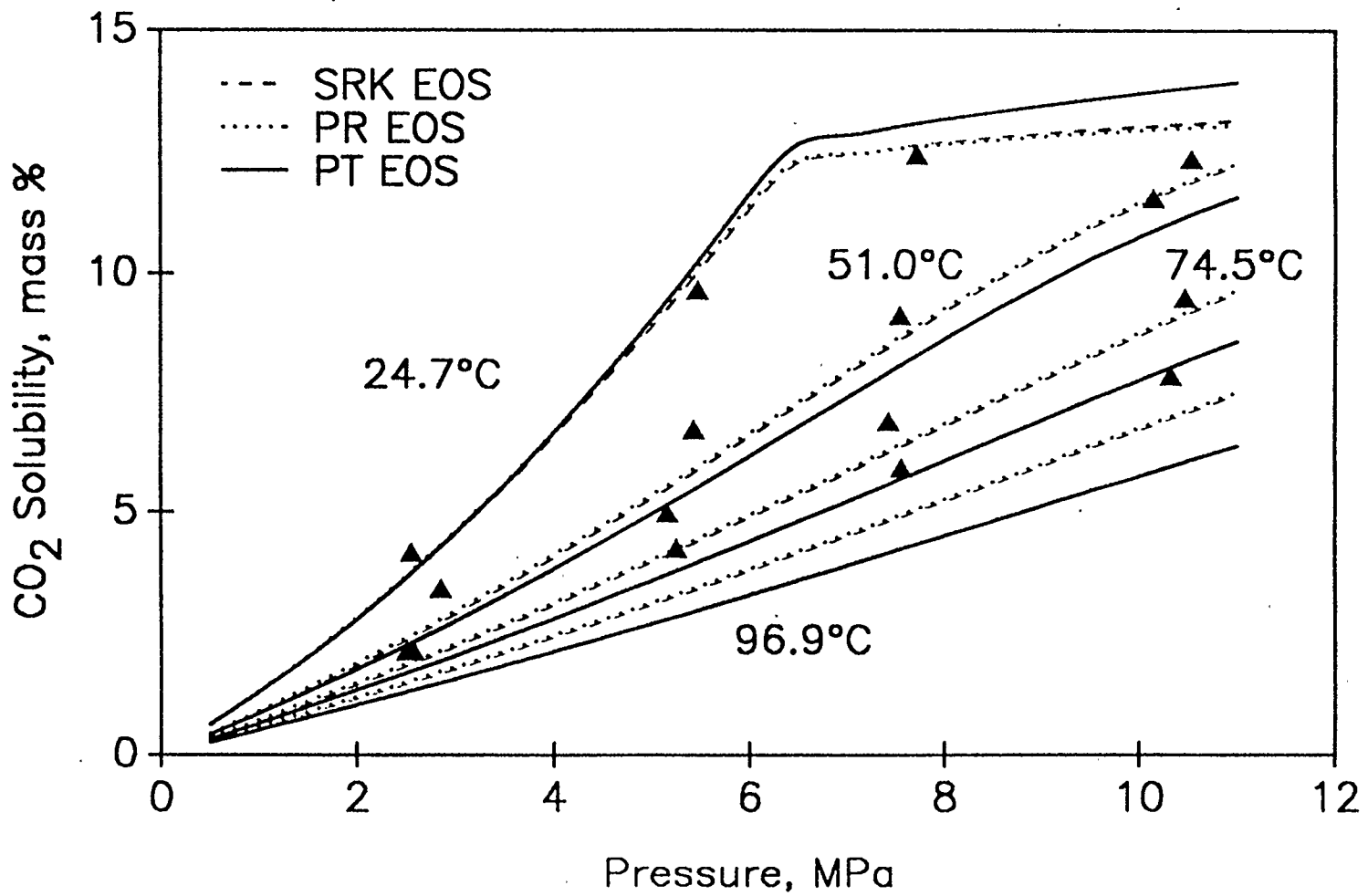


Figure 6.5: Whole Bitumen CO₂-Solubility Data Correlated with the Twu Characterization

Since the P-R and the S-R-K equations give such similar results (and this holds for the other cuts as well as for the whole bitumen), further discussion will exclude the latter equation. With the exception of the actual regressed values of the interaction parameter, any statement made about the P-R equation holds true for the S-R-K equation as well in terms of performance of the different characterizations. The lack of any improvement in correlation with the P-T EOS at the cost of an additional parameter will exclude it from further discussion. It is possible that the use of Equations 2.63 and 2.64 with the values of ω that are encountered is not justified. The EOS will be mentioned again, however, in the discussion of the correlation of the gas-saturated density data.

6.5 Correlation of Bitumen Fraction Solubility Data

Correlation of the gas-solubility data for the cuts was performed in the same manner as for the whole bitumen. Greater variations in the estimated properties of the pseudocomponents were encountered with the cuts than with the whole bitumen, and as such, varied results were observed. When results were compared for different cuts, some trends did become apparent.

6.5.1 Correlation of Cut 1 Solubility Data

Results from the correlation of Cut 1 experimental data with the P-R EOS are summarized in Table 6.5. The results are also plotted for the 24.7°C and 97.8°C isotherms in Figure 6.6. Although the data extend to a maximum pressure of only around 6 MPa, the plots have been extrapolated to 11 MPa to check the behaviour of the correlation when extrapolated to the pressure range of the other bitumen fraction data.

TABLE 6.5

Comparison of Characterizations for the Correlation of
Cut 1 Solubility Data with the P-R EOS

Characterization	Optimized k_{ij}	95% Confidence Interval	Residual	AAD
Kesler-Lee	0.110	0.004	15.5	6.8%
Cavett	0.16	0.01	66.2	14.5%
Sim-Daubert	0.120	0.004	17.0	7.2%
Whitson	0.103	0.004	16.9	7.1%
Twu	0.122	0.005	19.5	7.7%
Watanasiri	0.122	0.004	16.8	7.0%

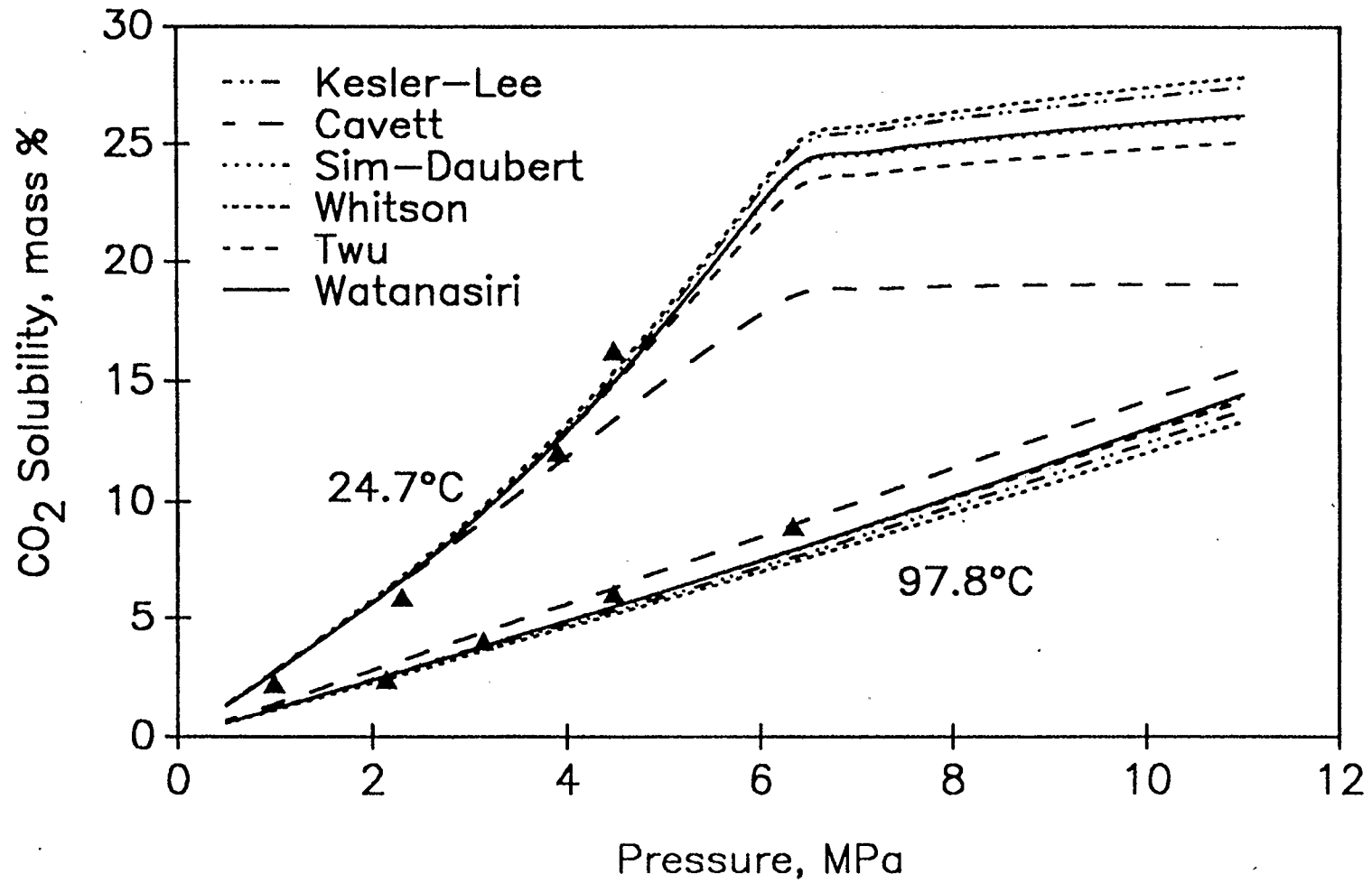


Figure 6.6: Cut 1 CO₂-Solubility Data Correlated with the P-R EOS

Five of the six characterizations gave similar results. The residual value of 66.2 obtained with the Cavett characterization is very much higher than the values obtained with the other characterizations. In Figure 6.6, it appears that this characterization tends to under-predict the effect of temperature on the solubility, and hence the residual is quite high. This is most noticeable when the room-temperature isotherm is extrapolated into the liquid-CO₂ region and the predicted solubility values fall off markedly from those predicted by the other correlations. A possible explanation for this behaviour may be found in Figures 6.1 and 6.2, where the estimated critical temperature of Cut 1 from the Cavett correlation is 200 K higher than those from the other correlations, and the estimated critical pressure is very high as well.

6.5.2 Correlation of Cut 2 Solubility Data

Correlation of Cut 2 solubility data with the six Cut 2 characterizations gave much more consistent results than the correlations for Cut 1. The residuals for all six characterizations (shown in Table 6.6) are below the degrees of freedom in the model. The isotherms shown in Figure 6.7 (at 24.5°C and 101.5°C) are very similar as well. Even the Cavett characterization correlates the data well, and as shown in Figures 6.1 and 6.2, the critical temperature estimation for Cut 2 is no less anomalous than it is for Cut 1. The critical pressure estimate, however, is similar to the estimates from the other correlations.

TABLE 6.6
 Comparison of Characterizations for the Correlation of
 Cut 2 Solubility Data with the P-R EOS

Characterization	Optimized k_{ij}	95% Confidence Interval	Residual	AAD
Kesler-Lee	0.10001	$1(10^{-5})$	7.6	3.6%
Cavett	0.089	0.003	15.9	4.7%
Sim-Daubert	0.1062	0.0007	5.6	3.2%
Whitson	0.113	0.002	6.0	4.3%
Twu	0.1118	0.0004	6.1	4.2%
Watanasiri	0.105	0.001	6.5	3.6%

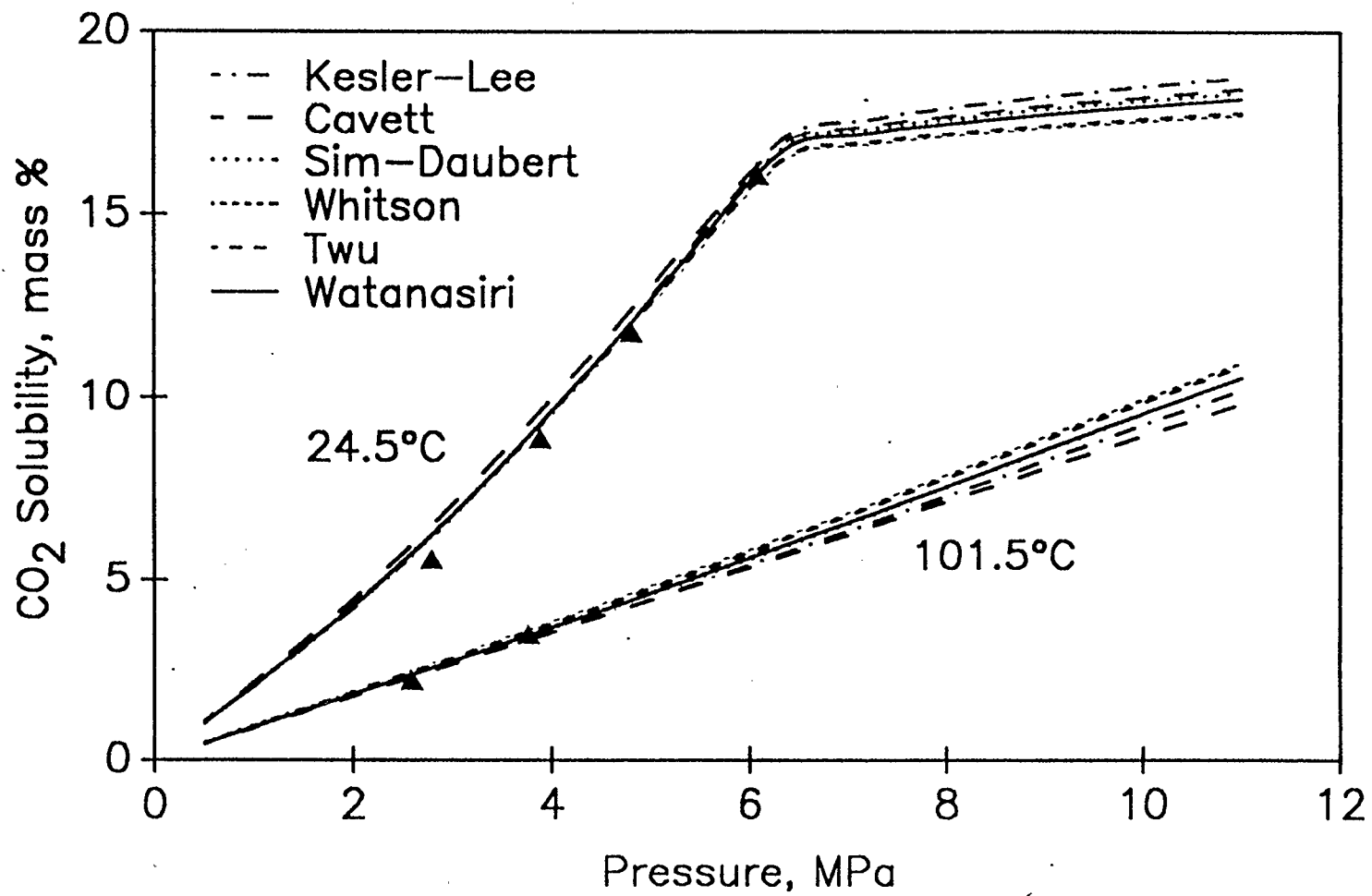


Figure 6.7: Cut 2 CO₂-Solubility Data Correlated with the P-R EOS

6.5.3 Correlation of Cut 3 Solubility Data

Correlation of the Cut 3 experimental solubility data showed much more varied results than that of the Cut 1 and Cut 2 data. As can be seen in Figure 6.8, some characterizations under-predict the effect of temperature on the CO_2 -solubility, while some over-predict. The Kesler-Lee characterization provides the best correlation (a residual of 15.3), and the Twu characterization also correlates the data well. The results are compared in Table 6.7.

6.5.4 Correlation of Cut 4 Solubility Data

Results of the correlation of the Cut 4 data are given in Table 6.8, and are plotted in Figure 6.9. Once again, the effect of temperature is over-predicted by some characterizations (such as Cavett and Sim-Daubert) and is under-predicted by others (such as Watanasiri). For this cut, the characterizations that provided the best results were those from the Kesler-Lee and the Whitson correlations.

6.5.5 Correlation of Cut 5 Solubility Data

Only four characterizations were used to correlate the Cut 5 experimental data. The Whitson and Watanasiri characterizations were omitted because of their low critical pressure estimations, which proved to be difficult to use in the calculations. That is, flash calculations would not converge for a number of data points. Results are given in Table 6.9 and in Figure 6.10. Surprisingly, the characterization that gave the best match of the data for this cut was the Cavett characterization.

TABLE 6.7
Comparison of Characterizations for the Correlation of
Cut 3 Solubility Data with the P-R EOS

Characterization	Optimized k_{ij}	95% Confidence Interval	Residual	AAD
Kesler-Lee	0.0907	0.0003	15.3	8.8%
Cavett	0.0585	0.0007	85.0	19.3%
Sim-Daubert	0.0783	0.0002	33.1	13.5%
Whitson	0.1141	0.0004	44.6	8.9%
Twu	0.0891	0.0004	16.3	9.2%
Watanasiri	0.132	0.002	91.6	11.8%

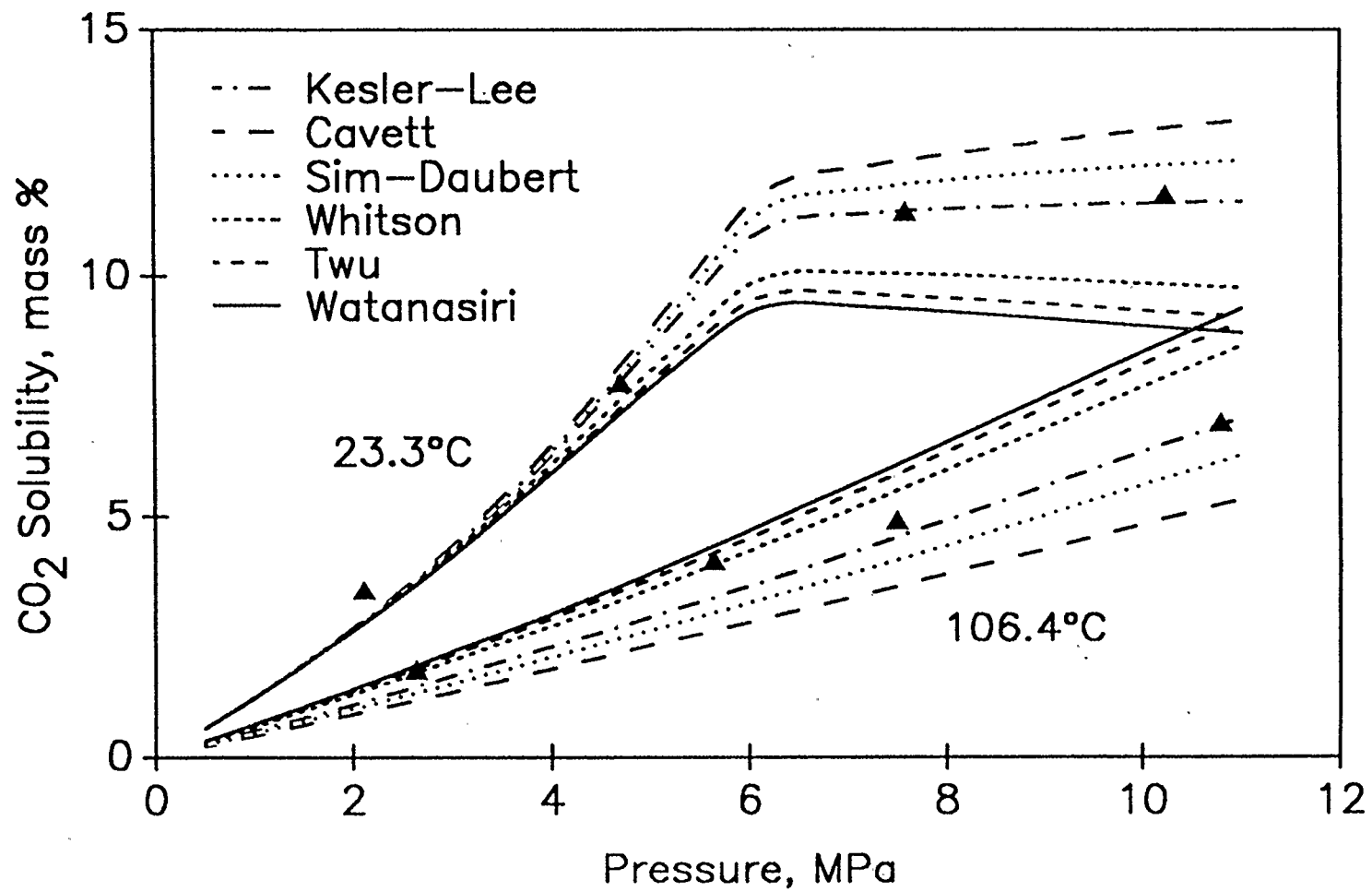


Figure 6.8: Cut 3 CO₂-Solubility Data Correlated with the P-R EOS

TABLE 6.8
 Comparison of Characterizations for the Correlation of
 Cut 4 Solubility Data with the P-R EOS

Characterization	Optimized k_{ij}	95% Confidence Interval	Residual	AAD
Kesler-Lee	0.094	0.006	7.5	8.5%
Cavett	0.0247	0.0001	57.0	20.8%
Sim-Daubert	0.0593	0.0002	25.3	14.9%
Whitson	0.1378	0.0002	6.2	6.9%
Twu	0.0790	0.0001	13.2	11.3%
Watanasiri	0.1947	0.0009	21.3	10.6%

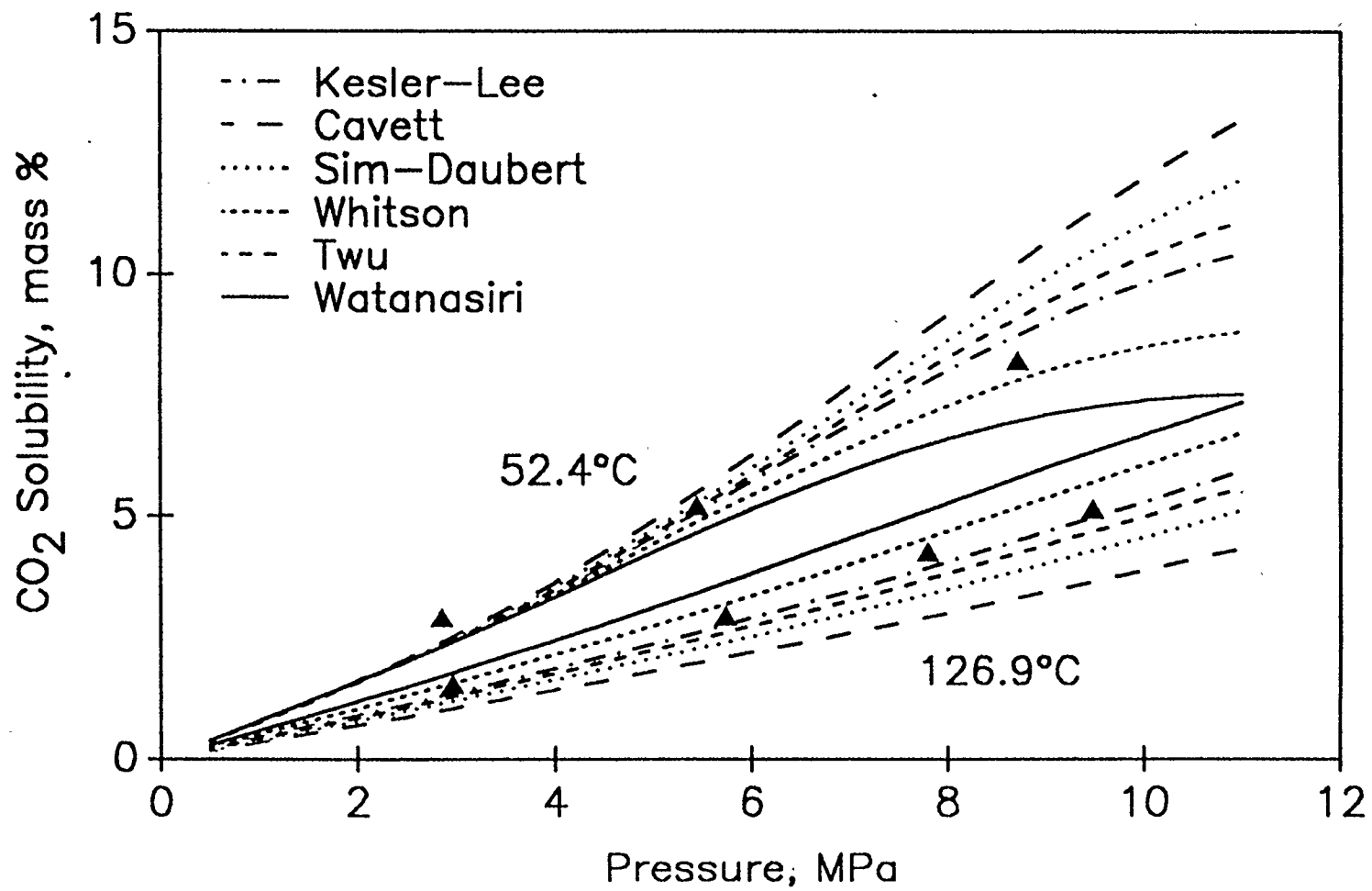


Figure 6.9: Cut 4 CO₂-Solubility Data Correlated with the P-R EOS

TABLE 6.9

Comparison of Characterizations for the Correlation of
Cut 5 Solubility Data with the P-R EOS

Characterization	Optimized k_{ij}	95% Confidence Interval	Residual	AAD
Kesler-Lee	0.05	0.04	15.7	23.4%
Cavett	-0.23	0.02	13.0	24.7%
Sim-Daubert	-0.09	0.03	16.6	25.7%
Twu	-0.12	0.03	16.5	26.1%

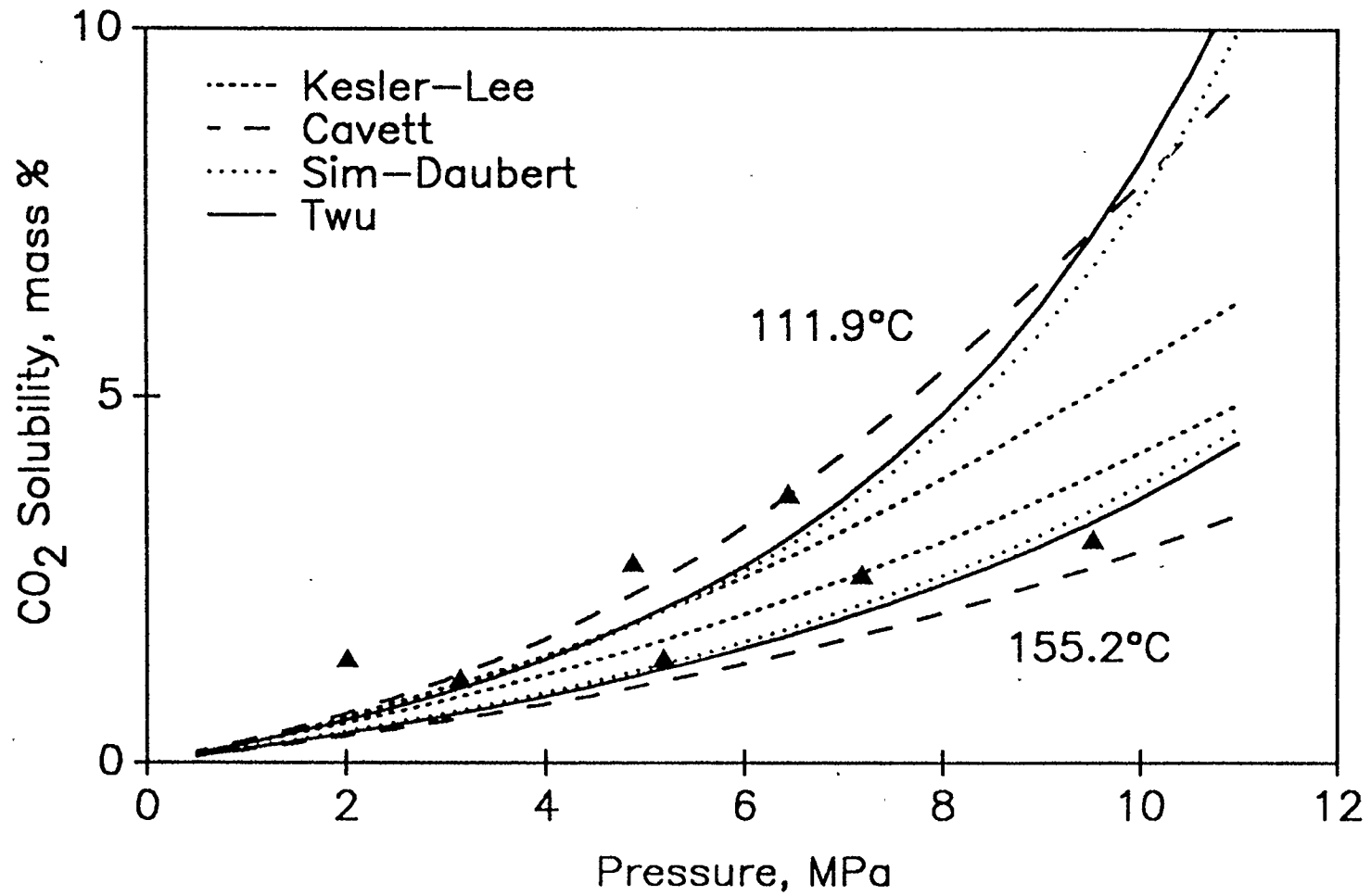


Figure 6.10: Cut 5 CO₂-Solubility Data Correlated with the P-R EOS

6.6 Temperature-Dependence of the Interaction Parameter

As can be seen in Figure 6.4, the prediction of the effect of temperature on the solubility of CO_2 in the bitumen varies from characterization to characterization. If the interaction parameter is allowed to vary with temperature, it is likely that correlation would be improved. To investigate temperature dependence in the CO_2 -pseudocomponent interaction parameter, the following equation was chosen:

$$k_{ij} = k_{\alpha} + k_{\beta} \cdot (T - 25) \quad (6.5)$$

where T is the temperature in $^{\circ}\text{C}$.

Results for the correlation of the whole bitumen data with Equation 6.5 are given in Table 6.10. In almost all cases, correlation of the data is improved — the sole exception being the Twu characterization, for which no improvement was observed. There is no consistency, however, in the values of k_{β} obtained for the characterizations: For three of the characterizations positive values are obtained, while for two others negative values are obtained. For the Cavett characterization, this variation in temperature resulted in an interaction parameter of 0.0580 at 25°C and a value of -0.0049 at 100°C . At the other end of the spectrum, for the Watanasiri characterization, values of 0.1180 and 0.1558 were obtained for the same temperatures.

TABLE 6.10

Comparison of Characterizations for the Correlation of Whole Bitumen Solubility Data
with Temperature Dependent Interaction Parameters

Characterization	Optimized k_{α}	95% Confidence Interval	Optimized k_{β}	95% Confidence Interval	Residual	AAD
Kesler-Lee	0.089	0.003	-0.0002	0.0001	11.8	7.2%
Cavett	0.079	0.006	-0.0008	0.0002	36.1	9.5%
Sim-Daubert	0.085	0.003	-0.0004	0.0001	11.7	7.3%
Whitson	0.104	0.003	0.0003	0.0001	5.2	4.8%
Twu	0.091	0.004	0.0000	0.0002	13.9	8.4%
Watanasiri	0.108	0.003	0.0004	0.0001	4.8	4.4%

Correlated with the P-R EOS

Because of the inconsistency of the k_{β} values obtained for these characterizations of the whole bitumen, and because similar results were obtained for the other cuts, no calculations were made with temperature dependent CO_2 -pseudocomponent interaction parameters with the P-R EOS. Suffice it to say that improvements can be made if temperature dependence is introduced, but no real trends are observed in the correlations. It would appear that introducing this dependence only overcomes the inability of the characterizations to accurately correlate the data.

6.7 Correlation of Density Data

Although the P-T EOS was found to be inferior in correlating CO_2 -solubility data, the introduction of a variable critical compressibility factor makes it much better suited to correlate the gas-saturated density data than either the P-R or S-R-K equations. The density values obtained from the P-T EOS were, however, not very good when the characterizations of Chapter 5 were used. For example, when the Cut 4 solubility data were correlated, density predictions for the first data point (54°C , 8 720 kPa) ranged from 1 098 kg/m^3 (Cavett) to 296 kg/m^3 (Watanasiri). The experimental value is 1 020 kg/m^3 .

In an attempt to improve the correlation of the density data, a sensitivity analysis of the characterization parameters (T_c , P_c , ω , and k_{ij}) showed that density predictions were sensitive to the critical constants and the acentric factor, but not to the interaction parameter. The interaction parameter could therefore not be considered a candidate for improving density predictions. Only one correlation is available for the acentric factor, and the estimates for the six samples do not appear

unreasonable; hence, this parameter is excluded as well. Of the two critical properties, the critical pressure estimates, particularly for the heavier cuts, appear to behave more unreasonably than the critical temperature estimates.

It was postulated that the critical pressure of a bitumen fraction could be estimated by matching the density data. The solubility data could then be correlated by optimizing the interaction parameter. The optimized critical pressures could also be compared for the different characterizations, since at this point the only thing that would differentiate the characterizations would be the critical temperature estimates. Ultimately, this approach may result in some sort of relationship between critical temperature and critical pressure of the cut.

6.7.1 Estimation of Critical Pressure from Density Data

Correlation of the experimental density data was performed in the following manner: A binary interaction parameter was regressed to correlate the solubility data; the critical pressure of the pseudocomponent was regressed to correlate the density data; and finally, the interaction parameter was again regressed to match the solubility data.

Unfortunately, the prediction of the effect of temperature on the CO₂-solubility is under-predicted. Because of this, only the optimized critical pressure values were correlated in terms of the critical temperature and molar mass of the pseudocomponent with the following equation:

$$P_c = \left(267\,155 + 142.3 \cdot T_c \right) \cdot MW^{-1} \quad (6.6)$$

where T_c is in Kelvin and MW is in g/mol.

While the density of the cuts has been correlated to within 5% of the experimental data, the true variation of the density with temperature is not accurately modeled. It can be seen in Figure 6.11 that the predicted variation in the density is slight compared with the variations indicated by the data. As a result of this observation, it was decided a temperature dependence in the b -term of the P-T EOS would be appropriate. The form of temperature dependence chosen was that of Trebble and Bishnoi (1987):

$$b = b_c \cdot \beta(T) \quad (6.7)$$

where

$$\beta(T) = 1 + q \cdot \left(1 - T_r + \ln(T_r) \right) \quad T \leq T_c \quad (6.8)$$

$$\beta(T) = 1 \quad T > T_c \quad (6.9)$$

The value of q is obtained from:

$$q = 0.17959 + 0.23471\omega \quad (6.10)$$

The addition of this form of temperature dependence in the b -term of the P-T EOS was found to improve the correlation of the density data for the whole bitumen and Cuts 1 and 2, but the effect of temperature on the density of Cuts 3, 4, and 5 was found to be over-predicted. Correlation of the CO₂-solubility was still quite inadequate, as was the case when only the solubility data were being correlated. As such, temperature dependence in the CO₂-pseudocomponent interaction parameter (Equation 6.5) was included as well.

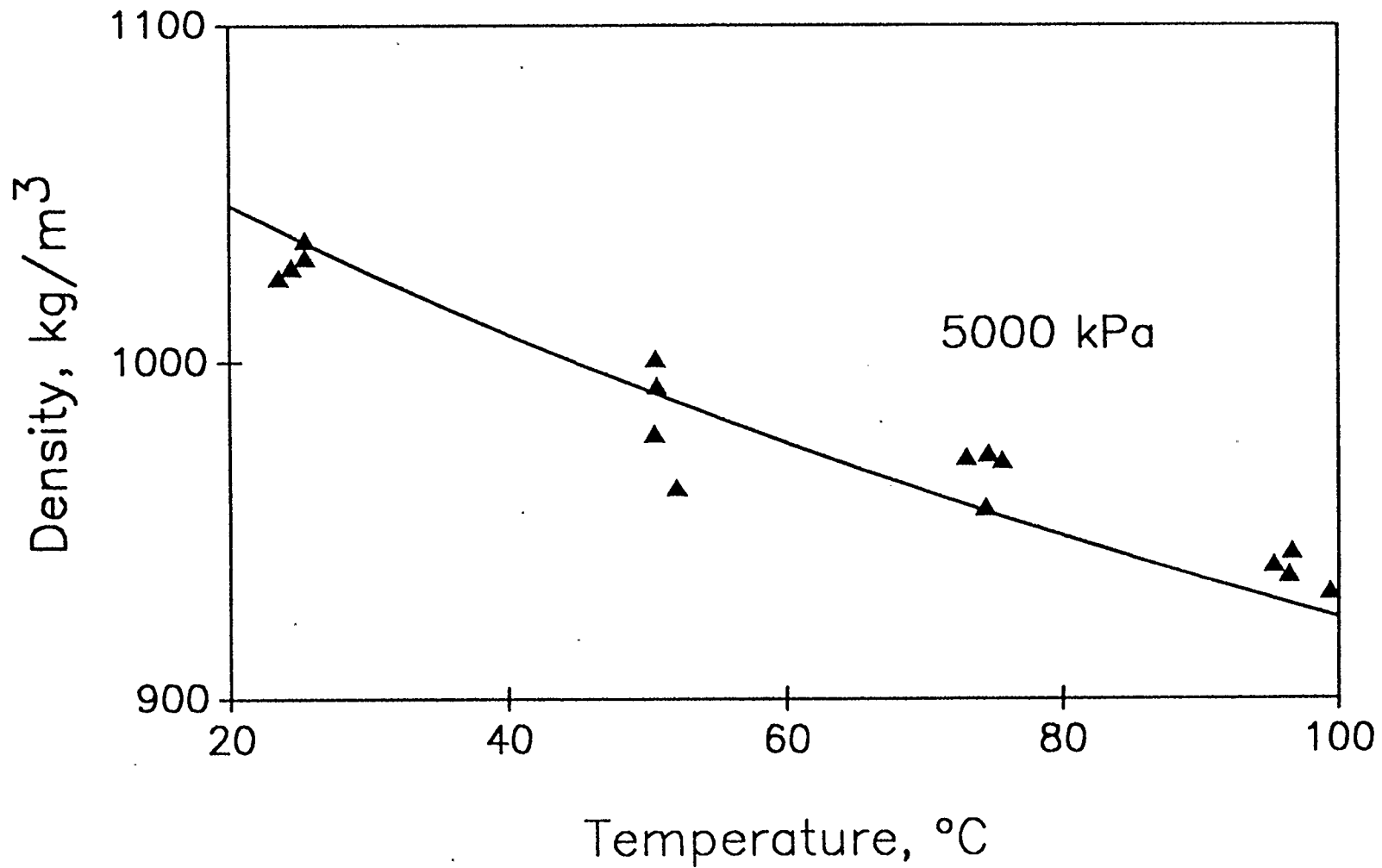


Figure 6.11: Cut 3 Density Data Correlated with the P-T EOS and the Kesler-Lee Characterization

Shown in Table 6.11 are the characterizations that gave the lowest overall residual (the sum of the density and the solubility residuals) for each cut. Regressed critical pressures and interaction parameters are given in Appendix C. Figures 6.12 through 6.17 show density data correlated with the characterization that provided the lowest residual for each cut.

The pseudocomponent critical pressures obtained from the correlation of the density data for the cuts may be again correlated with the following equation:

$$P_c = \left(58\,615 + 472.3 \cdot T_c \right) \cdot MW^{-1} \quad (6.11)$$

where P_c is in kPa, and T_c is in Kelvin. The correlation coefficient is about 0.98 for this equation. Unfortunately, there are no trends in the values obtained for k_α and k_β .

6.8 Use of Regressed Critical Pressure with the P-R EOS

In an attempt to generalize interaction parameters regressed with the P-R EOS (Tables 6.4 through 6.8) in terms of some readily measurable property of the cuts, it was found that trends in the parameters did not extend to the heavier cuts, as the optimization used the parameters to overcome errors introduced by unreasonable characterizations. To alleviate this problem, the critical pressure correlation obtained in the previous section (Equation 6.6) was used to estimate the pseudocomponent critical pressures, and the solubility data were recorrelated with the P-R EOS.

TABLE 6.11
Correlation of Sample Solubility and Density Data
with the P-T EOS

Sample	Characterization	Residual	AAD solubility	AAD density
whole bitumen	Kesler-Lee	55.8	9.6%	1.1%
Cut 1	Watanasiri	143.8	6.9%	2.1%
Cut 2	Sim-Daubert	73.4	3.6%	1.4%
Cut 3	Kesler-Lee	206.2	12.2%	2.3%
Cut 4	Twu	197.2	14.8%	2.3%
Cut 5	Cavett	765.4	28.1%	5.7%

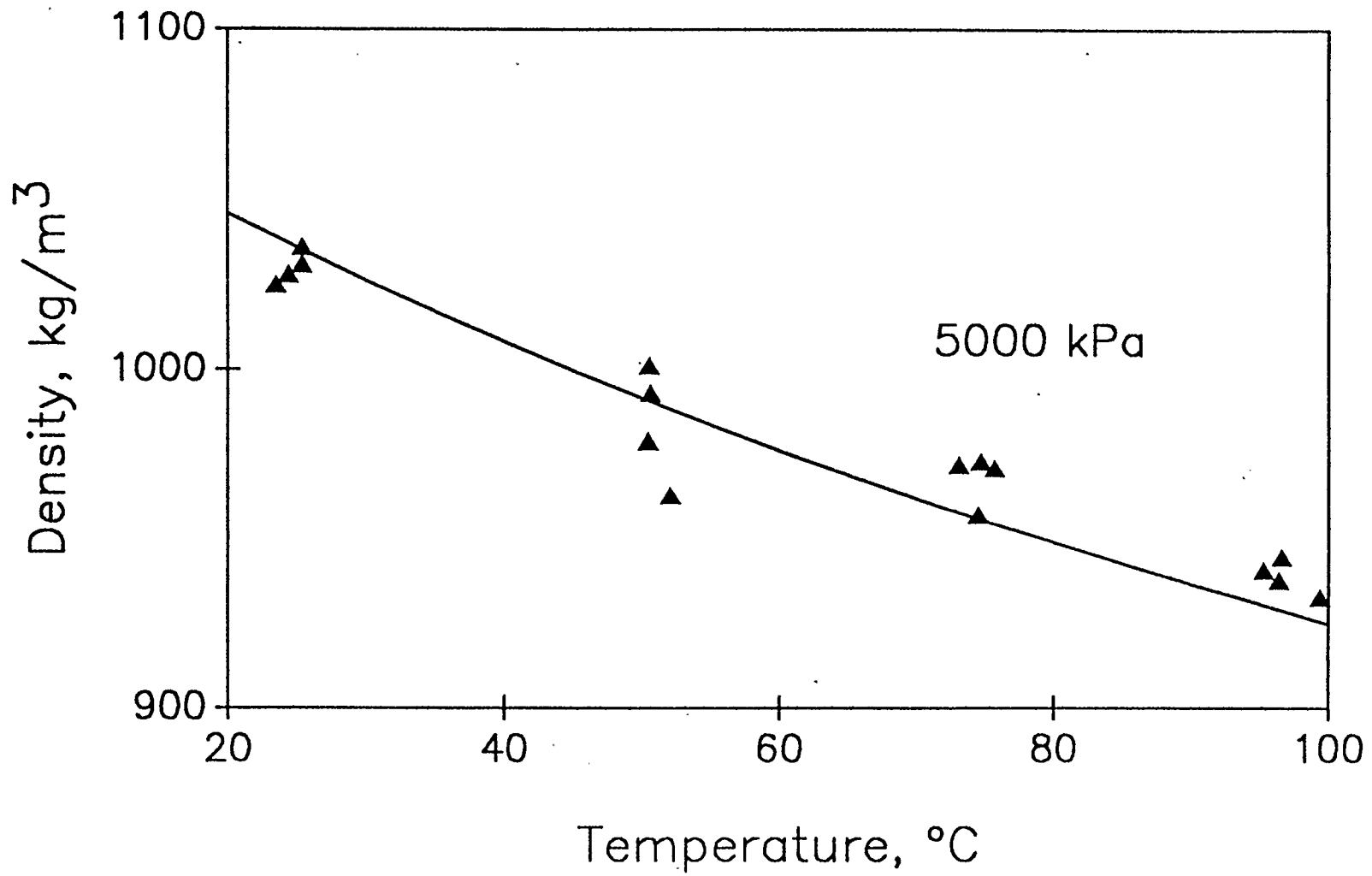


Figure 6.12: Whole Bitumen CO₂-Solubility and Density Data Correlated with the P-T EOS

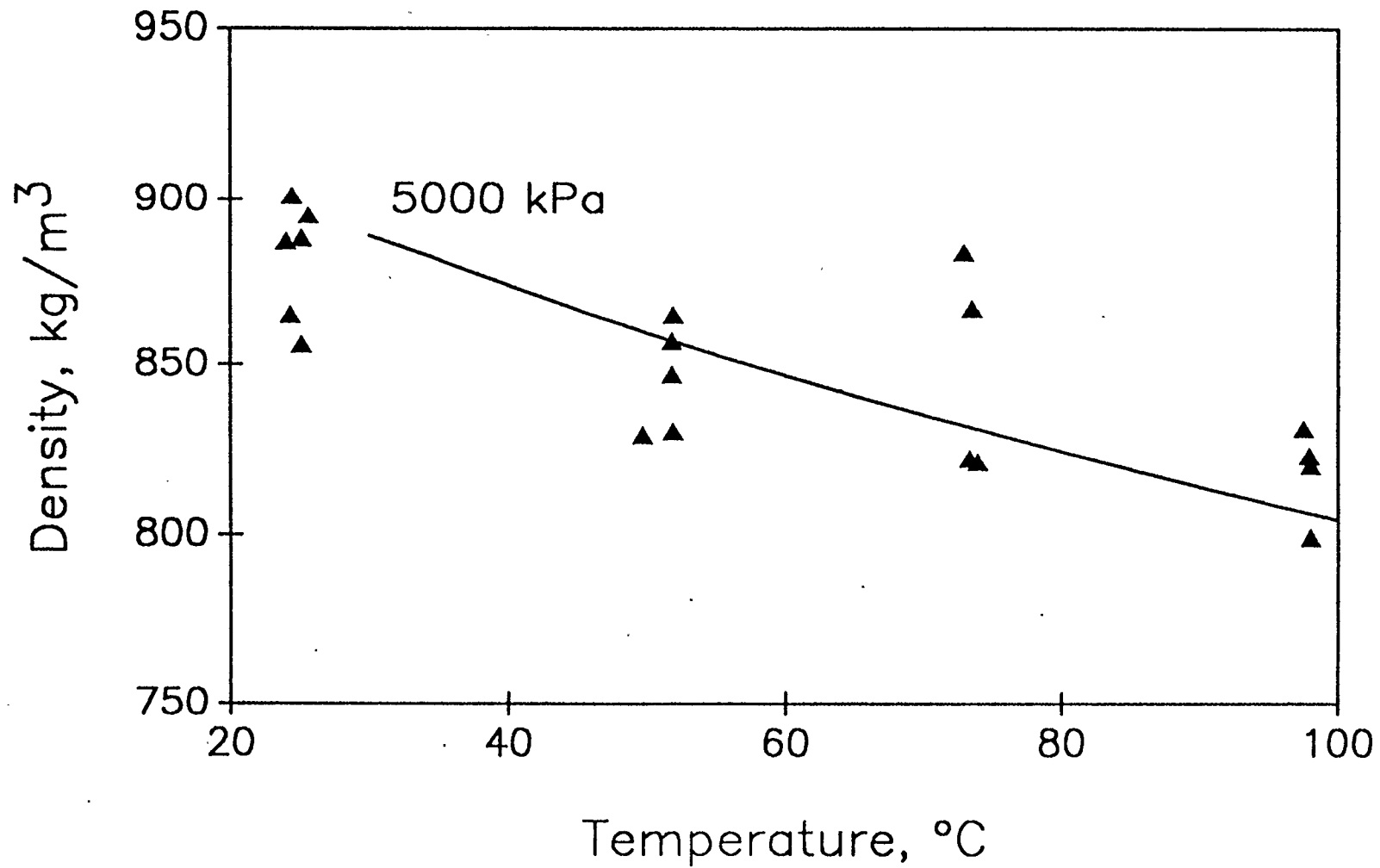


Figure 6.13: Cut 1 CO₂-Solubility and Density Data Correlated with the P-T EOS

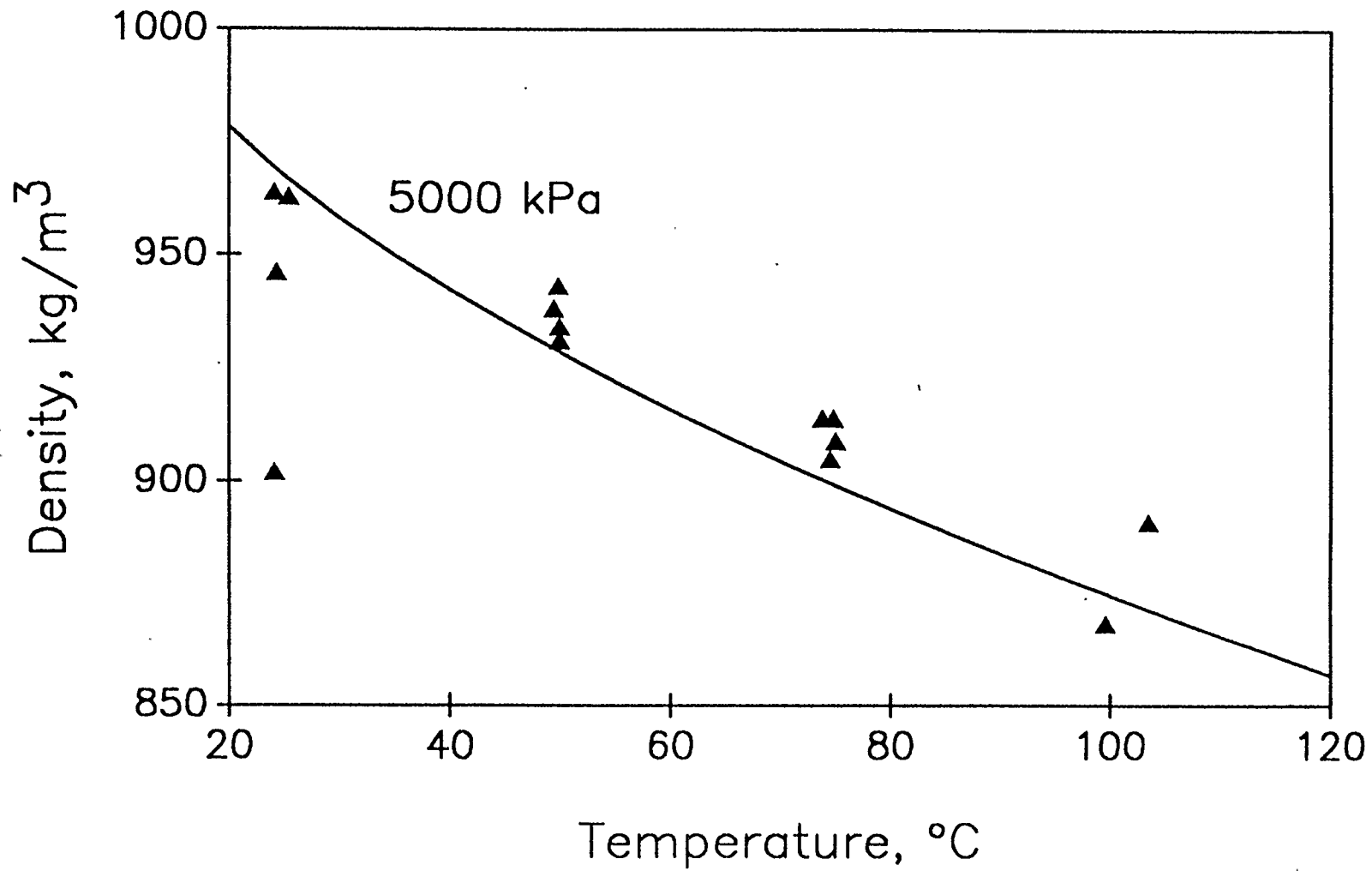


Figure 6.14: Cut 2 CO₂-Solubility and Density Data Correlated with the P-T EOS

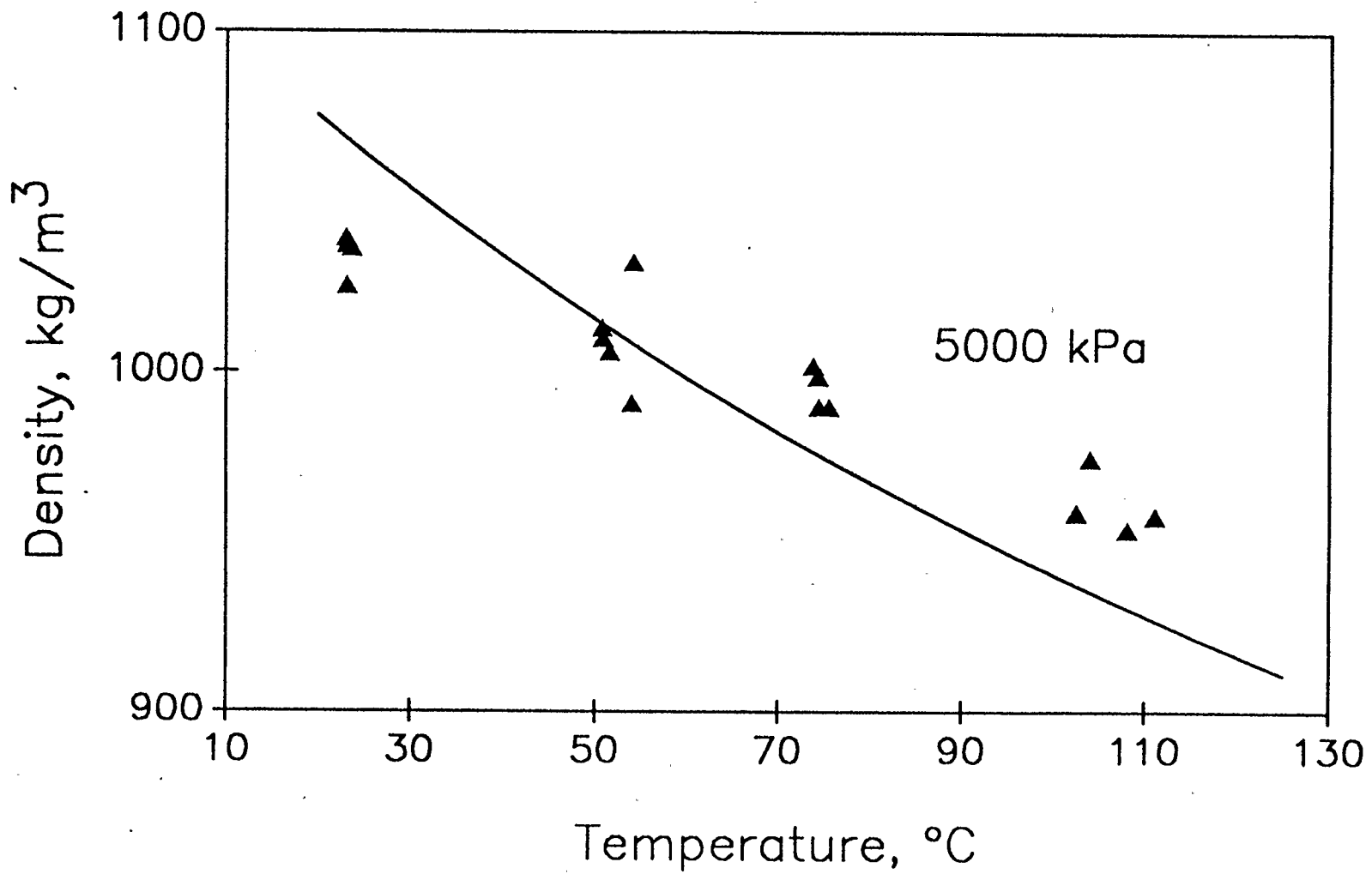


Figure 6.15: Cut 3 CO₂-Solubility and Density Data Correlated with the P-T EOS

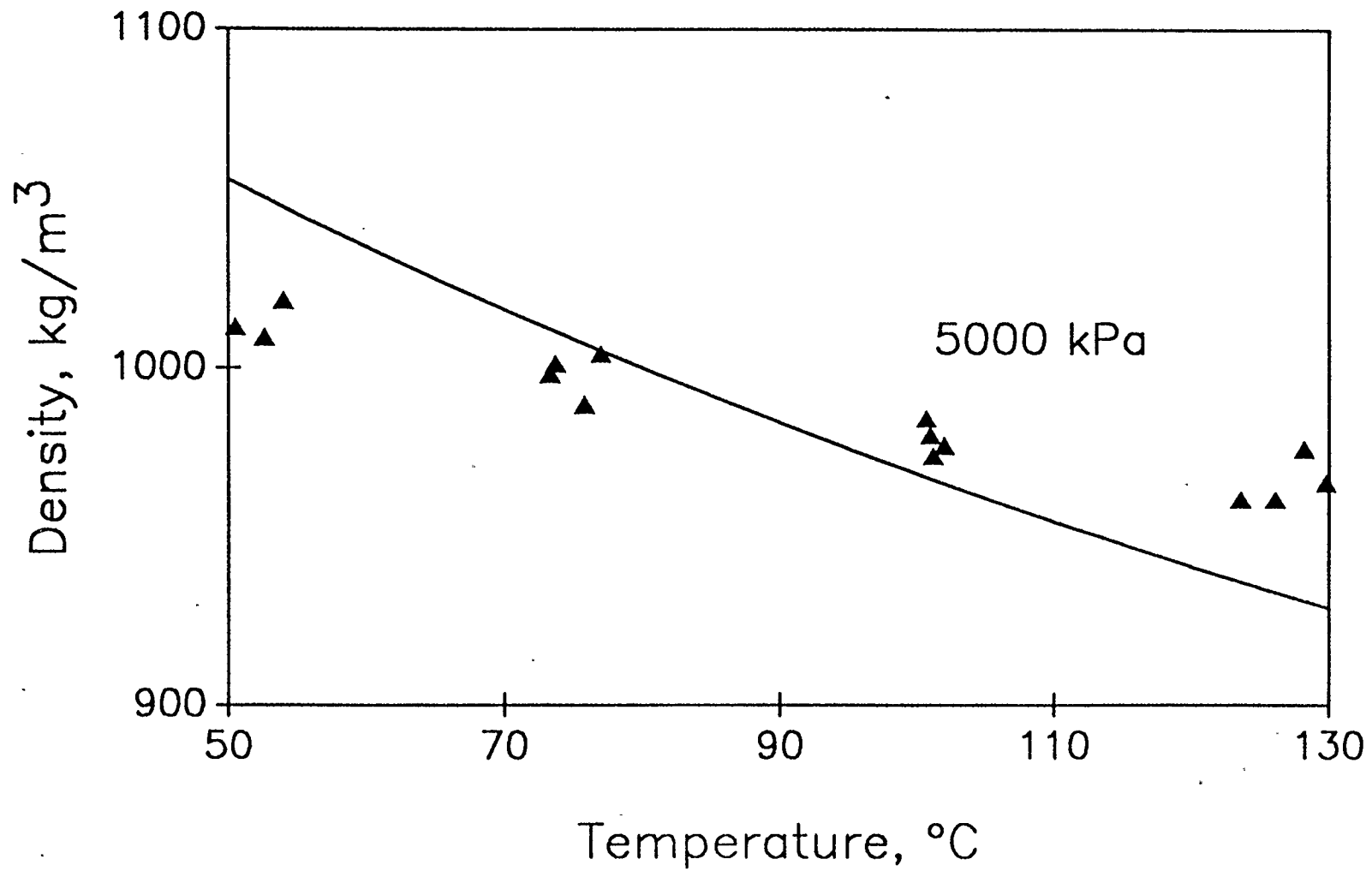


Figure 6.16: Cut 4 CO₂-Solubility and Density Data Correlated with the P-T EOS

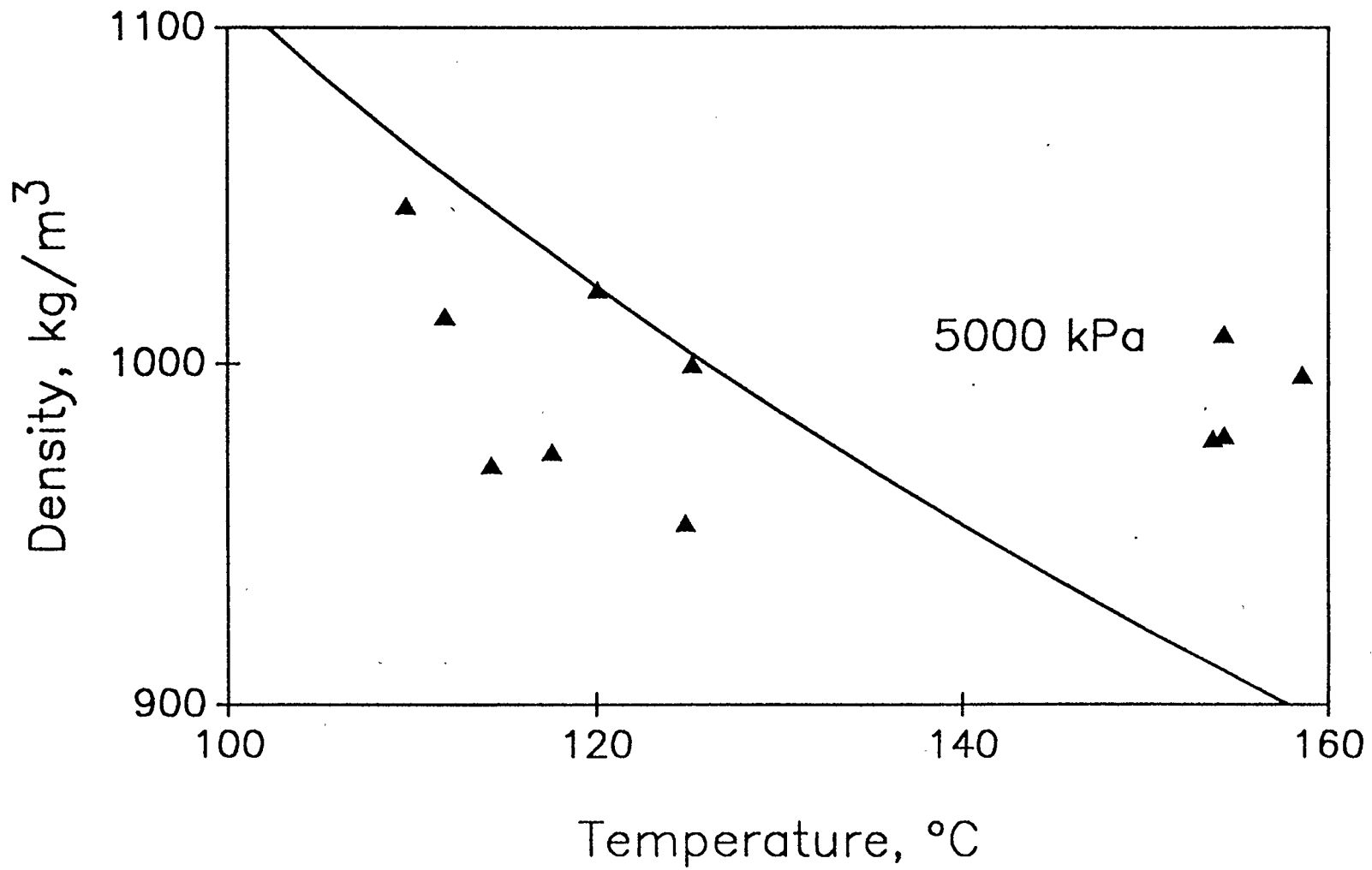


Figure 6.17: Cut 5 CO₂-Solubility and Density Data Correlated with the P-T EOS

The CO₂-pseudocomponent interaction parameters resulting from this correlation show consistent trends from cut to cut for all of the characterizations considered. These parameters may themselves be correlated with the following equation:

$$k_{ij} = 0.1255 - 1.71(10^{-6}) MW T_c^{0.5} \quad (6.12)$$

where MW is the molar mass of the pseudocomponent, and T_c is the critical temperature of the pseudocomponent in Kelvin. Figures 6.18 and 6.19 show the data for Cuts 2 and 4 correlated with the P-R EOS and Equations 6.11 and 6.12.

Densities of the gas-saturated fractions as predicted by the P-R EOS with the use of Equation 6.6 were very consistent, although inaccurate. Values deviating by approximately 20% of the experimental densities were obtained, which is expected from the P-R EOS.

6.9 Summary

The performance of the critical property correlations examined in this work varied from cut to cut, but a few general statements still may be made.

All correlations provided realistic estimates of the critical temperatures of the cuts, but the estimates from the Cavett correlation clearly do not have enough variation from cut to cut. As a result, the Cavett characterizations generally could not correlate the data as well as the other characterizations.

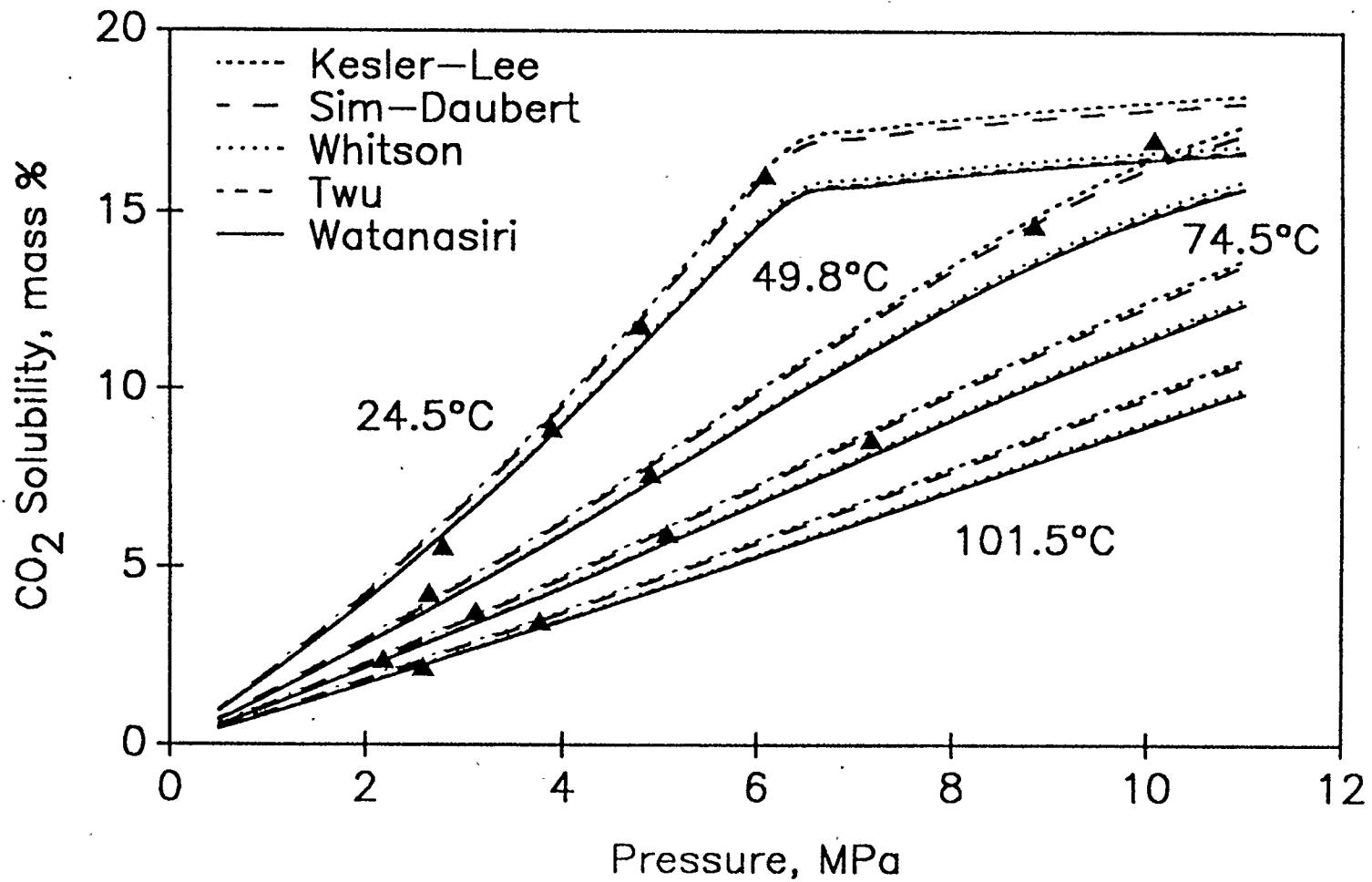


Figure 6.18: Cut 2 CO₂-Solubility Data Correlated with the P-R EOS and P_c Estimated from Equation 6.6

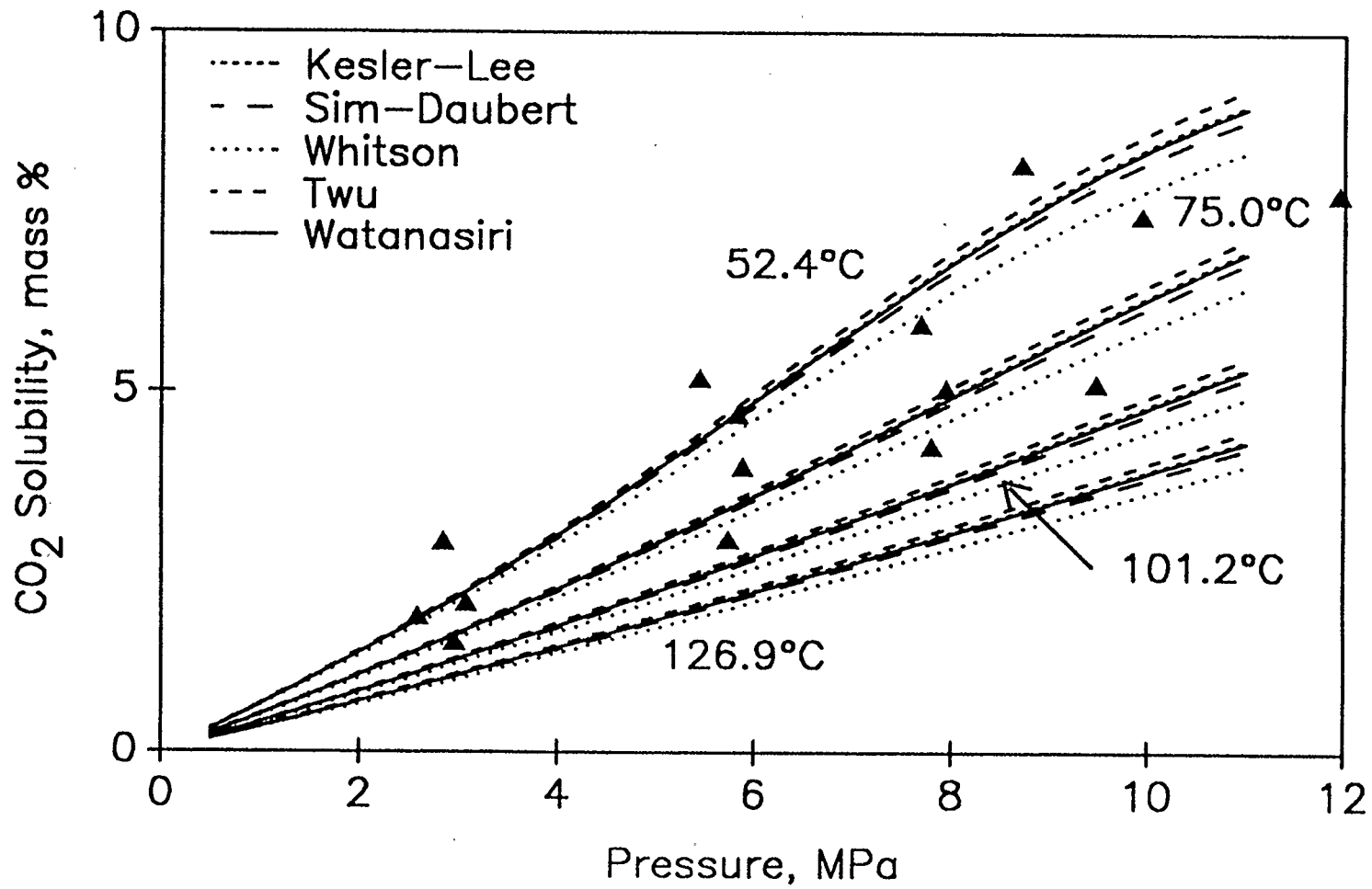


Figure 6.19: Cut 4 CO₂-Solubility Data Correlated with the P-R EOS and P_c Estimated from Equation 6.6

The estimates of critical pressure provided by the six correlations for the lighter cuts, while varied, may all be considered realistic. For the heavier cuts, especially Cut 5, a number of the correlations give unacceptable estimates. The Kesler-Lee, Whitson, and Watanasiri *et al.* correlations estimate values of P_c that are much too low. The Cavett correlation, as has been noted, gives an estimate for Cut 5 that is higher than that of Cut 4, and this was found to give unreasonable density predictions. The correlations of Sim and Daubert and of Twu gave quite good estimates, but it should be noted that further extrapolation of the Twu correlation may cause problems because of the negative values of α in Equation 2.18.

The correlations of optimized critical pressures (Equations 6.6 and 6.11) provide much more reasonable estimates of the critical pressure of the heavier cuts. These correlations have been developed with only the data from this work, and extrapolation to other characterizations and other bitumens may not be justified. In fact, the form of these equations suggest that some sort of inversion in P_c estimations for heavier cuts may occur (as with the Cavett and Twu correlations) if the ratio of T_c to MW were to vary differently than as was found in this project.

As only one correlation of acentric factor of the three examined was found to give consistent estimations for all five cuts, no real conclusions may be made about its validity. The estimations did appear realistic, however.

The correlation of the CO_2 -pseudocomponent interaction parameters

given by Equation 6.12 appears to accurately correlate the data regardless of the characterization used. This is, of course, assuming that the characterization is representative of the cut, and that the interaction parameter is not being used to overcome inadequacies in the characterization.

CHAPTER 7

WHOLE BITUMEN GAS-SOLUBILITY PREDICTIONS

While the CO_2 -solubility and density of the whole bitumen was successfully correlated in Chapter 6 using characterizations consisting of a single pseudocomponent, the method cannot be called truly predictive. Furthermore, the use of a single pseudocomponent characterization to represent the bitumen limits the applicability of the characterization to cases where no separation of the bitumen will occur.

To develop a characterization of the bitumen that may be extended to other property predictions, and that could be used in calculations in a truly predictive manner, more than just one pseudocomponent is required to represent the bitumen. With the information about the bitumen fractions obtained by correlating the CO_2 -solubility data, a characterization consisting of five pseudocomponents — each of which represents one of the cuts — would be ideal. Since this type of characterization would be composed of pseudocomponents which represent actual fractions of the bitumen, and not just theoretical fractions, one would expect that predictions of the whole bitumen behaviour would be quite accurate. Any inaccuracies could possibly be attributed to interactions amongst constituents in the bitumen.

To check the validity of this predictive type of calculation, six different characterizations of the whole bitumen were used to predict the CO_2 -solubility of the whole bitumen. Each characterization consisted of the five pseudocomponents used to correlate the solubility data of the

cuts. The six different characterizations arose from the six critical property correlations used for the pseudocomponents. As such, the characterizations were called the Kesler-Lee, Cavett, Sim-Daubert, Whitson, Twu, and Watanasiri characterizations.

The critical temperatures of the pseudocomponents were estimated from the critical temperature correlations outlined in Chapter 2, as were the acentric factors. The critical pressures were estimated with Equation 6.6, and binary interaction parameters for each CO₂-pseudocomponent pair were estimated from Equation 6.12. Initially, pseudocomponent-pseudocomponent binary interaction parameters were assumed to be zero. The P-R EOS was used for calculating the CO₂-solubility.

Unfortunately, the behaviour of the CO₂-saturated whole bitumen predicted by this method did not match the experimental data in Table 5.1. Generally, predictions of CO₂-solubility differed a great deal from the data, and in the liquid-CO₂ region separation of Cut 5 from the rest of the bitumen was predicted. It became apparent that interactions between the bitumen constituents could not be ignored.

To represent these interactions, a number of schemes to generate pseudocomponent-pseudocomponent interaction parameters were investigated. The following equation was found to work the best:

$$k_{i,j} = \left[-4.2155 + 0.001108T + 1.955(10^{-4})T^2 \right] \cdot \left| MW_i - MW_j \right|^{0.5} / 1000 \quad (7.1)$$

Here, T is the temperature in Celsius, $|MW_i - MW_j|$ represents the differences in molar masses between the pseudocomponents. This correla-

tion was arrived at by regressing values of $(MW_H - MW_L)^{0.5} / 1000$ for the data points at each of the four temperatures, and then correlating these values in terms of a polynomial. Typical values range from -0.195 for Cut 1-Cut 5 interaction at 25°C, to -0.022 for Cut 1-Cut 2 interaction at 25°C.

The introduction of Equation 7.1 dramatically improved the CO₂-solubility predictions generated by five of the six characterizations. The exception was the Cavett correlation, for which radically different parameters in the first term of Equation 7.1 were required. Average absolute deviations in predictions of the whole bitumen solubility data for these five characterizations are given in Table 7.1. A plot of the predictions is given in Figure 7.1.

TABLE 7.1
Prediction of Whole Bitumen Solubility Data using
Five-Pseudocomponent Characterizations

Characterization	Residual	AAD
Kesler-Lee	6.9	5.8%
Cavett	241.1	23.5%
Sim-Daubert	7.7	5.9%
Whitson	17.3	8.2%
Twu	12.8	6.8%
Watanasiri	9.8	6.6%

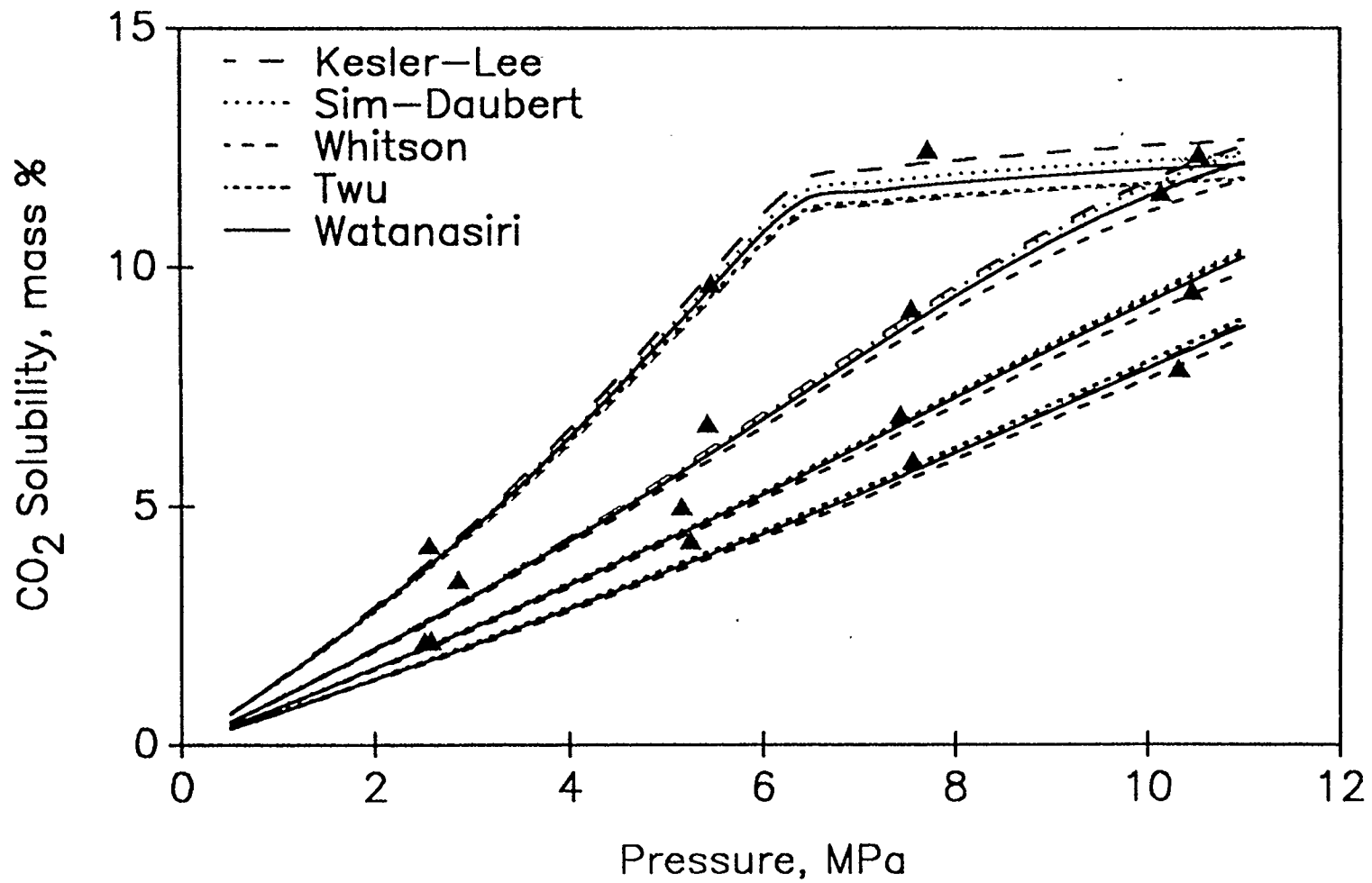


Figure 7.1: Whole Bitumen CO₂-Solubility Predictions

CONCLUSIONS AND RECOMMENDATIONS

Conclusions

A number of conclusions may be made about the data provided in this work, and about the correlation of that data. First, the behaviour of CO_2 -saturated bitumen fractions is similar to the behaviour of CO_2 -saturated whole bitumen, in terms of the dramatic decrease in viscosity and the phase behaviour. This similarity is more apparent with the heavier cuts than with the lighter cuts.

A double-log correlation used to correlate gas-free bitumen viscosity in the past was found to correlate the bitumen fraction viscosity data as well. The results suggest a possible relationship between the parameters in the correlation and the fraction molar mass. A simple mixing rule for bitumen fractions that considers the molar mass of the fractions was proposed.

The correlation of the CO_2 -solubility data was successfully performed using equation-of-state based methods, with the cuts represented by pseudocomponents. Six different correlations were used to estimate the critical properties of the pseudocomponents, and all were found to adequately correlate the data. The optimized binary interaction parameters, however, did not show any trends with respect to the cuts.

The Patel-Teja equation-of-state was found to be inferior to the Peng-Robinson and Soave-Redlich-Kwong equations for correlating the CO_2 -solubility of the cuts. The P-T EOS was found to correlate the density of the cuts well when the critical pressures of the pseudocompo-

nents were optimized. It did not, however, adequately correlate the effect of temperature on the density. The use of a temperature dependent b -term in the EOS improved the correlation of the density data for the lighter cuts, but significantly over-predicted the effect on the heavier cuts. Temperature dependence in the CO_2 -pseudocomponent binary interaction parameters was required to adequately correlate the CO_2 -solubility data.

Pseudocomponent critical pressures obtained from regression of the density data with the P-T EOS were found to be well correlated in terms of the molar mass and critical temperature of the pseudocomponent. When these critical pressures were used with the P-R EOS to correlate the solubility data, the regressed interaction parameters were found to exhibit trends that could be correlated in terms of the molar mass and critical temperature of the pseudocomponent as well.

The pseudocomponents used to correlate the CO_2 -solubility data of the fractions were successfully used in a five-pseudocomponent bitumen characterization to predict the solubility of CO_2 in the whole bitumen. Interactions between the pseudocomponents were taken into account with a proposed correlation for pseudocomponent-pseudocomponent interaction in terms of the critical temperatures and molar masses of the pseudocomponents.

Recommendations

A number of questions are still left unanswered, and only further work in this area will put them to rest. First, the results of the

correlation of the data can really only be applied to the CO₂-Cold Lake bitumen system. More work is needed with other bitumens and other gases to validate the trends that were observed in this work.

A second area which may benefit from further exploration is the use of the Patel-Teja equation to correlate both the CO₂-solubility and the density data. The introduction of temperature dependence to the *b*-term in the EOS improves correlation of the density of the lighter cuts, but correlation of the solubility still requires temperature-dependent interaction parameters.

A third area which requires more investigation is the interactions between the bitumen constituents. The best way to investigate this further would be to examine fractions of other bitumens, or to examine the dissolution of other gases in bitumen fractions.

Finally, an area that was left untouched in this work is the correlation of the gas-saturated bitumen fraction viscosities. The dramatic variations in viscosity between the cuts could provide the information required to refine bitumen viscosity prediction methods.

REFERENCES

- Bishnoi, P.R., R.A. Heidemann, and M.K. Shah, "Calculation of Thermodynamic Properties of Bitumen Systems", The Oil Sands of Canada-Venezuela Symposium Proceedings, CIM Special Volume 17, D.A. Redford and A.G. Winestock, Ed. (1977).
- Black, C., and C.H. Twu, "Correlations and Prediction of Thermodynamic Properties for Heavy Petroleum Shale Oils, Tar Sands, and Coal Liquids", AIChE 1983 Spring National Meeting, Houston, U.S.A.
- Cavett, R.H., "Physical Data for Distillation Calculations — Vapor-Liquid Equilibria", 27th mid-year meeting of API, Division of Refining, San Francisco, (1962).
- Eastick, R.R., and A.K. Mehrotra, "Viscosity Data and Correlation for Mixtures of Bitumen Fractions", Submitted to Fuel Processing Technology, June (1989).
- Edmister, W.C., "Applied Hydrocarbon Thermodynamics — Part 4: Compressibility Factors and Equations of State", Petr. Ref., 37(4), pp. 173-179 (1958).
- Fu, C.-T., V.R. Puttagunta, and G. Vilcsak, "Vapor-Liquid Equilibrium Properties for Pseudo-Binary Mixtures of CO₂-Athabasca Bitumen and N₂-Athabasca Bitumen", AOSTRA J. Res., 2(2), pp. 73-81 (1985).
- Fu, C.-T., V.R. Puttagunta, and G. Vilcsak, "Gas Solubility of Methane and Ethane in Cold Lake Bitumen at *in situ* Conditions", J. Can. Pet. Tech., 27(4), pp. 79-85 (1988).
- Fu, C.-T., R. Puttagunta, L. Baumber, and C. Hsi, "Pseudo-critical Properties of Heavy Oils and Bitumens", Fluid Phase Equil., 30, pp. 281-295 (1986).

- Jacobs, F.A., J.K. Donnelly, J. Stanislav, and W.Y. Svrcek, "Viscosity of Gas-saturated Bitumen", *J. Can. Pet. Tech.*, 19(4), pp. 46-50 (1980).
- James, N.E., "A Model for the Prediction of the Solubility of Bitumen in Hydrocarbon Diluents", M. Sc. Thesis, Department of Chemical and Petroleum Engineering, University of Calgary (1987).
- Johnson, S.E., W.Y. Svrcek, and A.K. Mehrotra, "Viscosity Prediction of Athabasca Bitumen Using the Extended Principle of Corresponding States", *Ind. Eng. Chem. Research*, 26(11), pp. 2290-2298 (1987).
- Kesler, M.G. and B.I. Lee, "Improve Prediction of Enthalpy of Fractions", *Hydrocarbon Proc.*, 55(3), pp. 153-158 (1976).
- Khan, M.A.B., A.K. Mehrotra, and W.Y. Svrcek, "Viscosity Models for Gas-Free Athabasca Bitumen", *J. Can. Pet. Tech.*, 23(3), pp. 47-53 (1984).
- Mehrotra, A.K., R.R. Eastick, and W.Y. Svrcek, "Viscosity of Cold Lake Bitumen and its Fractions", *Can. J. Chem. Eng.*, in press (1989a).
- Mehrotra, A.K., G.S. Patience, and W.Y. Svrcek, "Calculation of Gas-Solubility in Wabasca Bitumen", *J. Can. Pet. Tech.*, 28(3), pp. 81-83 (1989b).
- Mehrotra, A.K., M. Sarkar, and W.Y. Svrcek, "Bitumen Density and Gas Solubility Predictions Using the Peng-Robinson Equation of State", *AOSTRA J. Res.*, 1(4), pp. 215-229 (1985).
- Mehrotra, A.K. and W.Y. Svrcek, "Correlations for Properties of Bitumen Saturated with CO₂, CH₄, N₂, and Experiments with Combustion Gas Mixtures", *J. Can. Pet. Tech.*, 21(6) pp. 95-104 (1982).

- Mehrotra, A.K. and W.Y. Svrcek, "Measurement and Correlation of Viscosity, Density and Gas Solubility for Marguerite Lake Bitumen Saturated with Carbon Dioxide", AOSTRA J. Res., 1(1), pp. 51-62 (1984).
- Mehrotra, A.K. and W.Y. Svrcek, "Viscosity, Density and Gas Solubility Data for Oil Sand Bitumens. Part I: Athabasca Bitumen Saturated with CO and C₂H₆", AOSTRA J. Res., 1(4), pp. 263-268 (1985a).
- Mehrotra, A.K. and W.Y. Svrcek, "Viscosity, Density and Gas Solubility Data for Oil Sand Bitumens. Part II: Peace River Bitumen Saturated with N₂, CO, CH₄, CO₂ and C₂H₆", AOSTRA J. Res., 1(4), pp. 269-279 (1985b).
- Mehrotra, A.K. and W.Y. Svrcek, "Viscosity, Density and Gas Solubility Data for Oil Sand Bitumens Part III: Wabasca Bitumen Saturated with N₂, CO, CH₄, CO₂, and C₂H₆", AOSTRA J. Res., 2(2), pp. 83-93 (1985c).
- Mehrotra, A.K. and W.Y. Svrcek, "Corresponding States Method for Calculating Bitumen Viscosity", J. Can. Pet. Tech., 26(5), pp. 60-66 (1987).
- Mehrotra, A.K. and W.Y. Svrcek, "Properties of Cold Lake Bitumen Saturated with Pure Gases and Gas Mixtures", Can. J. Chem. Eng., 66(4), pp. 656-665 (1988a).
- Mehrotra, A.K. and W.Y. Svrcek, "Correlation and Prediction of Gas Solubility in Cold Lake Bitumen", Can. J. Chem. Eng., 66(4), pp. 666-670 (1988b).
- Mehrotra, A.K. and W.Y. Svrcek, "Characterization of Athabasca Bitumen for Gas Solubility Calculations", J. Can. Pet. Tech, 27(6), pp. 107-110 (1988c).
- Nghiem, L.X., K. Aziz, and Y.K. Li, "A Robust Iterative Method for Flash Calculations Using the Soave-Redlich-Kwong or the Peng-Robinson Equation of State", S. Pet. Eng. J., pp. 521-530, June (1983).

- Patel, N.C. and A.S. Teja, "A New Cubic Equation of State for Fluids and Fluid Mixtures", *Chem. Eng. Sci.*, **37**(3), pp. 463-473 (1982).
- Pedersen, K.S., P. Thomassen, and A. Fredenslund, "Thermodynamics of Petroleum Mixtures Containing Heavy Hydrocarbons. 1. Phase Envelope Calculations by Use of the Soave-Redlich-Kwong Equation of State", *I&EC Proc. Des. Dev.*, **23**(1), pp. 163-170 (1984).
- Peng, D.-Y. and D.B. Robinson, "A New Two-Constant Equation of State", *Ind. Eng. Chem. Fundam.*, **15**(1), pp. 59-64 (1976).
- Press, W.H, B.P. Flannery, S.A. Teukolsky, and W.T. Vetterling, "Numerical Recipes in C — The Art of Scientific Computing", Cambridge University Press (1988).
- Reid, R.C., J.M. Prausnitz, and T.K. Sherwood, "The Properties of Gases and Liquids", Second Ed., McGraw Hill (1977).
- Riazi, M.R., and T.E. Daubert, "Simplify Property Predictions", *Hydrocarbon Proc.*, **59**(3), pp. 115-116 (1980).
- Sim, W.J. and T.E. Daubert, "Prediction of Vapor-Liquid Equilibria of Undefined Mixtures", *Ind. Eng. Chem. Process. Des. Dev.*, **19**(3), pp. 386-393 (1980).
- Soave, G., "Equilibrium Constants from a Modified Redlich-Kwong Equation of State", *Chem. Eng. Sci.*, **27**, pp. 1197-1203 (1972).
- Svrcek, W.Y., and A.K. Mehrotra, "Gas Solubility, Viscosity and Density Measurements for Athabasca Bitumen", *J. Can. Pet. Tech.*, **21**(4), pp. 31-38 (1982).
- Svrcek, W.Y., and A.K. Mehrotra, "One Parameter Correlation for Bitumen Viscosity", *Chem. Eng. Res. Des.*, **66**(4), pp. 323-327 (1988).

Svrcek, W.Y., and A.K. Mehrotra, "Properties of Peace River Bitumen Saturated with Field Gas Mixtures", J. Can. Pet. Tech., 28(2), pp. 50-56 (1989).

Treble, M.A., and P.R. Bishnoi, "Development of a New Four-Parameter Cubic Equation of State", Fluid Phase Equil., 35, pp. 1-18 (1987).

Twu, C.H., "An Internally Consistent Correlation for Predicting the Critical Properties and Molecular Weights of Petroleum and Coal-Tar Liquids", Fluid Phase Equil., 16, pp. 137-150 (1984).

Watanasiri, S., V.H. Owens, and K.E. Starling, "Correlations for Estimating Critical Constants, Acentric Factor, and Dipole Moment for Undefined Coal-Fluid Fractions", Ind. Eng. Chem. Process Des. Dev., 24(2), pp. 294-296 (1985).

Whitson, C.H., "Characterizing Hydrocarbon Plus Fractions", Paper #EUR 183, EUROPEC Conference, London, October 21-24 (1980).

Yu, J.M., S.H. Huang, and M. Radosz, "Phase Behaviour of Reservoir Fluids: Supercritical Carbon Dioxide and Cold Lake Bitumen", 5th Int. Conf. on Fluid Properties and Phase Equilibria for Chemical Process Design, Banff, Alberta, 95:1-8 (1989).

"The Thermodynamic and Transport Properties of Bitumens and Heavy Oils", AOSTRA, Chapter 4 (1984).

APPENDIX A

Constants in the Cavett Correlations

The Cavett correlations (Cavett, 1962) were presented in Chapter 2 as Equations 2.4 and 2.5. The constants in these equations follow.

$a_0 =$	768.07121	$b_0 =$	2.8290406
$a_1 =$	1.7133693	$b_1 =$	0.9412019 (10^{-3})
$a_2 =$	-0.10834003 (10^{-2})	$b_2 =$	-0.30474749 (10^{-5})
$a_3 =$	-0.89212579 (10^{-2})	$b_3 =$	-0.20876110 (10^{-4})
$a_4 =$	0.38890584 (10^{-6})	$b_4 =$	0.15184103 (10^{-8})
$a_5 =$	0.53094920 (10^{-5})	$b_5 =$	0.1047899 (10^{-7})
$a_6 =$	0.32711600 (10^{-7})	$b_6 =$	-0.48271599 (10^{-7})
		$b_7 =$	0.13949619 (10^{-9})

APPENDIX B

SIMDIST Distillation Data

Temperatures in °C

Mass percent Distilled	Whole Bitumen	Cut 1	Cut 2	Cut 3	Cut 4
0	236	168	228	391	437
1	252	176	245	430	469
2	263	186	263	440	484
3	272	193	273	447	495
4	279	198	280	452	504
5	285	202	286	456	511
6	292	205	292	460	518
7	299	208	297	463	524
8	305	210	302	466	529
9	312	212	306	469	534
10	317	214	310	472	539
11	323	216	314	474	543
12	328	219	317	476	547
13	333	221	320	479	551
14	339	223	323	481	555
15	344	225	325	483	558
16	349	226	328	485	—
17	354	228	330	487	—
18	359	230	333	488	—
19	364	232	335	490	—
20	369	234	338	492	—
21	374	236	340	494	—
22	379	237	342	495	—
23	384	239	344	497	—
24	389	241	346	498	—
25	394	243	348	500	—
26	399	244	350	501	—
27	405	246	352	503	—
28	410	247	354	504	—
29	415	249	356	506	—
30	420	250	358	507	—
31	425	251	360	509	—
32	429	253	362	510	—
33	434	254	364	511	—
34	439	256	365	513	—
35	444	257	367	514	—
36	448	259	369	516	—
37	453	260	371	517	—
38	458	261	373	518	—
39	463	263	375	520	—
40	468	264	377	521	—
41	473	265	378	522	—
42	478	267	380	523	—
43	483	268	382	525	—
44	488	269	384	526	—
45	493	271	386	527	—

Mass percent Distilled	Whole Bitumen	Cut 1	Cut 2	Cut 3	Cut 4
46	498	272	387	529	—
47	503	273	389	530	—
48	509	274	391	531	—
49	514	275	393	533	—
50	519	276	395	534	—
51	525	277	397	535	—
52	531	278	399	536	—
53	536	279	400	538	—
54	543	280	402	539	—
55	548	281	404	540	—
56	553	282	406	542	—
57	559	283	408	543	—
58	—	284	410	544	—
59	—	286	411	545	—
60	—	287	413	547	—
61	—	288	415	548	—
62	—	290	417	549	—
63	—	291	419	551	—
64	—	292	420	552	—
65	—	294	422	553	—
66	—	295	424	555	—
67	—	297	426	556	—
68	—	298	427	557	—
69	—	299	429	559	—
70	—	301	431	560	—
71	—	302	433	—	—
72	—	304	434	—	—
73	—	305	436	—	—
74	—	307	438	—	—
75	—	308	440	—	—
76	—	310	442	—	—
77	—	312	444	—	—
78	—	313	445	—	—
79	—	315	447	—	—
80	—	317	449	—	—
81	—	318	451	—	—
82	—	320	453	—	—
83	—	322	456	—	—
84	—	324	458	—	—
85	—	326	460	—	—
86	—	328	462	—	—
87	—	330	465	—	—
88	—	332	468	—	—
89	—	335	470	—	—
90	—	337	473	—	—
91	—	340	476	—	—
92	—	343	479	—	—
93	—	346	483	—	—
94	—	350	487	—	—
95	—	354	492	—	—

Mass percent Distilled	Whole Bitumen	Cut 1	Cut 2	Cut 3	Cut 4
96	—	359	497	—	—
97	—	366	504	—	—
98	—	374	513	—	—
99	—	387	527	—	—
100	—	400	539	—	—

APPENDIX C

Supplement to Chapter 6

Critical Pressures and Interaction Parameters

Regressed with the P-T EOS

Whole Bitumen

Characterization	P_c (kPa)	k_α	k_β	Residual
Kesler-Lee	712	-0.0282	-0.0009	55.8
Cavett	772	-0.0449	-0.0016	179.0
Sim-Daubert	718	-0.0324	-0.0008	56.5
Whitson	731	-0.0357	-0.0009	63.0
Twu	718	-0.0331	-0.0008	56.5
Watanasiri	720	-0.0304	-0.0010	65.4

Cut 1

Characterization	P_c (kPa)	k_α	k_β	Residual
Kesler-Lee	1745	0.0772	0.0000	145.4
Cavett	2045	0.0349	-0.0006	193.3
Sim-Daubert	1744	0.0796	0.0000	145.7
Whitson	1777	0.0751	0.0000	148.4
Twu	1788	0.0709	0.0000	148.7
Watanasiri	1721	0.0827	-0.0006	143.8

Cut 2

Characterization	P_c (kPa)	k_α	k_β	Residual
Kesler-Lee	1281	0.0320	0.0000	102.7
Cavett	1509	0.0124	-0.0020	331.6
Sim-Daubert	1286	0.0409	-0.0003	73.4
Whitson	1315	0.0339	-0.0004	74.7
Twu	1319	0.0337	-0.0004	74.9
Watanasiri	1320	0.0286	0.0000	87.5

Cut 3

Characterization	P_c (kPa)	k_α	k_β	Residual
Kesler-Lee	624	-0.0428	-0.0009	206.3
Cavett	665	-0.0699	-0.0009	194.5
Sim-Daubert	629	-0.0491	-0.0008	213.0
Whitson	640	-0.0535	-0.0009	232.5
Twu	625	-0.0514	-0.0007	215.2
Watanasiri	626	-0.0431	-0.0009	203.0

Cut 4

Characterization	P_c (kPa)	k_α	k_β	Residual
Kesler-Lee	531	-0.0876	-0.0005	208.5
Cavett	556	-0.1022	-0.0005	270.4
Sim-Daubert	535	-0.0909	-0.0006	215.7
Whitson	542	-0.0897	-0.0008	229.5
Twu	527	-0.0854	-0.0006	197.2
Watanasiri	532	-0.0882	-0.0013	209.8

Cut 5

Characterization	P_c (kPa)	k_α	k_β	Residual
Kesler-Lee	138	-0.0282	-0.0009	102.7
Cavett	182	-0.0449	-0.0016	331.6
Sim-Daubert	158	-0.0324	-0.0008	73.4
Whitson	154	-0.0357	-0.0009	74.7
Twu	179	-0.0331	-0.0008	74.9
Watanasiri	155	-0.0304	-0.0010	87.5